Semi-organised structures in convective boundary layers

N. KLEEORIN

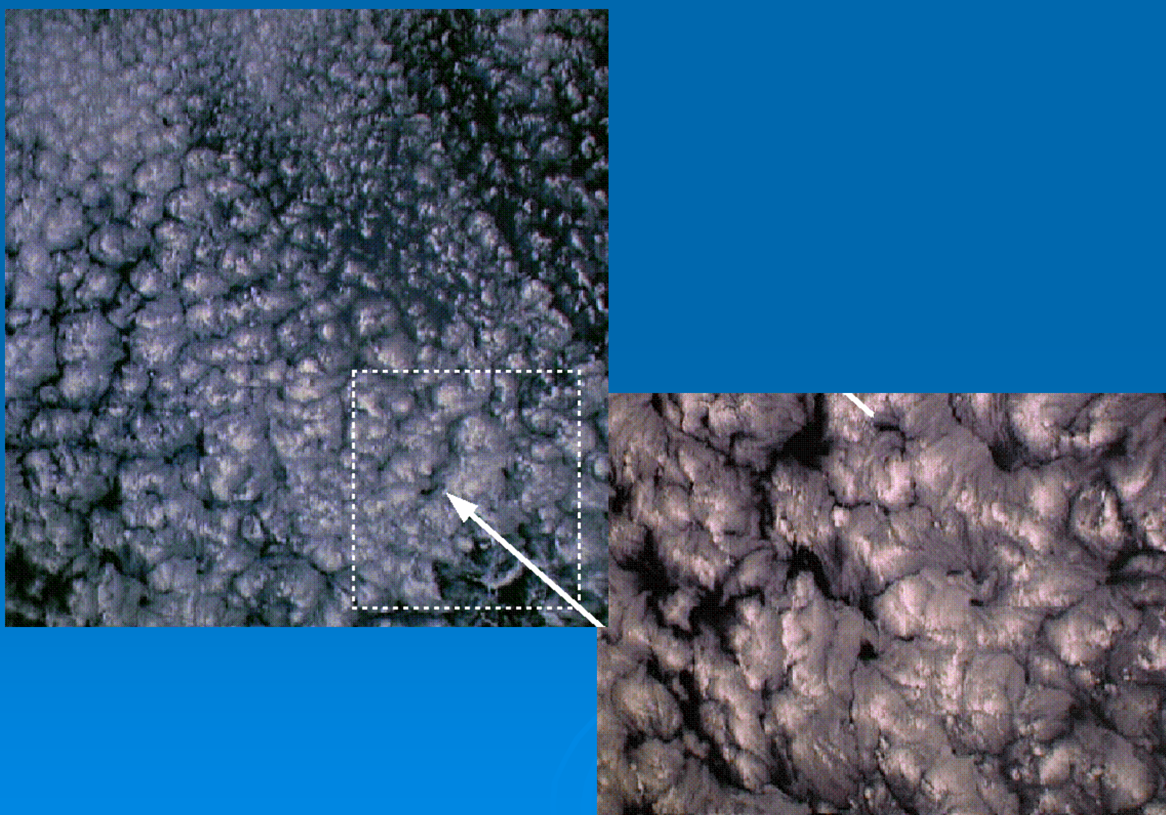

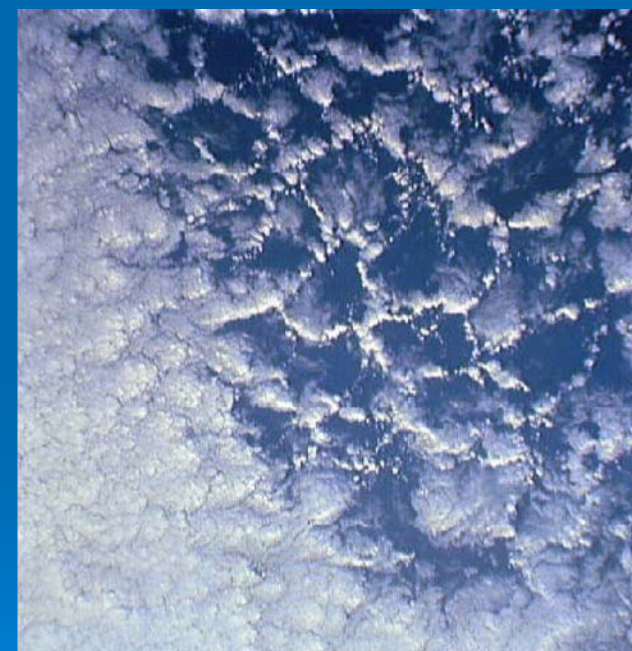

T. ELPERIN, I. ROGACHEVSKII,A. EIDELMAN, A. KREIN, A. MARKOVICH, I.GOLUBEV

Department of Mechanical Engineering
Ben-Gurion University of the Negev
Beer Sheva, ISRAEL

S. ZILITINKEVICH

Division of Atmospheric Sciences
Department of Physical Sciences
University of Helsinki, FINLAND

Outline

- Introduction
- Properties of coherent structures in atmospheric and laboratory turbulent convection
- Mechanisms of formation of coherent structures
- Theory and comparison with observations
- Experimental study of coherent structures
- Conclusions and future studies

Introduction

- **The atmospheric turbulent convection:**
  - the fully organized large-scale flow (the mean flow or mean wind)
  - the small-scale turbulent fluctuations,
  - long-lived large-scale coherent structures.
- **Two types of the coherent structures:**
  - cloud “streets”
  - cloud cells
- **The life-times and spatial scales of the coherent structures are much larger than the turbulent scales.**

Etling, D. and **Brown**, R. A., 1993. *Boundary-Layer Meteorol.*, **65**, 215—248.

Atkinson, B. W. and **Wu Zhang**, J., 1996. *Reviews of Geophysics*, **34**, 403—431.

Closed cloud cells over the Atlantic Ocean

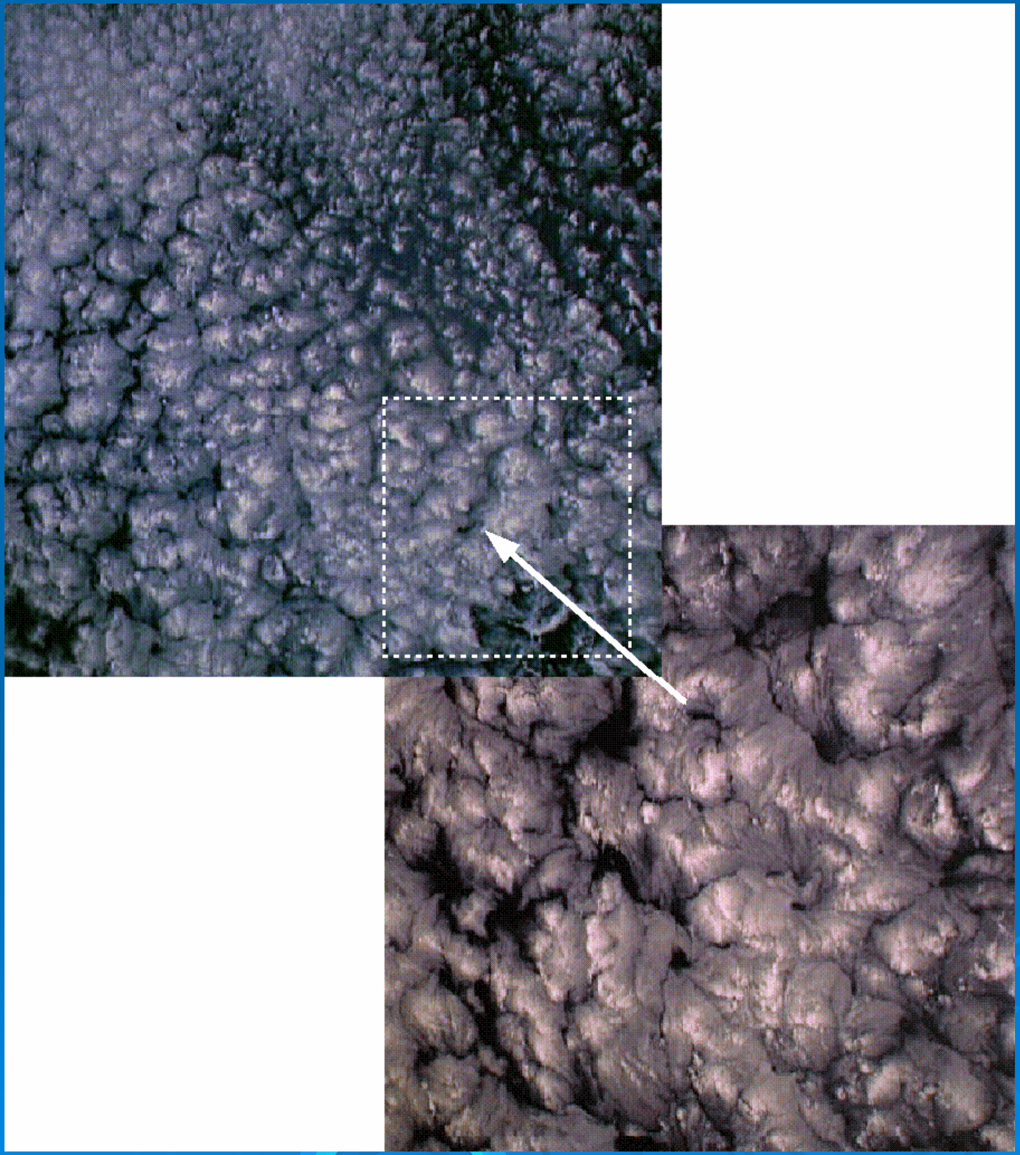

Open cloud cells over the Pacific Ocean

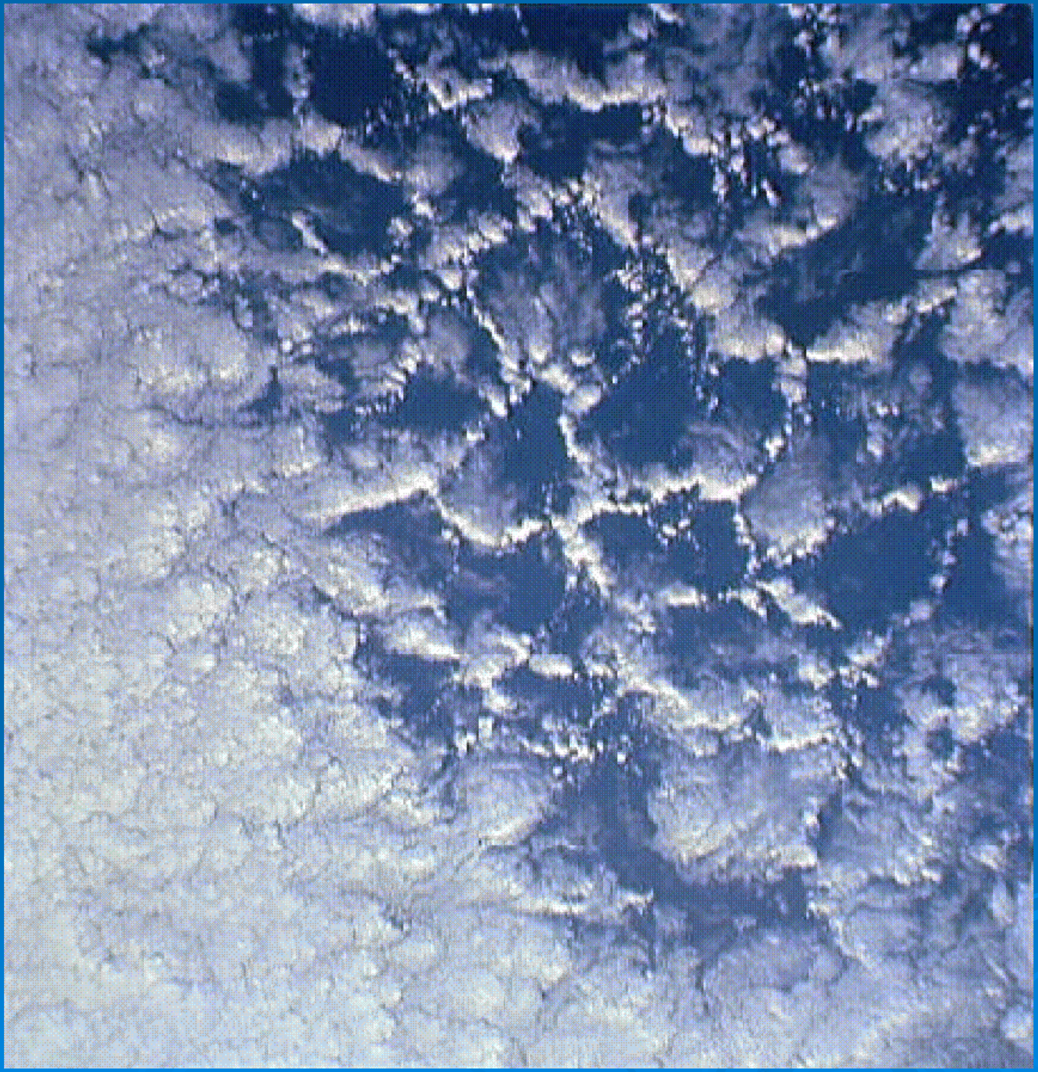

Example of Close Convective Cell

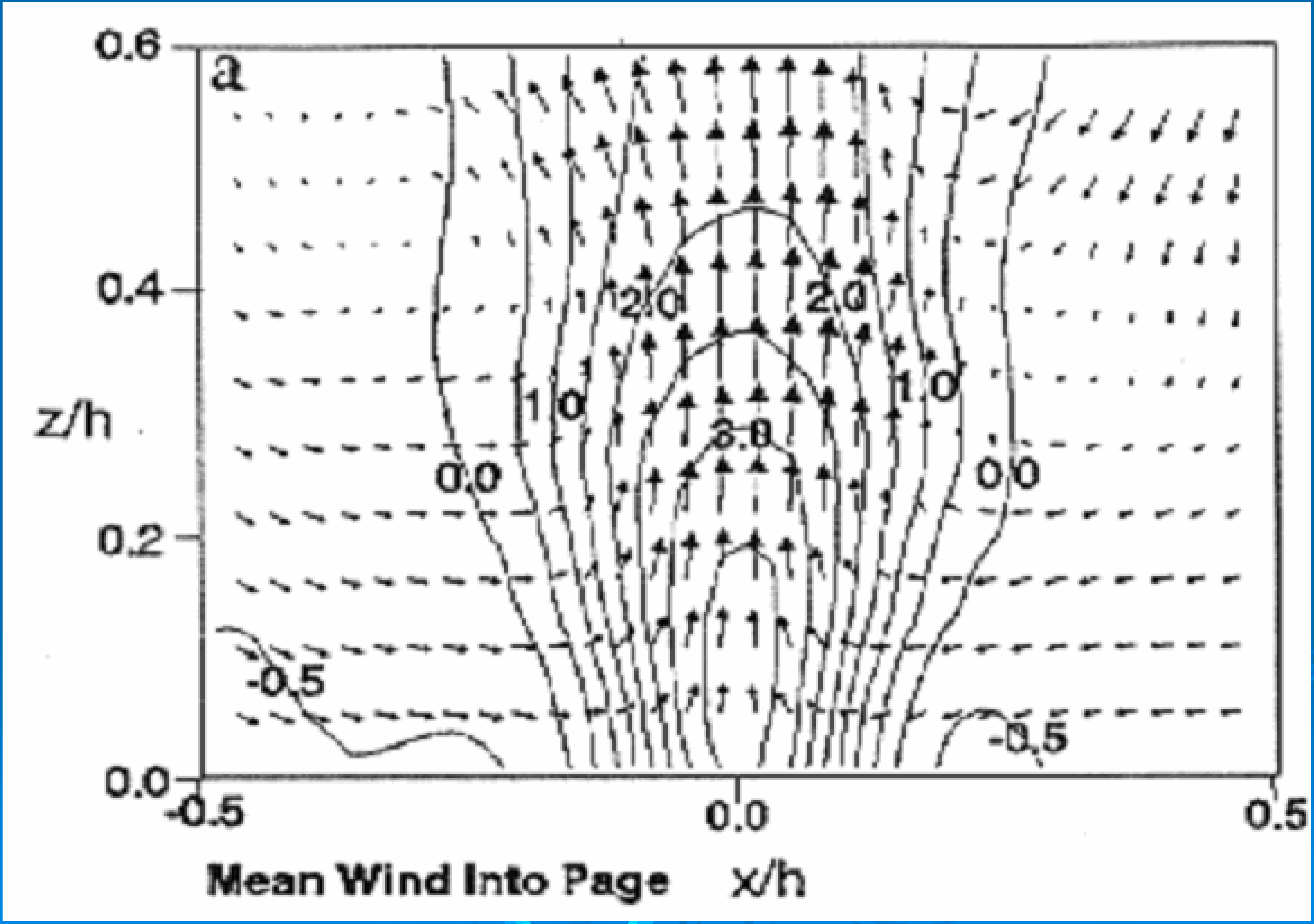

Unforced Convection: A=2

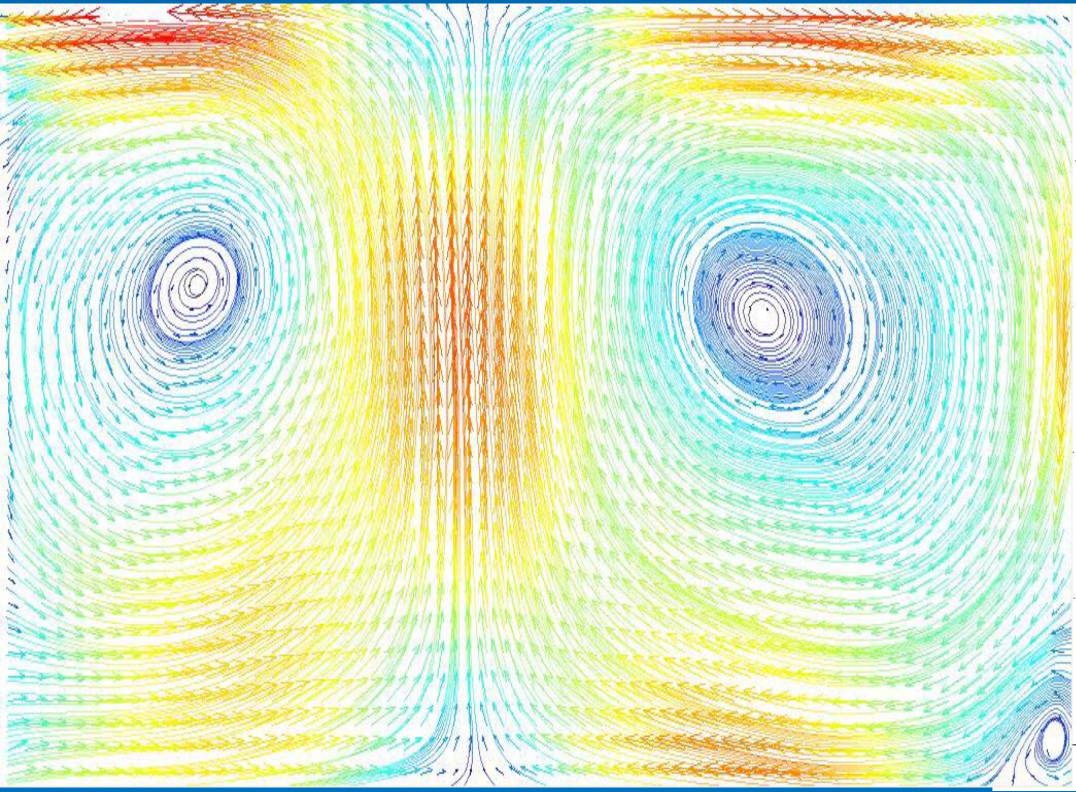

$\overline{U}(y,z)$

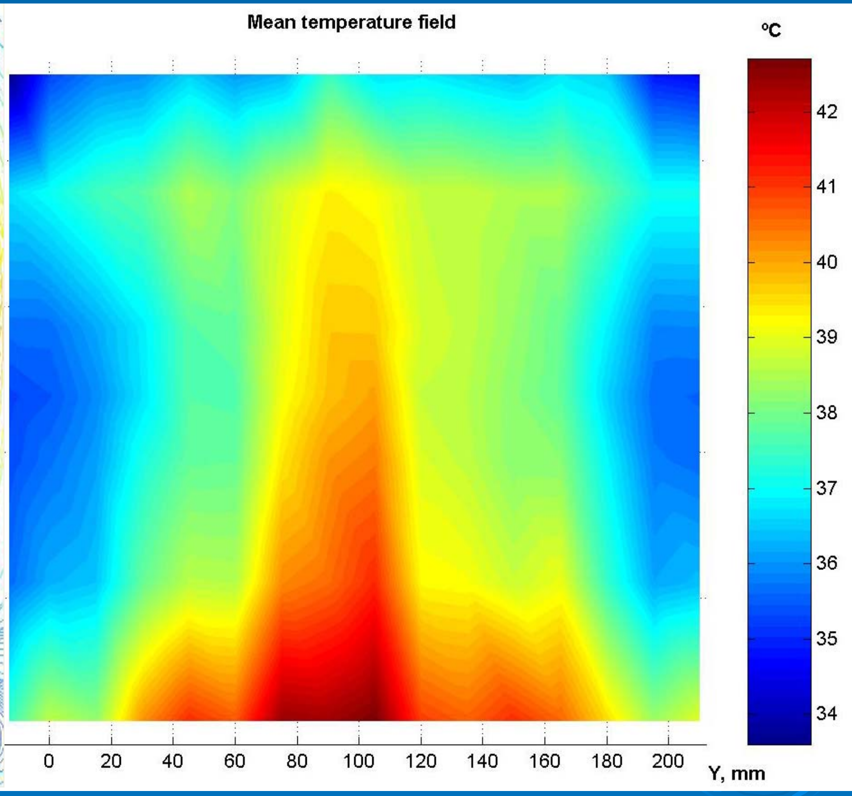

$\overline{T}(y,z)$

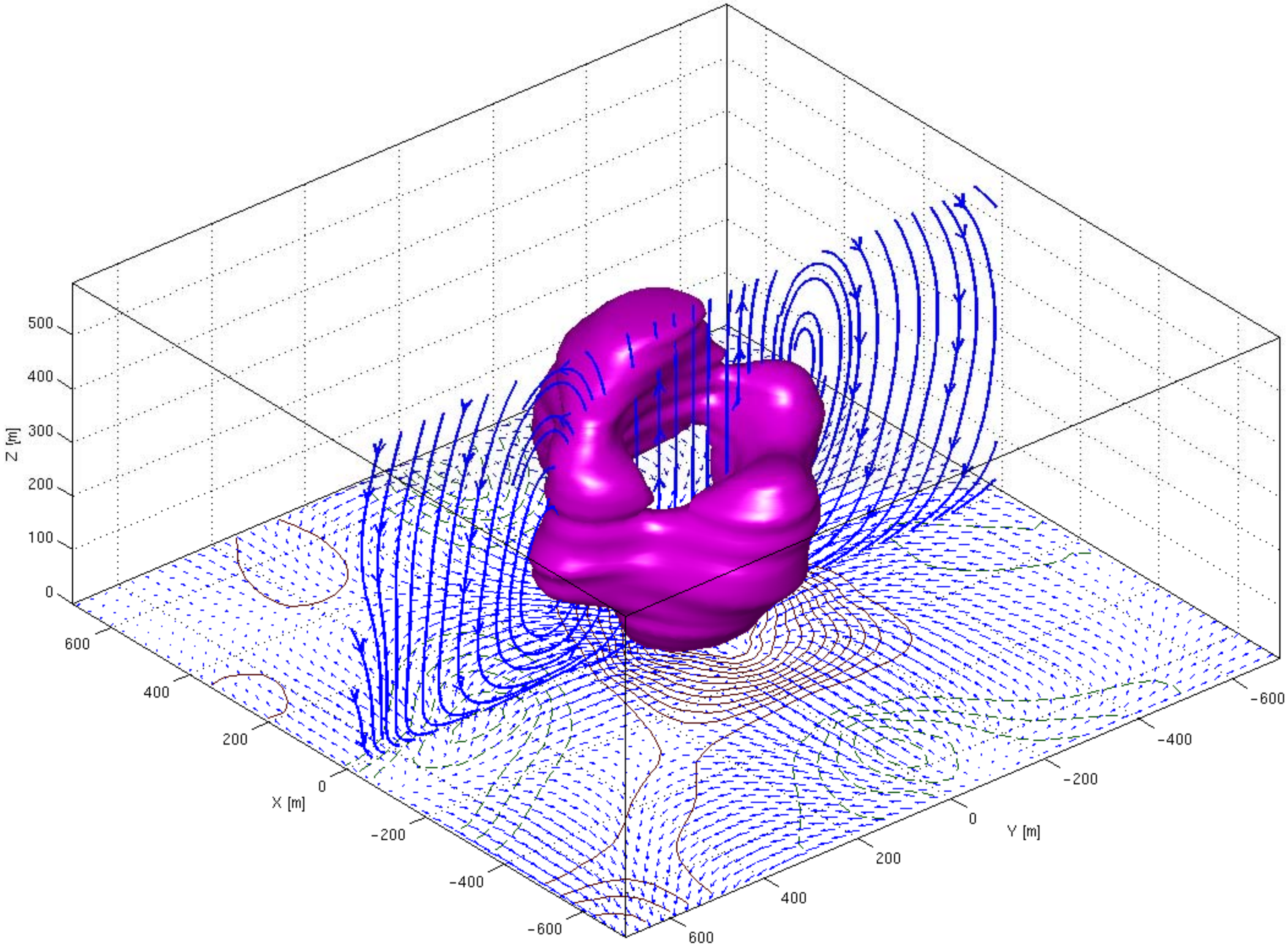

500
400
300
200
100
0
Z [m]
600
400
200
0
-200
-400
-600
X [m]
-600
-400
-200
0
200
400
600
Y [m]

Cloud “streets” over the Amazon River

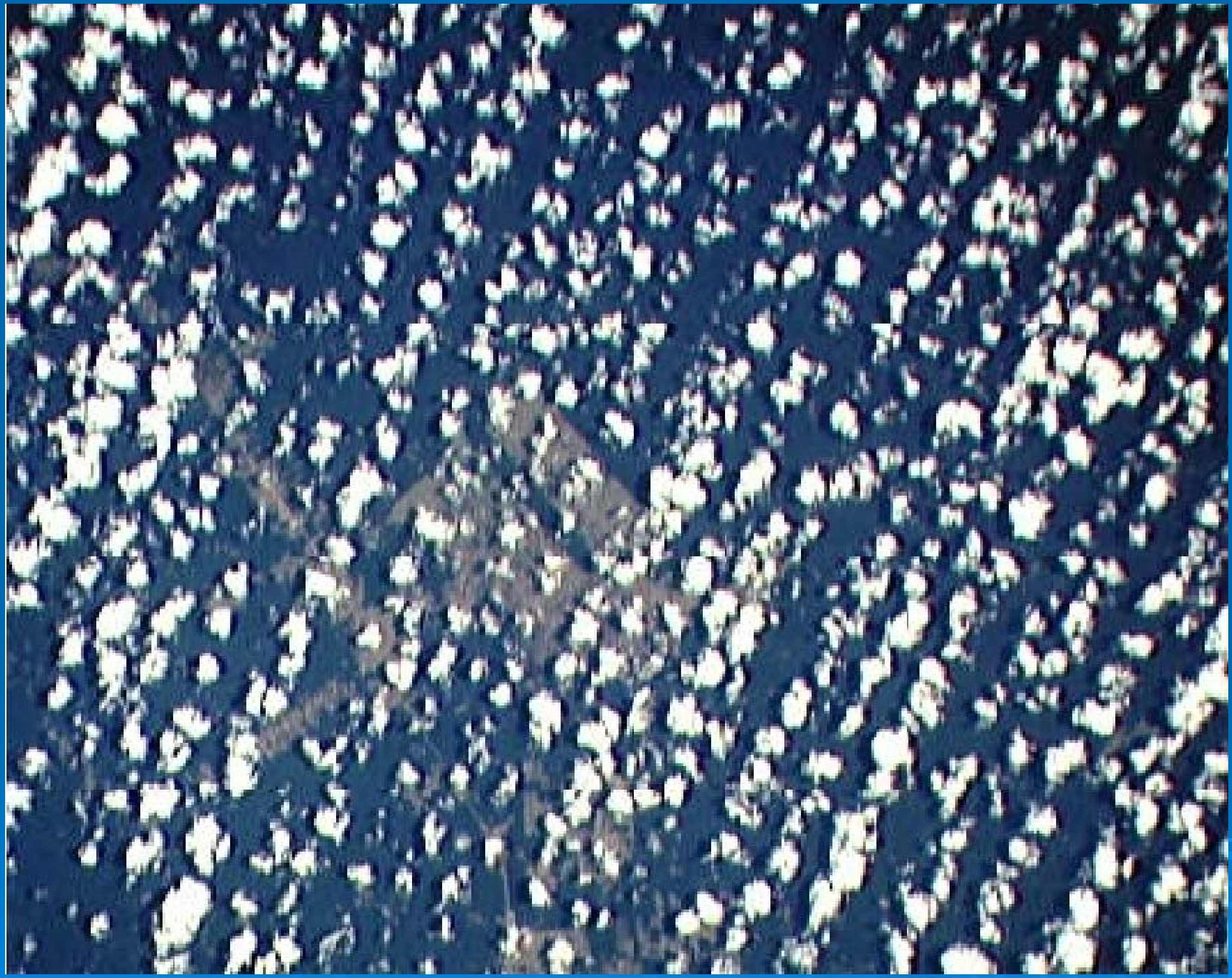

Cloud “streets” over Indian ocean

Equations for Atmospheric Flows

$$\rho \frac{D\,\mathbf{v}}{D\,t} = \mathbf{f}$$

$$\mathbf{f} = -\vec{\nabla} p + \mathbf{g}\,\rho + \mathrm{div}\,\hat{\sigma}_{\nu}$$

$$\frac{D\,T}{D\,t} = -\,\mathrm{div}\,\mathbf{F}_{\mu}$$

$$\mathbf{F}_{\mu} = -\kappa_{\mu} \vec{\nabla} T$$

$$\frac{\partial \rho}{\partial\, t} = -\mathrm{div}\,\rho\,\mathbf{v}$$

$$\frac{D}{D\,t} = \frac{\partial}{\partial\, t} + \mathbf{v} \cdot \vec{\nabla}$$

$$\mathrm{div}\,\hat{\sigma}_{\nu} = \rho\,\nu\,\Delta\,\mathbf{v}$$

Boussinesq Approximation

$$\left(\frac{\partial}{\partial t}+\mathbf{v}\cdot\vec{\nabla}\right)\mathbf{v}=-\vec{\nabla}\left(\frac{p}{\rho_0}\right)-\boldsymbol{\beta}\,\theta+\mathbf{f}_\nu(\mathbf{v}),$$

$$\left(\frac{\partial}{\partial t}+\mathbf{v}\cdot\vec{\nabla}\right)\theta=\frac{1}{T}\vec{\nabla}\cdot\left(\kappa T\,\vec{\nabla}\,\theta\right)$$

$$\mathrm{div}\,\rho_0\,\mathbf{v}=0$$

$$\boldsymbol{\beta}=\frac{\mathbf{g}}{T_0}\qquad \theta=T\left(\frac{p_0}{p}\right)^{(\gamma-1)/\gamma}\qquad \vec{\nabla}p_0=\rho_0\mathbf{g}$$

Laminar and Turbulent Flows

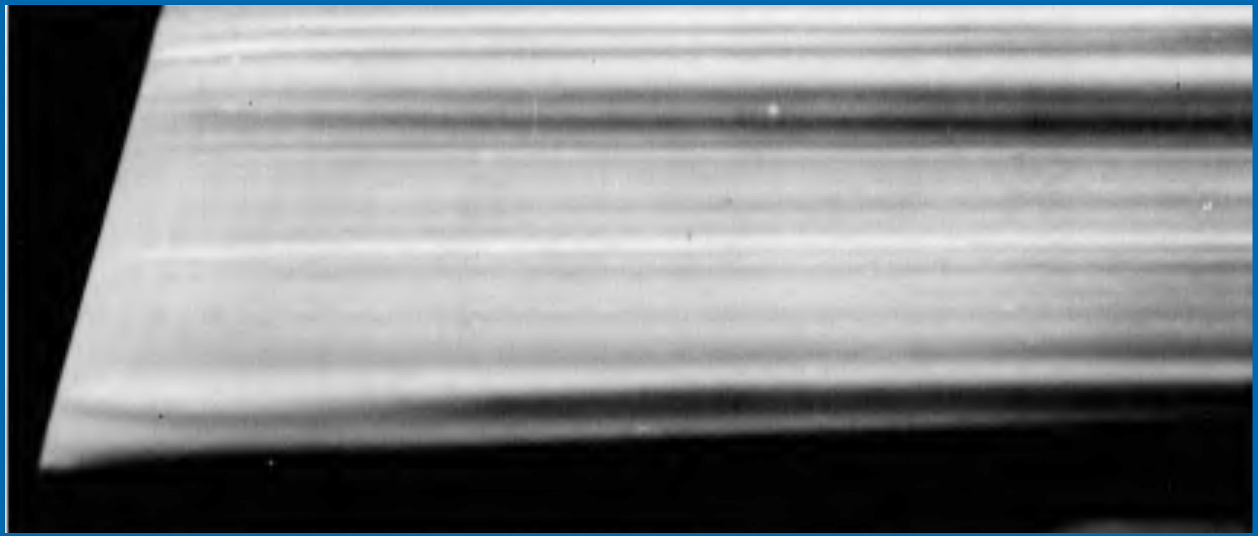

Laminar Boundary Layer

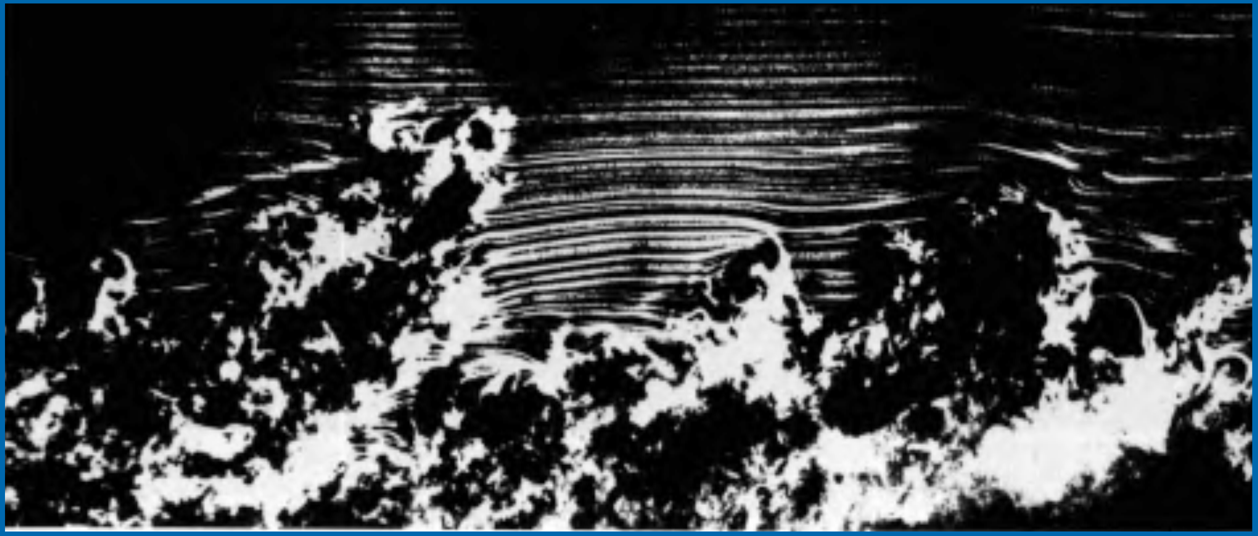

Turbulent Boundary Layer

Why Turbulence?

$$\frac{\text{inertial force}}{\text{viscous force}} \propto \frac{\mathrm{v}\, l}{\nu} = \mathrm{Re} \approx 10^{7} \div 10^{8}$$

$$\frac{\text{advective term}}{\text{diffusive term}} \propto \frac{\mathrm{v}\, l}{\kappa} = \mathrm{Pe} \approx 10^{7} \div 10^{8}$$

Why Not DNS?

Number degrees of freedom $\propto \mathrm{Re}^{9/4} \approx 10^{15} \div 10^{18}$

RANS Equations

Reynolds decomposition

$$\mathbf{v} = \overline{\mathbf{U}} + \mathbf{u}, \quad \theta = \overline{\Theta} + \theta', \quad \langle \mathbf{u} \rangle = 0, \quad \langle \theta' \rangle = 0$$

$$\left(\frac{\partial}{\partial t} + \overline{\mathbf{U}} \cdot \vec{\nabla} \right) \overline{\mathbf{U}} = -\vec{\nabla} \left(\frac{\overline{P}}{\rho_0} \right) + \operatorname{div} \hat{\tau} - \boldsymbol{\beta} \, \overline{\Theta} + \mathbf{f}_\nu \left(\overline{\mathbf{U}} \right) + 2 \overline{\mathbf{U}} \times \boldsymbol{\Omega},$$

$$\left(\frac{\partial}{\partial t} + \overline{\mathbf{U}} \cdot \vec{\nabla} \right) \overline{\Theta} = \frac{\overline{\mathbf{U}} \cdot \mathbf{e}}{\beta} N^2 - \operatorname{div} \left(\mathbf{F}_\mu + \mathbf{F}_T \right)$$

$$\left(\hat{\tau} \right)_{ij} = -\langle u_i u_j \rangle$$

$$N^2 = -\boldsymbol{\beta} \cdot \vec{\nabla} \overline{\Theta}$$

$$\mathbf{F}_T = \langle \mathbf{u} \, \theta' \rangle$$

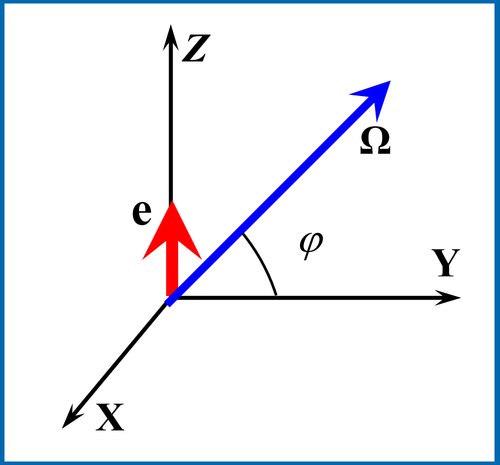

Experimental set-up

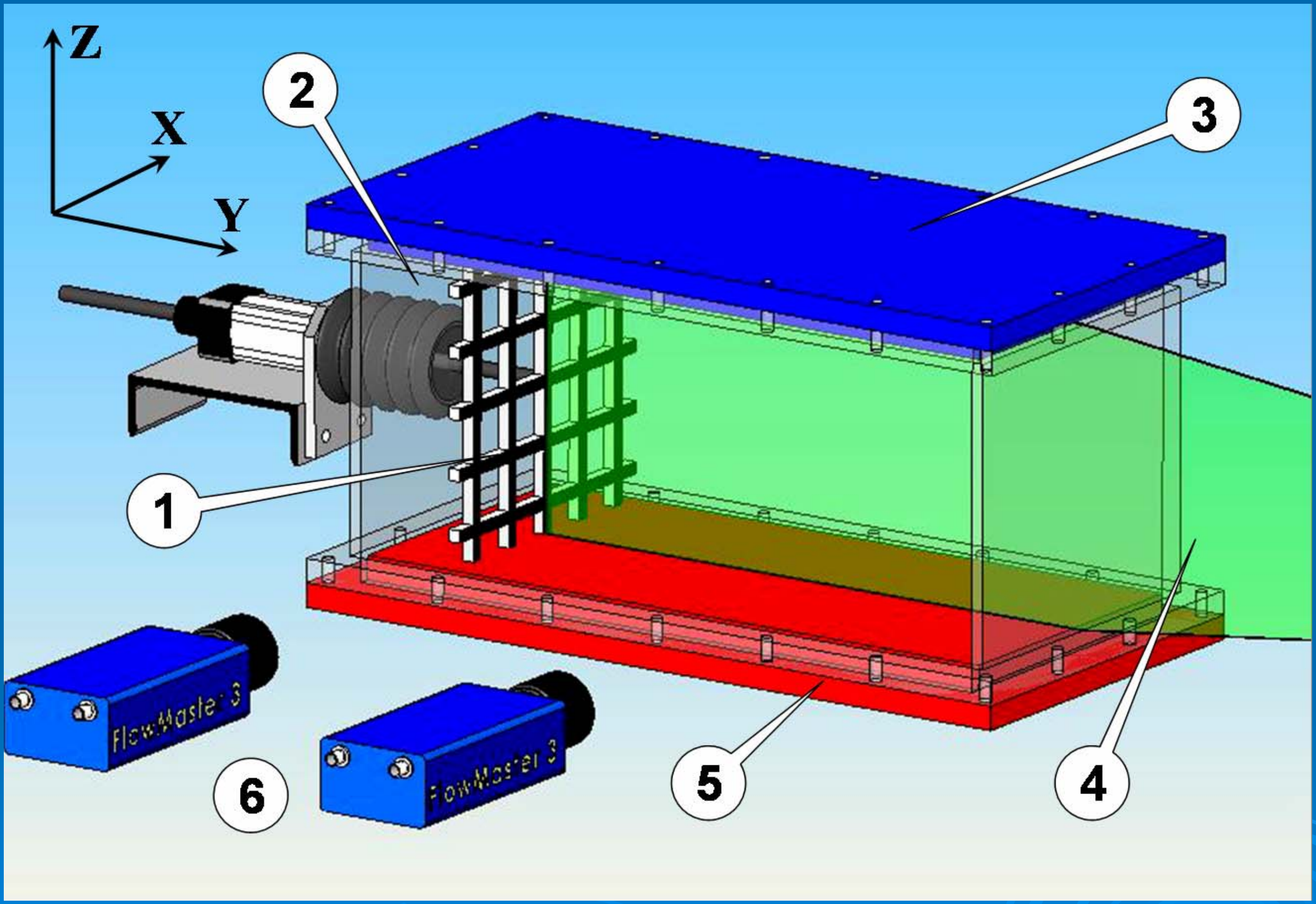

Laboratory Turbulent Convection

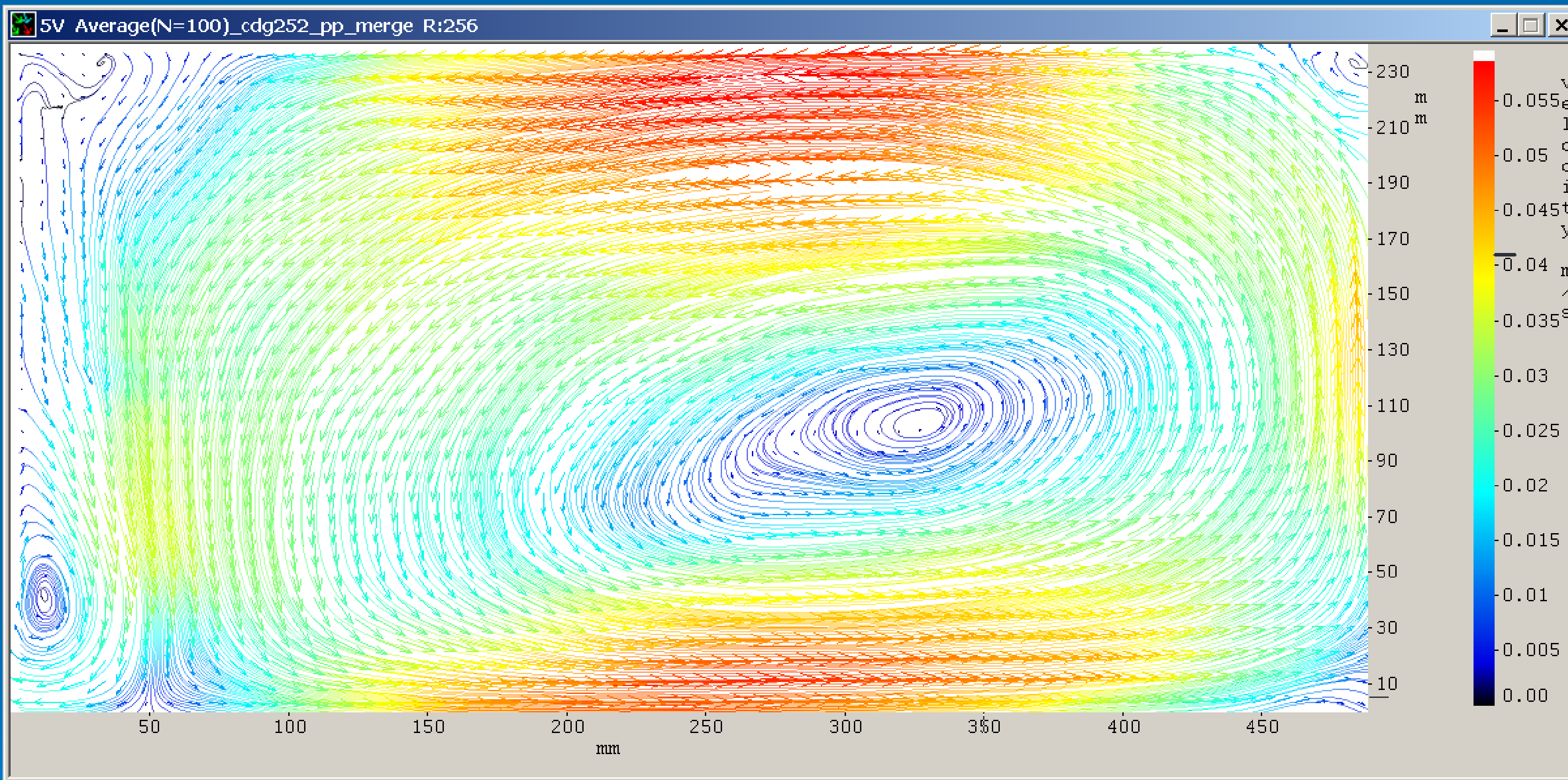

Before averaging

After averaging

Turbulent Eddies

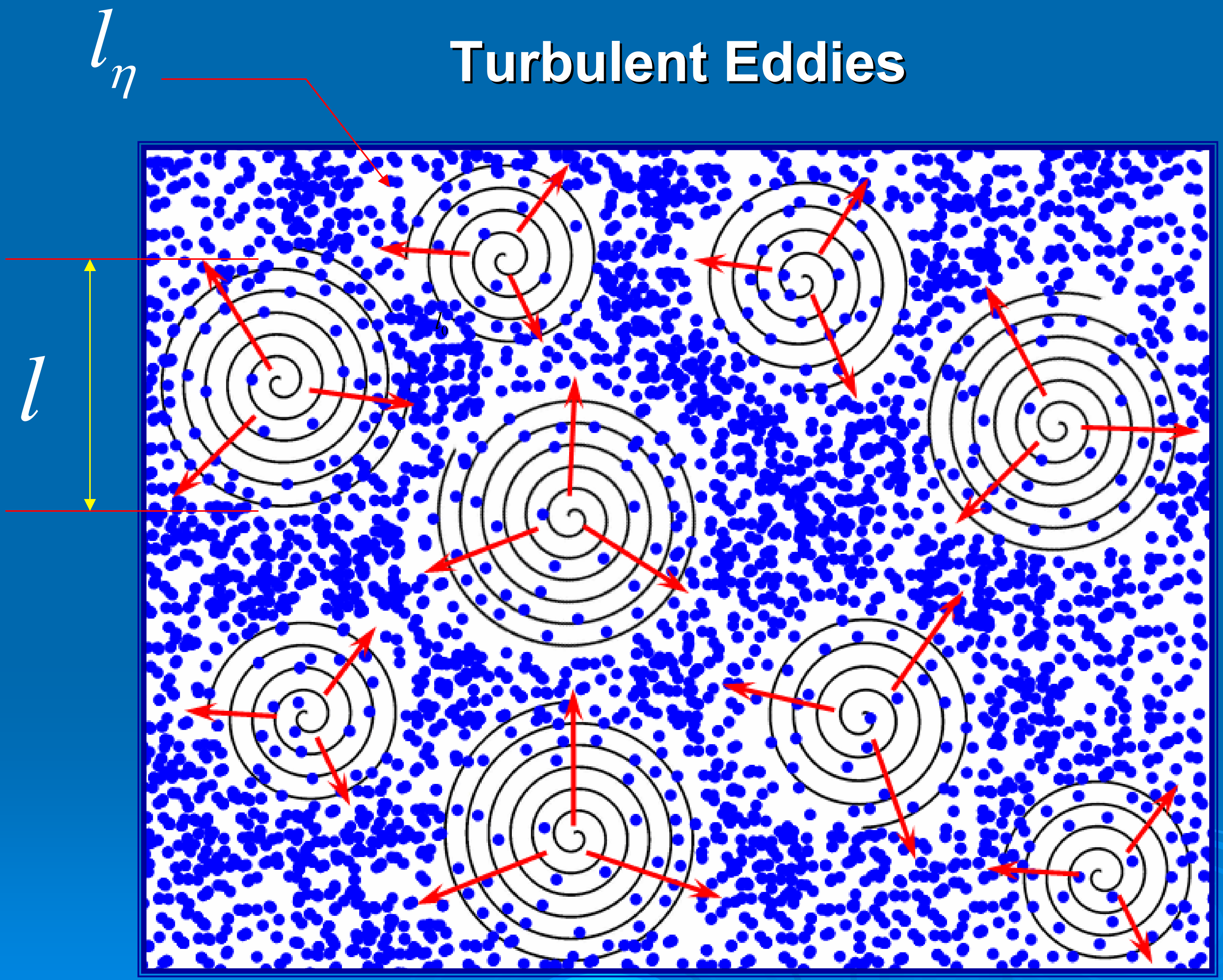

Budget Equation for TKE

$$\boxed{\frac{DE_K}{Dt} = \Pi_{tot} - T - D}$$

$$D = \nu\left\langle(\mathrm{rot}\,\mathbf{u})^2\right\rangle = \frac{\left\langle \mathbf{u}^2 \right\rangle}{\tau_0}$$

$$\Pi_{tot} = \Pi + g\cdot F\frac{1}{T}; \quad \Pi = K_M S^2; \quad S = \sqrt{\left(\nabla_i \bar{U}_j\right)\left(\nabla_i \bar{U}_j\right)}$$

Balance in R-space

$$\Pi_{tot} \approx D$$

Balance in K-space

$$T(k) \approx 0$$

$$T = \mathrm{div}\left(\mathbf{\Phi}_u\right)$$

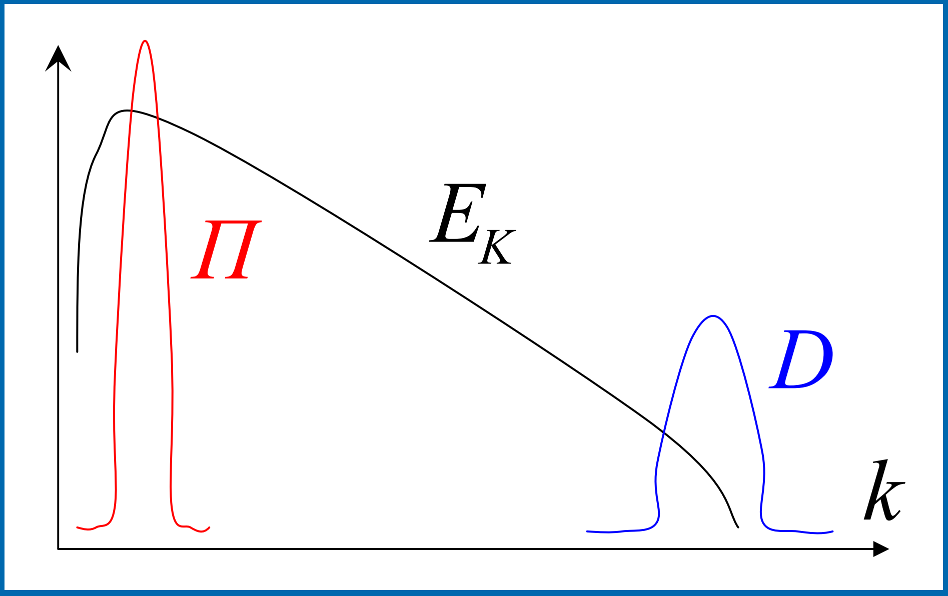

Boussinesq-Prandtl Model

$$\tau_{ij} = K_M \left(\nabla_i \overline{U}_j + \nabla_j \overline{U}_i \right) - \frac{\left\langle \mathbf{u}^2 \right\rangle}{3} \delta_{ij}$$

$$\mathbf{F} = -K_H \vec{\nabla} \overline{\Theta}$$

$$K_M \cong C_M \, u \, l, \qquad K_H \cong C_H \, u \, l, \quad \Pr_T = \frac{K_M}{K_H} = \frac{C_M}{C_H}$$

For example, in turbulent boundary layer $\quad l \approx \kappa z$

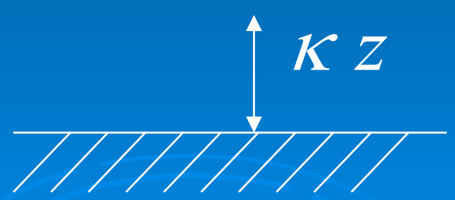

Heat flux

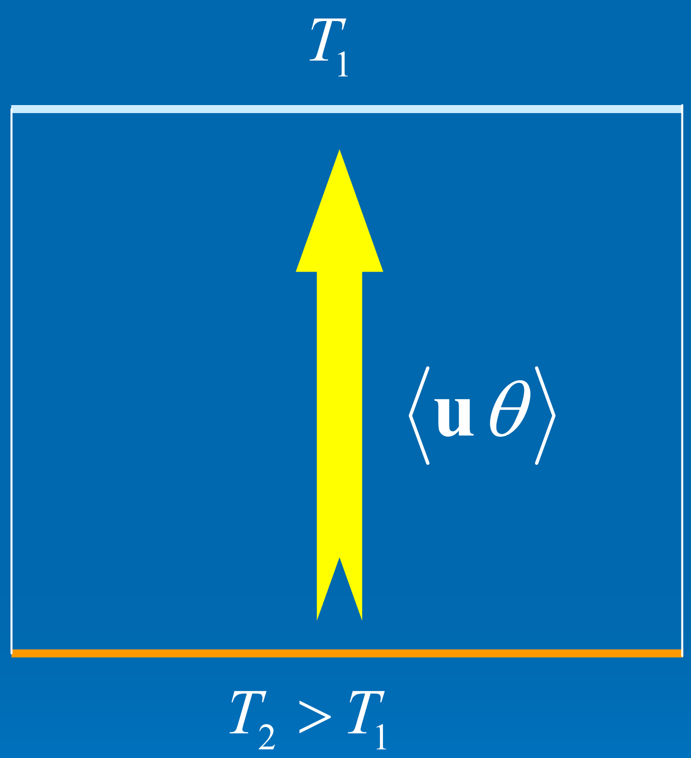

$$\langle \mathbf{u}\,\theta \rangle = -\kappa_T \vec{\nabla} T$$

$$\kappa_T \cong \frac{u_0\, l_0}{3}$$

Reyleigh Instability, Critical Reyleigh number

$$\left(\frac{\partial}{\partial t} - \Delta\right)\Delta V = Ra\,\Delta_\perp \Theta \qquad \Delta_\perp = \frac{\partial^2}{\partial^2 x} + \frac{\partial^2}{\partial^2 y}$$

$$\mathrm{Pr_T}\frac{\partial \Theta}{\partial t} - \Delta\Theta = V \qquad \Delta = \frac{\partial^2}{\partial^2 x} + \frac{\partial^2}{\partial^2 y} + \frac{\partial^2}{\partial^2 z}$$

$$\mathrm{Pr_T} = \frac{\nu_\mathrm{T}}{\kappa_\mathrm{T}}; \;\; \mathrm{Ra} = \frac{g\,\beta\,\Delta T\,L^3}{\nu_T\ \ \kappa_T}$$

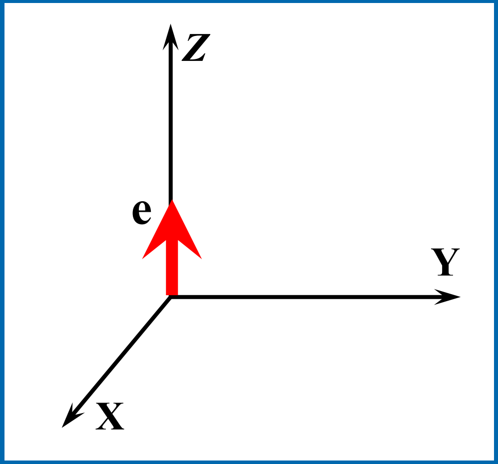

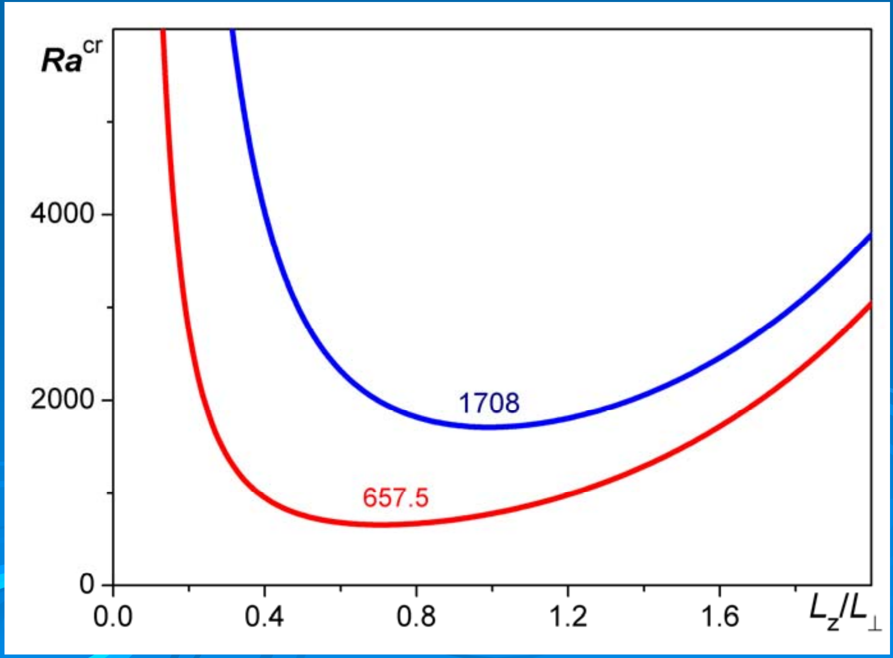

Temperature profiles

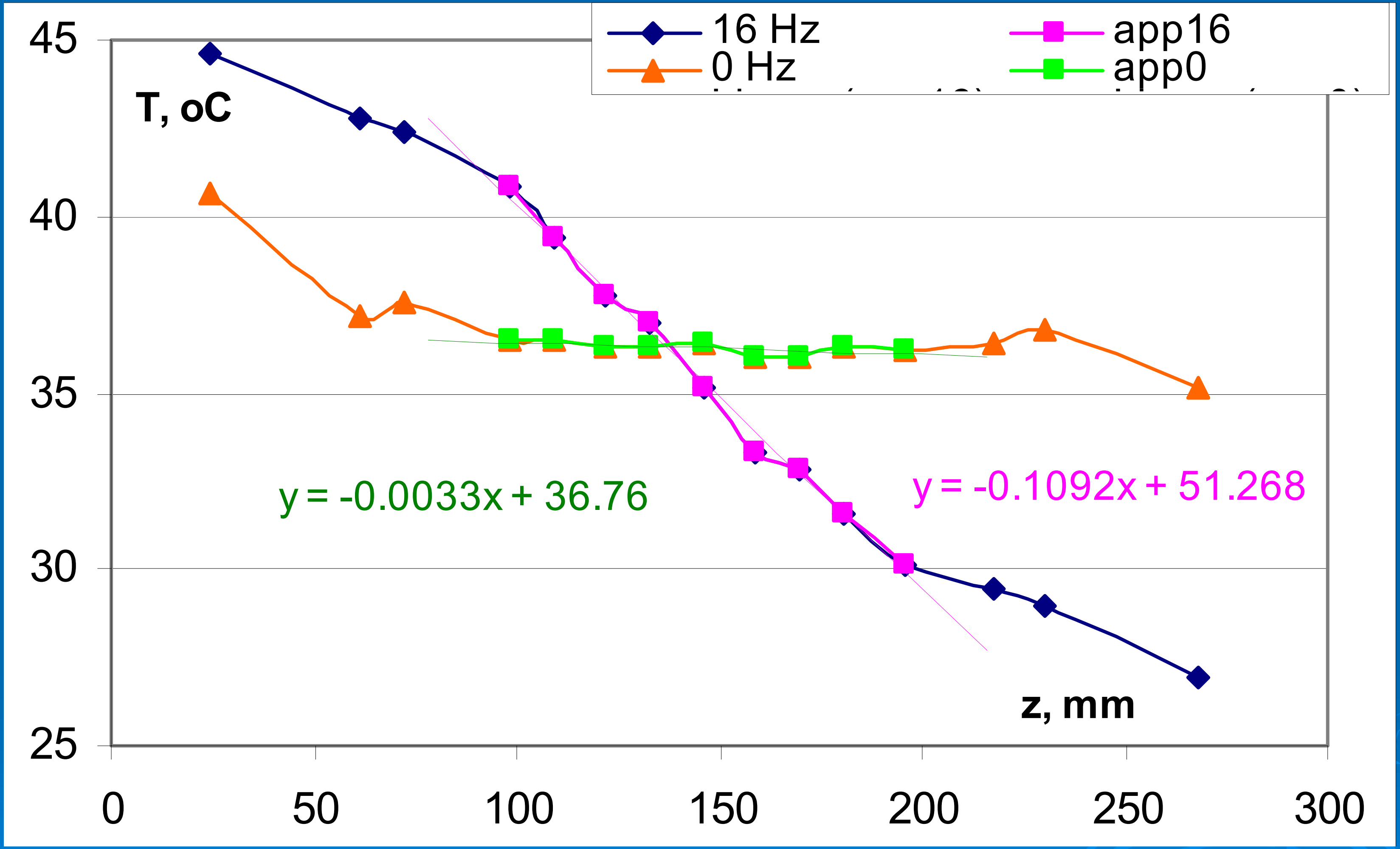

- Pure convection
- Convection and oscillating grids forcing

Experimental Parameters

- The r.m.s. vertical velocity $\sqrt{\langle u_z^2 \rangle} = 6 \div 10 \, \mathrm{cm}/\mathrm{s}$
- The integral scale $l_z = 2 \div 4 \, \mathrm{cm}$
- The mean velocity of SO structure $\overline{U}_z = 15 \div 20 \, \mathrm{cm}/\mathrm{s}$
- Rayleigh number $Ra = \dfrac{g\, \beta\, \Delta T\, L^3}{\nu \;\; \kappa} \approx (0.1 - 1.6) \times 10^8$

  $\left(\Delta T = 80\,^{\circ}K, \quad L = 30\, cm \right)$
- The effective Rayleigh number $Ra^{eff} = \dfrac{g\, \beta\, \Delta T\, L_T^3}{\nu_T \;\; \kappa_T} \approx 100 \div 625$

  $\left(\Delta T = 3 \div 5\, \mathrm{K}, \quad L_T = 20\, \mathrm{cm} \right)$

Problems

- The Rayleigh numbers based on the molecular transport coefficients are very large:

$$\boxed{Ra = \frac{g\,\beta\,\Delta T\,L^3}{\nu\ \ \kappa} \approx 10^{11} \div 10^{13}}$$

This corresponds to fully developed turbulent convection in atmospheric and laboratory flows.

- The effective Rayleigh numbers based on the turbulent transport coefficients (the turbulent viscosity and turbulent diffusivity) are not high.

$$\boxed{Ra^{eff} = \frac{g\,\beta\,\Delta T\,L^3}{\nu_T\ \ \kappa_T} \approx 10\,\mathrm{Pr}^{-1}\, Ra \big/ \mathrm{Re}_l^2 \approx 145}$$

They are less than the critical Rayleigh numbers required for the excitation of large-scale convection.

Hence the emergence of large-scale convective flows (which are observed in the atmospheric and laboratory flows) seems puzzling.

Interaction between mean-flow and turbulent objects

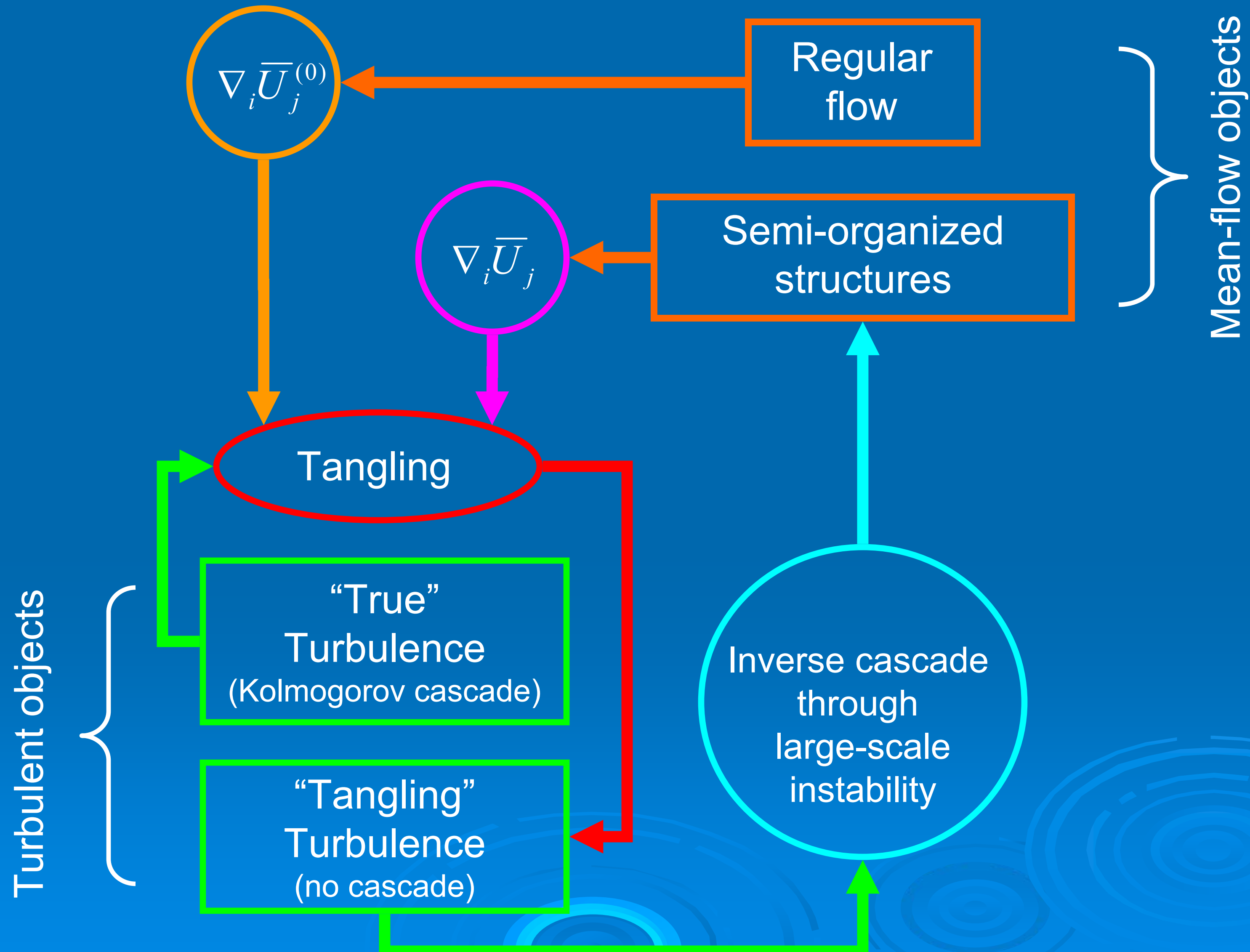

Tangling turbulence in sheared mean flow

Sheared mean flow

$\nabla \overline{U}^{(0)} \neq 0$

Kolmogorov turbulence

$\vec{u}$

"Tangling" turbulence

$\delta u \propto (\vec{u} \cdot \vec{\nabla})\, \overline{U}^{(0)}$

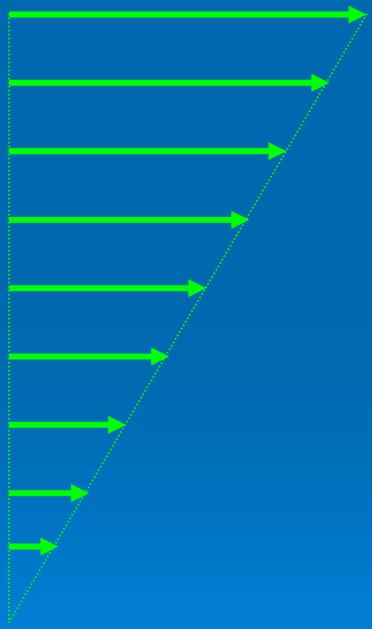

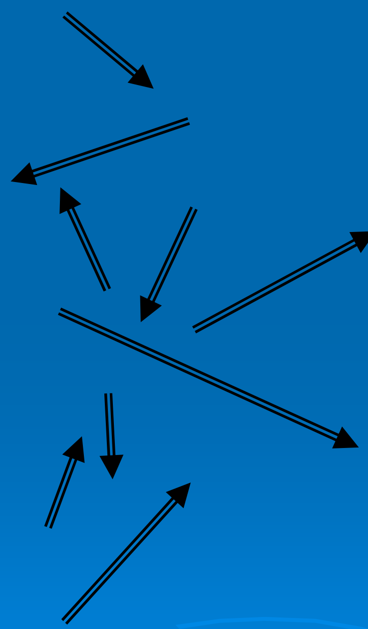

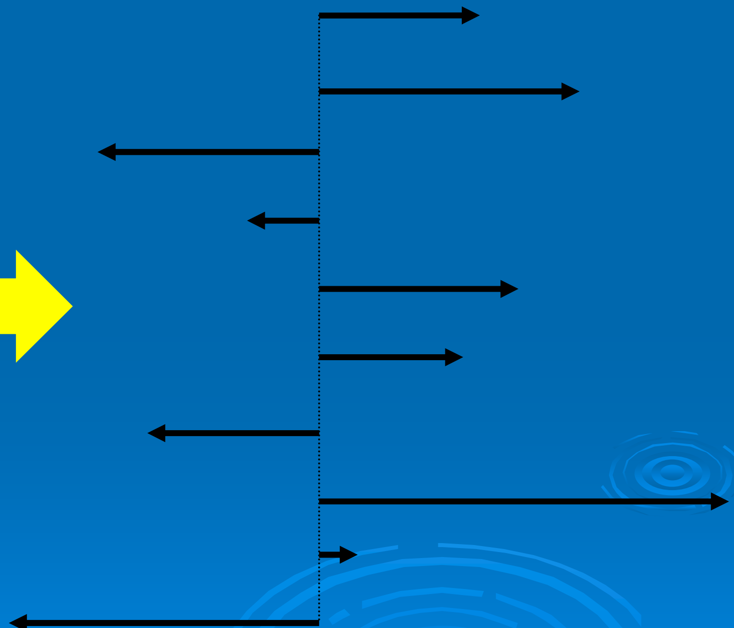

$k^{-5/3}$

Lumley (1967) $k^{-7/3}$

Heat flux

Traditional parameterization

$$\langle \theta\, \mathbf{u} \rangle = -\kappa_T\, \vec{\nabla}\, \overline{\Theta}$$

Modification of the heat flux by tangling turbulence

$$\boxed{\langle \theta\, \mathbf{u} \rangle = \mathbf{F}^* + \frac{\tau_0}{6}\left[-5\left(\vec{\nabla}\cdot\overline{\mathbf{U}}_\perp\right)\mathbf{F}_\parallel^* + \left(\alpha + \frac{3}{2}\right)\left(\overline{\mathbf{W}} \times \mathbf{F}_\parallel^*\right) + 3\left(\overline{\mathbf{W}}_\parallel \times \mathbf{F}_\parallel^*\right)\right]}$$

$$\mathbf{F}^* = -\kappa_T \vec{\nabla}\overline{\Theta} - \tau_0\left(\mathbf{F}_\parallel^* \cdot \nabla\right)\, \overline{\mathbf{U}}^{(0)}(z)$$

$$\overline{\mathbf{W}} = \vec{\nabla} \times \overline{\mathbf{U}}$$

Heat flux

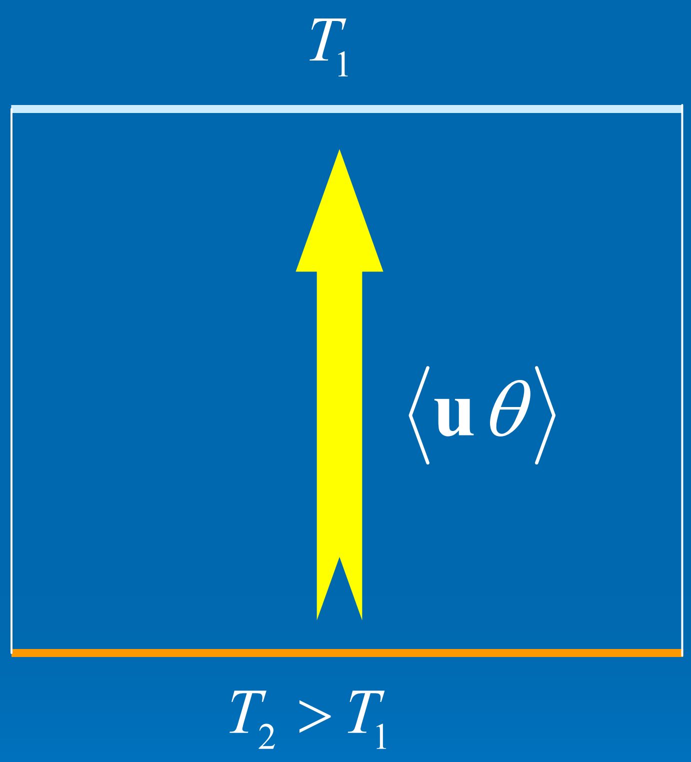

$$\langle \mathbf{u}\,\theta \rangle = -\kappa_T \vec{\nabla} T$$

$$\kappa_T \cong \frac{u_0\, l_0}{3}$$

Counter wind flux

$$\boxed{\mathbf{F}^* = -\kappa_T \vec{\nabla} \overline{\Theta} - \tau_0 \left(\mathbf{F}_{\parallel}^* \cdot \vec{\nabla} \right) \overline{\mathbf{U}}^{(0)}(z)}$$

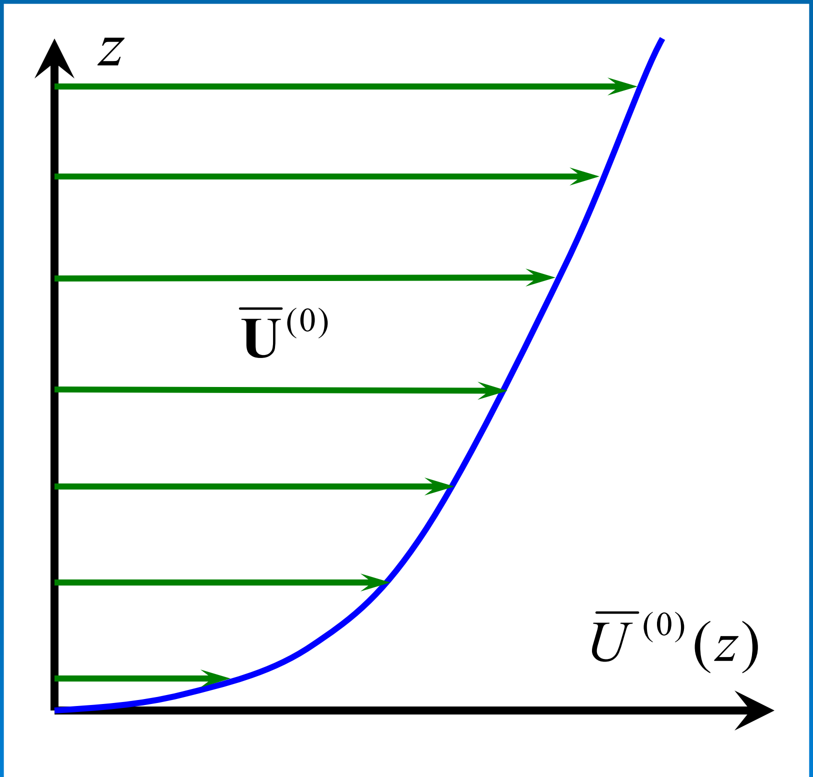

$$\frac{\partial \mathbf{u}}{\partial t} \propto -\left(\mathbf{u} \cdot \vec{\nabla} \right) \overline{\mathbf{U}}^{(0)} + \ldots$$

Tangling fluctuations

$$\delta \mathbf{u} \propto -\tau_0 \left(\mathbf{u} \cdot \vec{\nabla} \right) \overline{\mathbf{U}}^{(0)}$$

$$\boxed{\left\langle \theta \, \delta \mathbf{u} \right\rangle \propto -\tau_0 \left(\mathbf{F}_{\parallel}^* \cdot \nabla \right) \overline{\mathbf{U}}^{(0)}(z)}$$

$$\mathbf{F}_{\parallel}^* = \left\langle \theta \, \mathbf{u}_{\parallel} \right\rangle$$

Redistribution of a homogeneous vertical turbulent heat flux by a converging horizontal mean flow

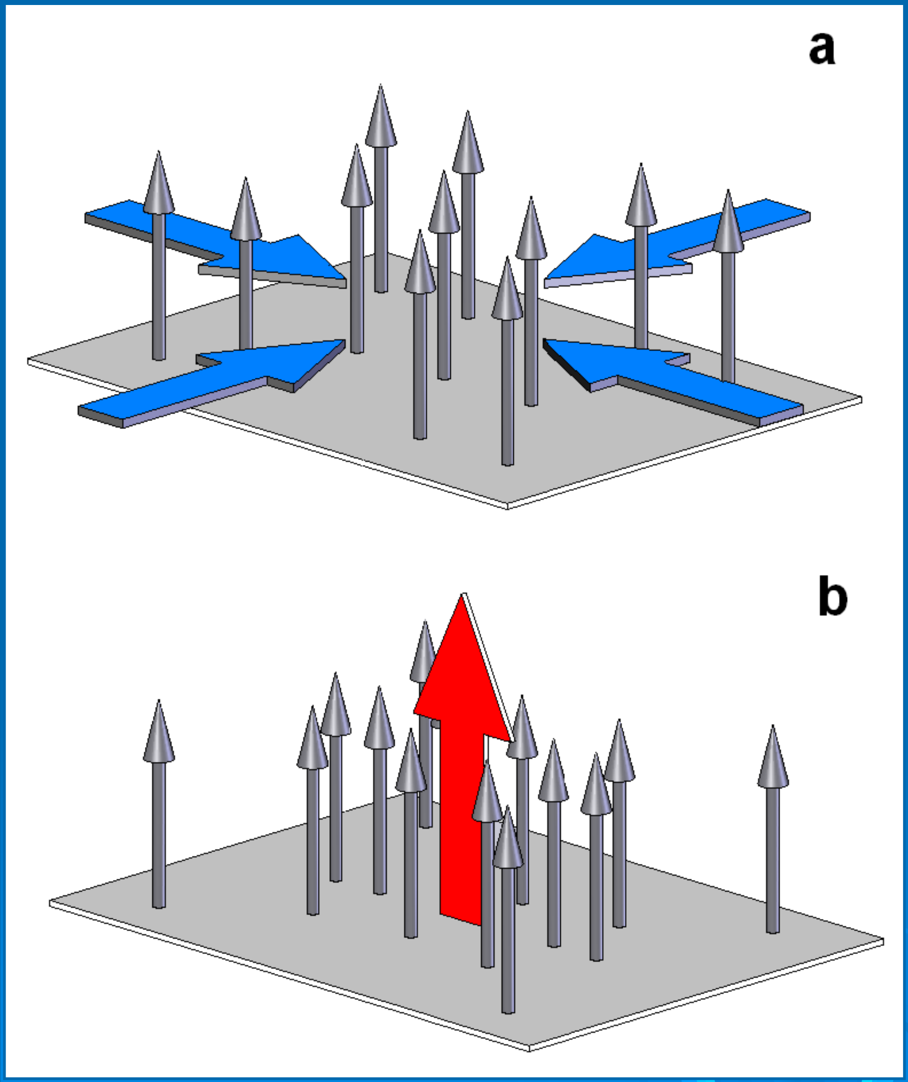

$$\boxed{\mathbf{F} \propto -\alpha\, \tau_0 \left(\vec{\nabla} \cdot \bar{\mathbf{U}}_{\perp} \right) \mathbf{F}_{\|}^{*}}$$

$$\mathbf{F}_{\|}^{*} = -\kappa_T\, \nabla \bar{\Theta}$$

α is the degree of thermal anisotropy,

The growth rate of convective wind instability

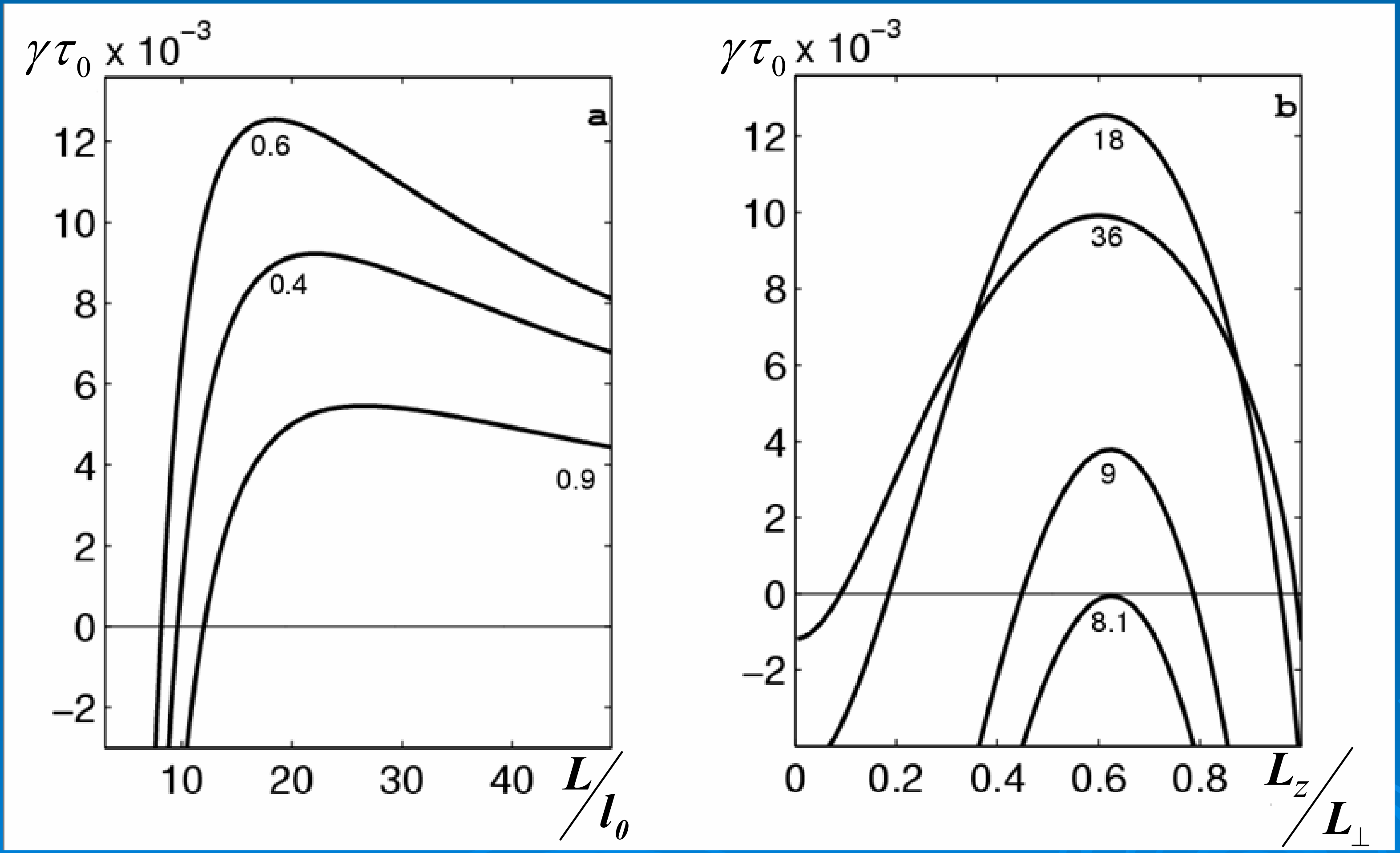

Convective-wind instability

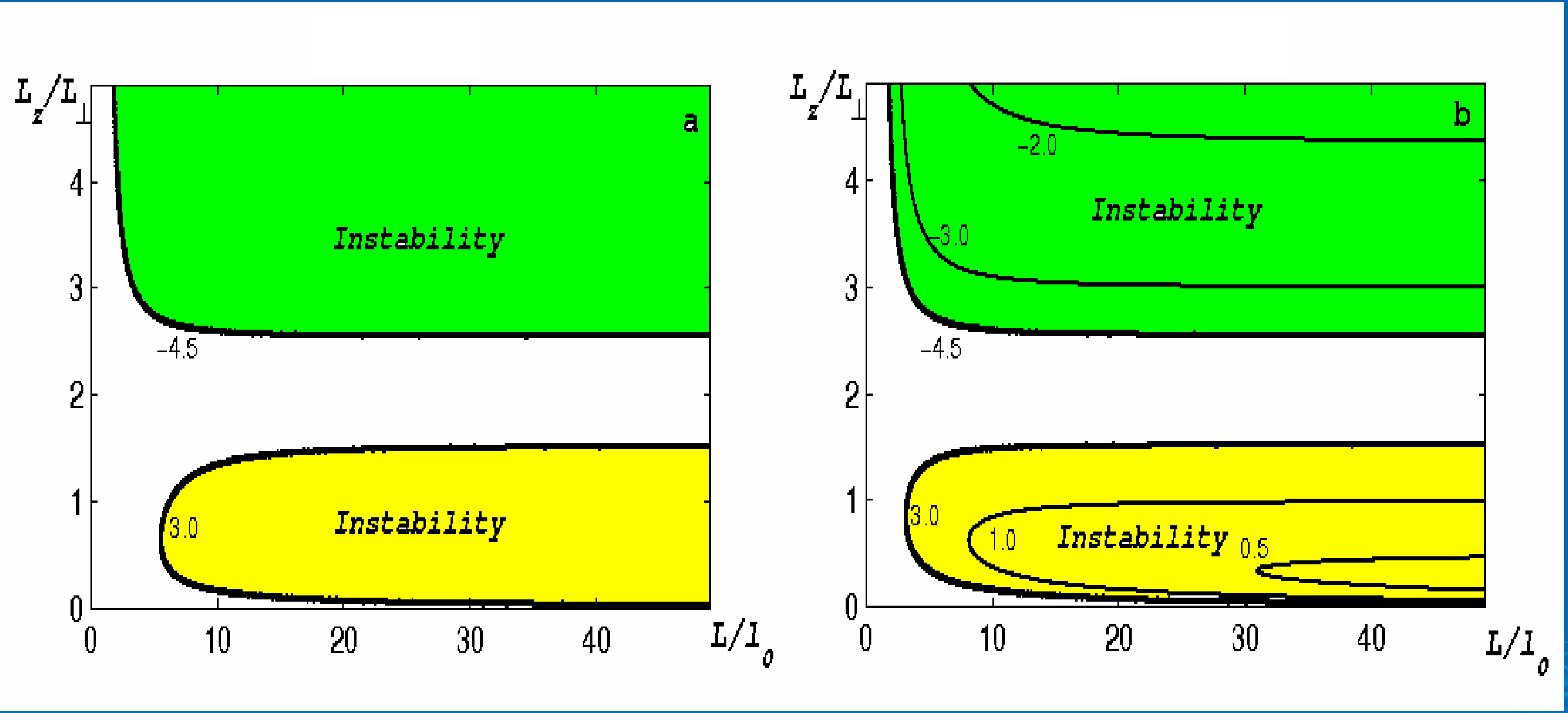

The range of parameters for which the convective-wind instability occurs for different anisotropy of turbulence.

Critical Reyleigh number

$$\left(\frac{\partial}{\partial t}-\Delta\right)\Delta V = Ra\Delta_{\perp}\Theta$$

$$\mathrm{Pr}_{\mathrm{T}}\frac{\partial\Theta}{\partial t}-\left(\Delta + b\nabla_z^2\right)\Theta = V + \mu\left(\frac{\mathrm{Pr}_{\mathrm{T}}}{Ra}\right)^{1/3}\left[10\Delta_{\perp}-5\Delta\right]V$$

$$\mu = \frac{4}{15}\left(\frac{6}{\zeta^2}\right)^{1/3}, \qquad \zeta = \frac{6gl_0}{u_0^2}\frac{\Delta\Theta}{T}, \qquad b = \frac{3(2+\gamma)}{2}$$

$$\mathrm{Pr}_{\mathrm{T}} = \frac{\nu_{\mathrm{T}}}{\kappa_{\mathrm{T}}}$$

Critical Rayleigh Number (free-free boundaries)

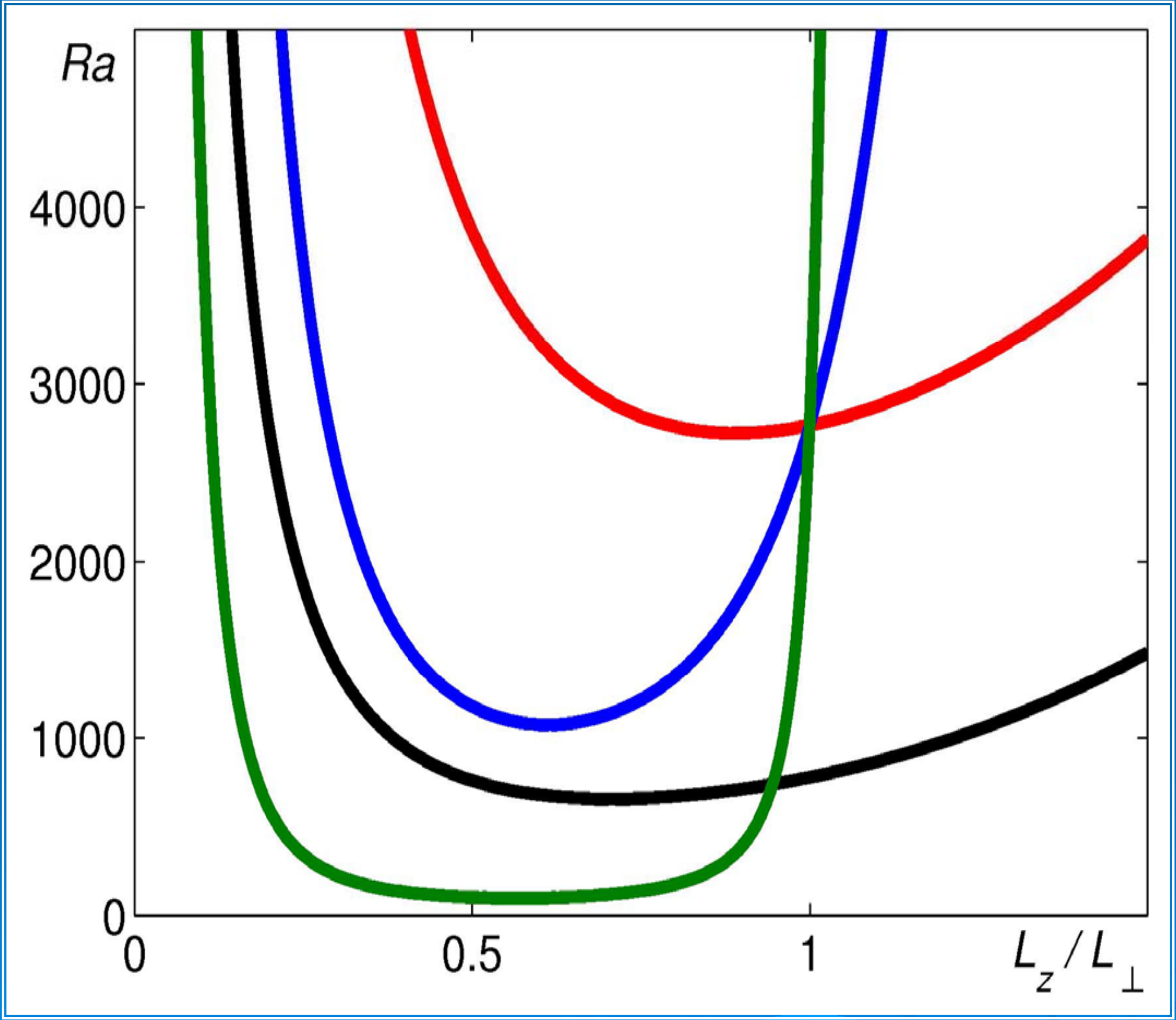

$Ra^{cr} = 657.5$

$\mu = 0$ $Ra^{cr} = 2722$

$\mu = 0.7$ $Ra^{cr} = 1076$

$\mu = 5$ $Ra^{cr} = 98$

$$\mu = 0.15\left(\frac{\gamma T_0}{\Delta T}\frac{u_0^2}{g l_0}\right)^{2/3}$$

Critical Rayleigh Number
(rigid-rigid boundaries)

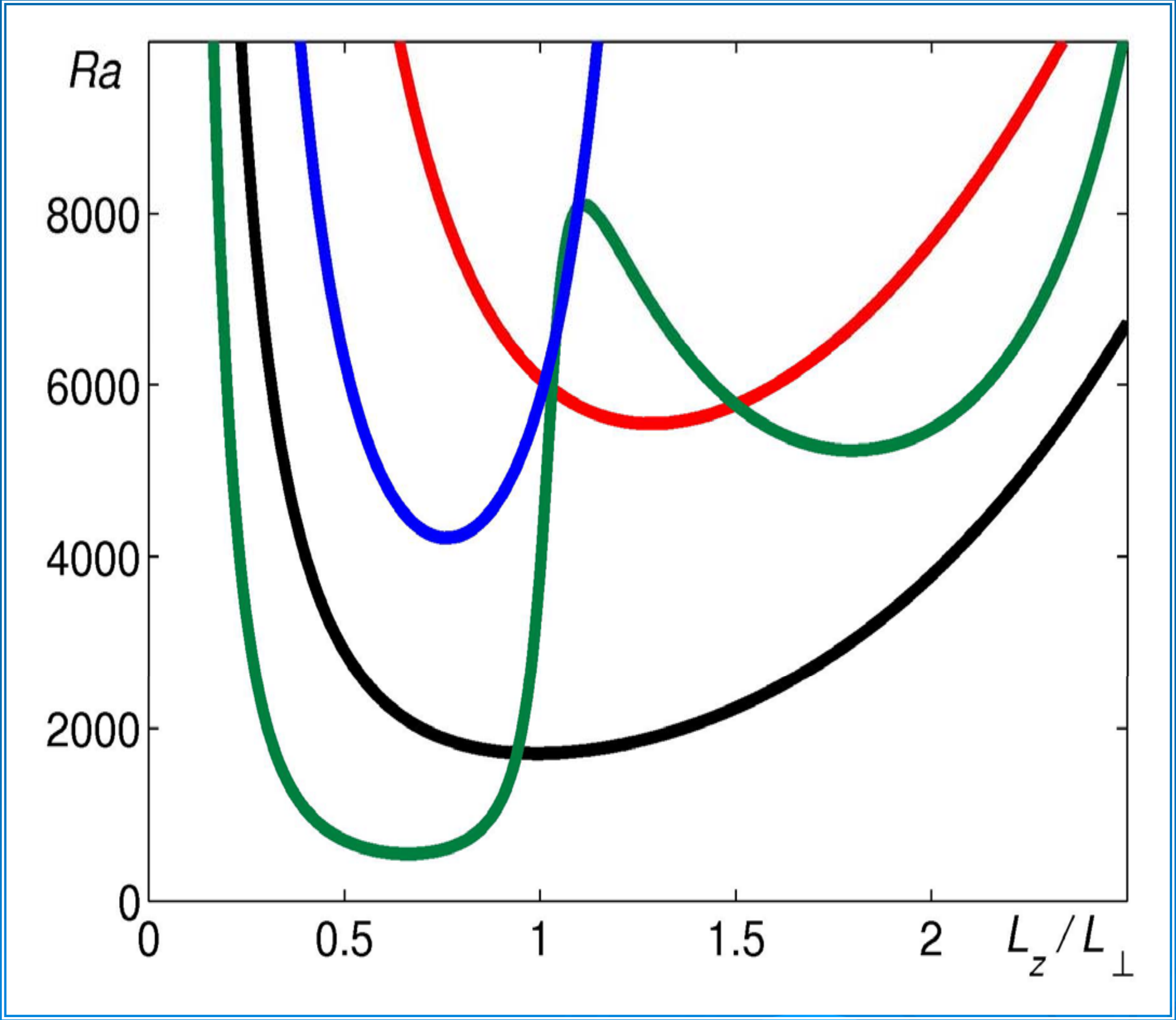

$Ra^{cr} = 1708$

$\mu = 0$ $Ra^{cr} = 5547$

$\mu = 0.7$ $Ra^{cr} = 4218$

$\mu = 5$ $Ra^{cr} = 549$

$$\mu = 0.15\left(\frac{\gamma T_0}{\Delta T}\frac{u_0^2}{g l_0}\right)^{2/3}$$

Cloud cells

	Observations	Theory
$L_z / L_\perp$	$0.05 \div 1$	$0 \div 1$
L / l_0	$5 \div 20$	$5 \div 15$
$T_{lifetime}$	Several hours	$\gamma^{-1} = (25 \div 100)\tau_0$ $= 1 \div 3\,h$

Mechanism of convective-shear instability

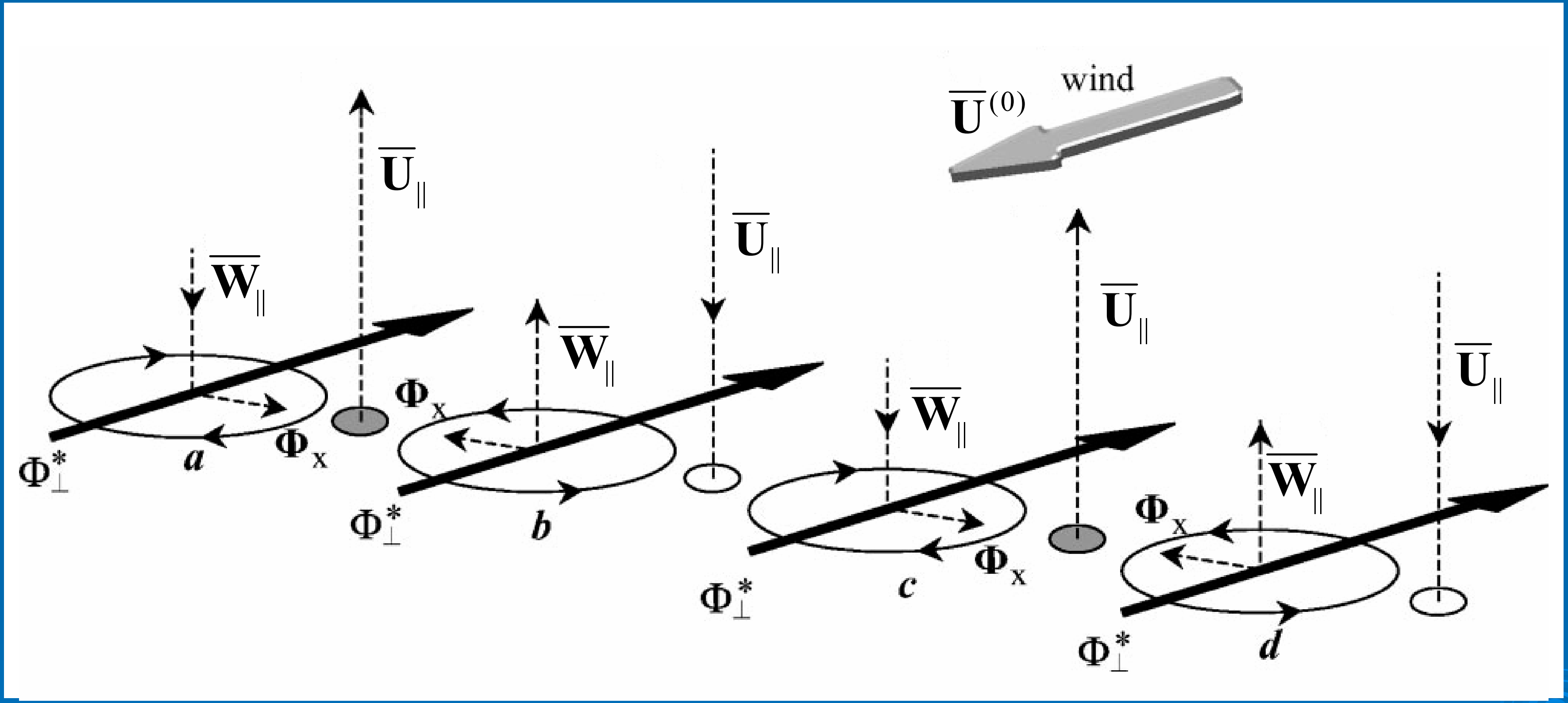

$$\mathbf{F} \propto \tau_0 \left(\bar{\mathbf{W}}_{\|} \times \mathbf{F}^{*} \right)$$

Convective-shear instability

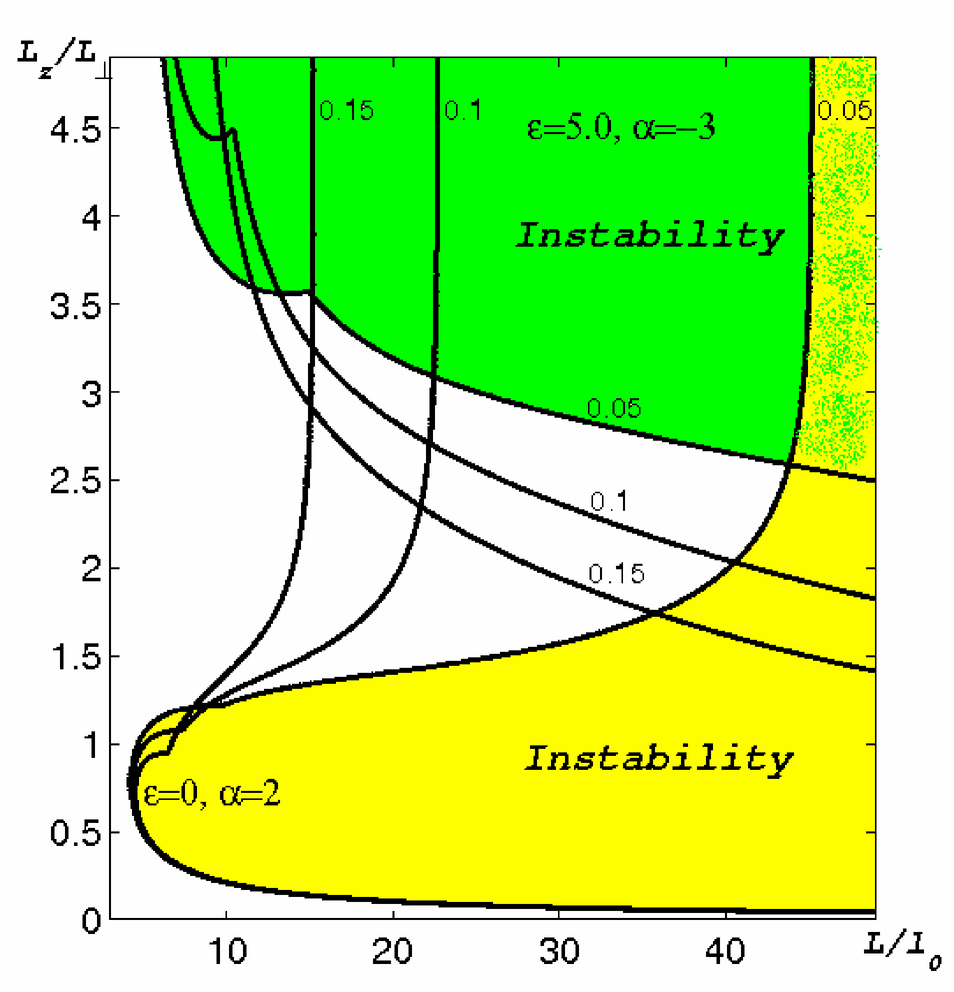

The range of parameters for which the convective-shear instability occurs for different values of shear and anisotropy.

Convective-shear waves

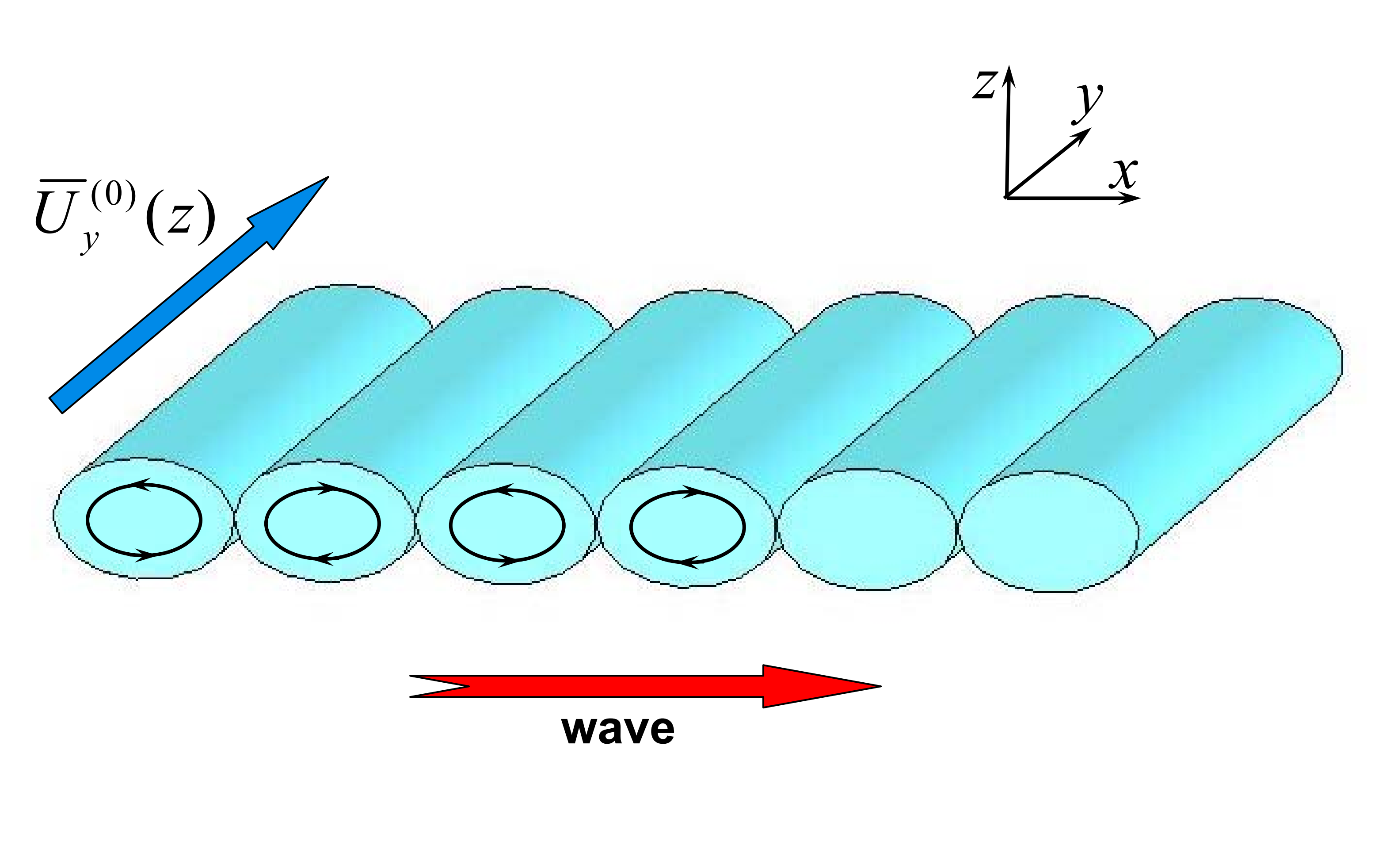

$$\overline{W}_z \propto \cos(\omega t - K x)$$

$$\overline{U}_z \propto \cos\left(\omega t - K x - \frac{\pi}{6}\right) \qquad \overline{\Theta} \propto \cos\left(\omega t - K x + \frac{\pi}{6}\right)$$

Cloud "streets"

	Observations	Theory
$L_z / L_\perp$	$0.14 \div 1$	$0 \div 1$
L / l_0	$10 \div 100$	$10 \div 100$
$T_{lifetime}$	$1 \div 72\ h$	$\gamma^{-1} = (25 \div 100)\tau_0$ $= 1 \div 3\,h$

Experimental set – up

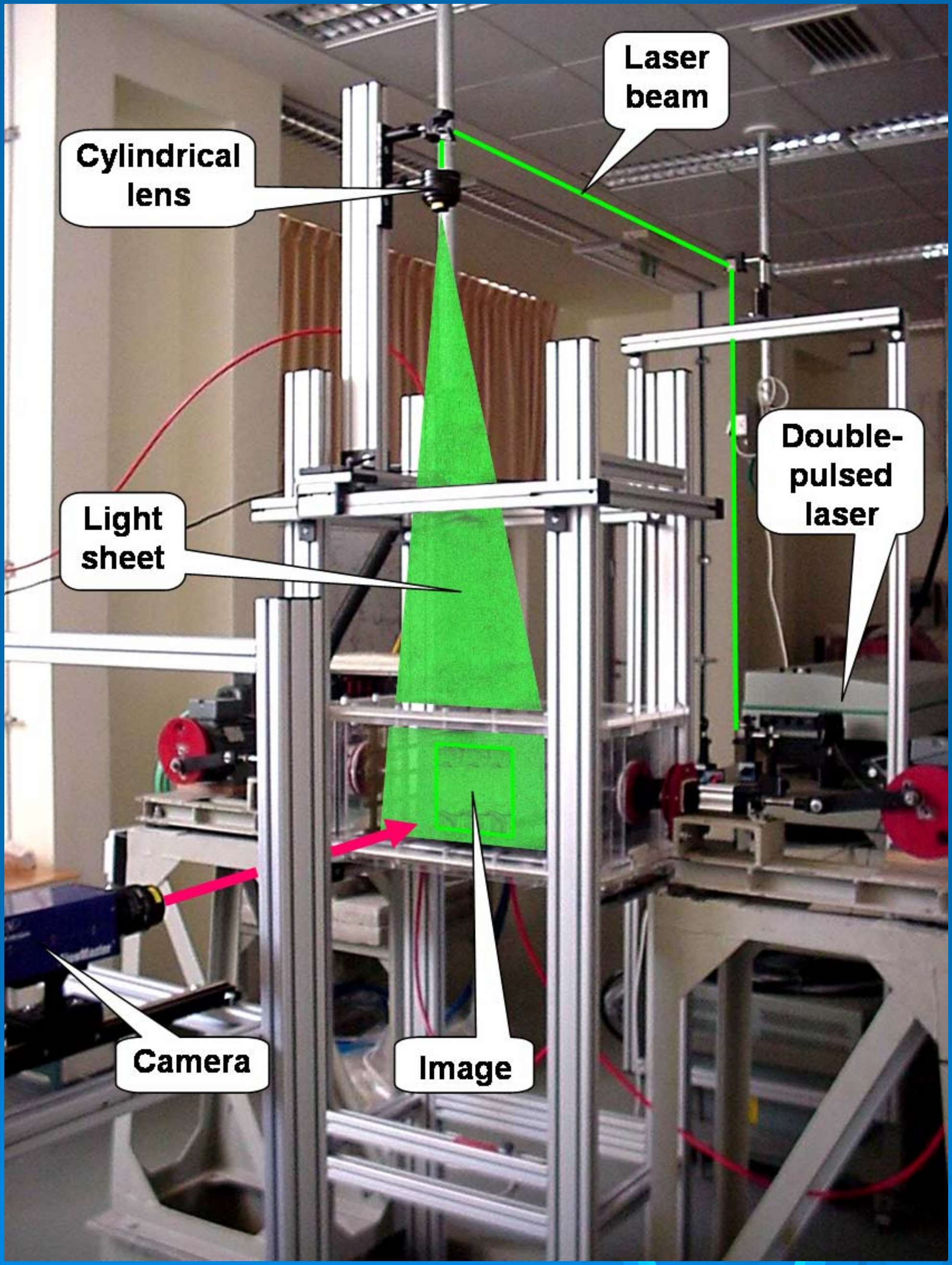

Experimental set-up

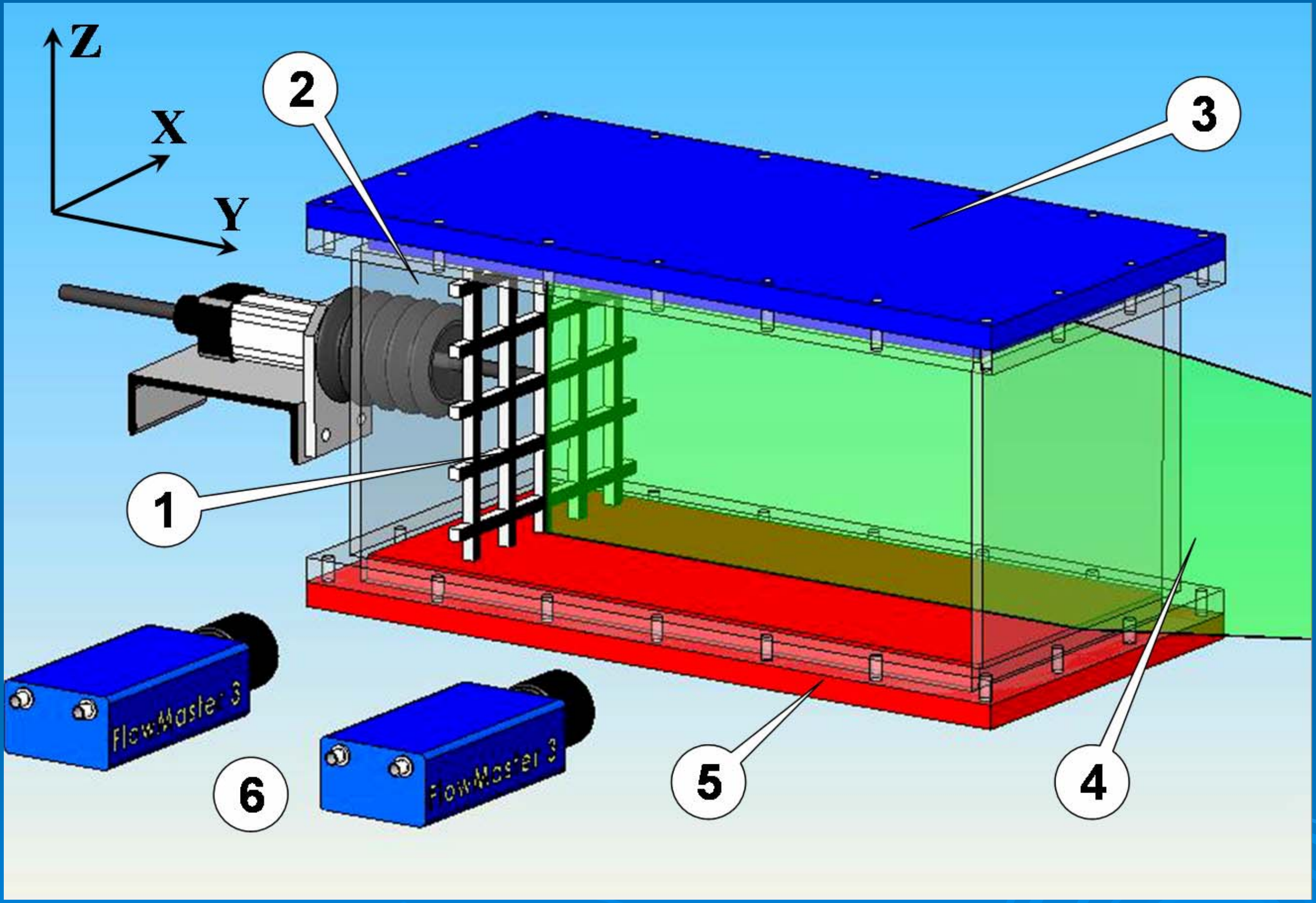

Laboratory Turbulent Convection

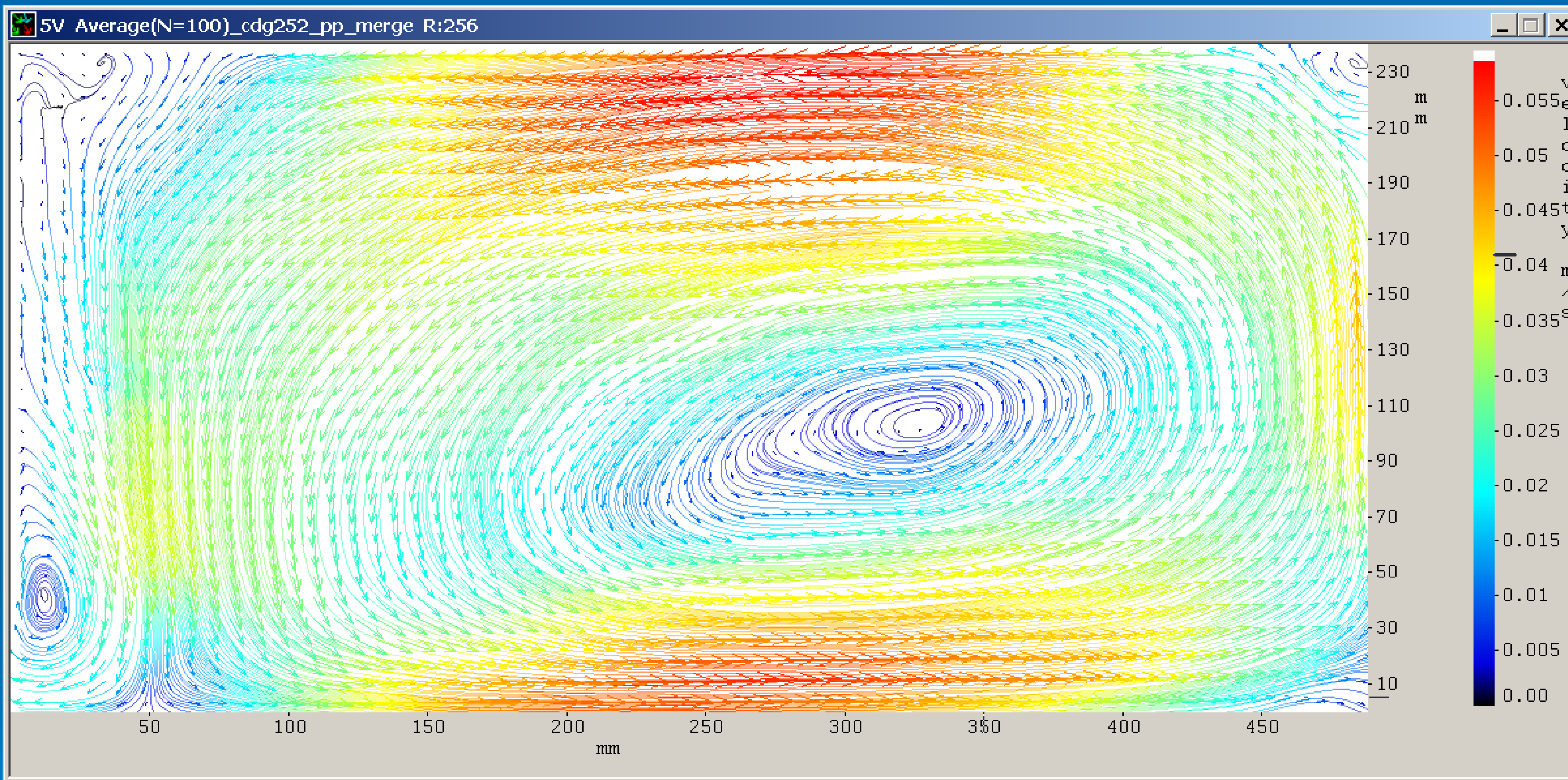

Before averaging

After averaging

Experimental Parameters

- The r.m.s. vertical velocity $\sqrt{\langle u_z^2 \rangle} = 6 \div 10 \, \text{cm}/\text{s}$
- The integral scale $l_z = 2 \div 4 \, \text{cm}$
- The mean velocity of SO structure $\overline{U}_z = 15 \div 20 \, \text{cm}/\text{s}$
- Rayleigh number $Ra = \dfrac{g\,\beta\,\Delta T\, L^3}{\nu\ \kappa} \approx (0.1 - 1.6) \times 10^8$

  $(\Delta T = 80\,^\circ K, \quad L = 30\, cm\ )$
- The effective Rayleigh number $Ra^{eff} = \dfrac{g\,\beta\,\Delta T\, L_T^3}{\nu_T\ \kappa_T} \approx 100 \div 625$

  $(\Delta T = 3 \div 5\,\text{K}, \quad L_T = 20\,\text{cm}\ )$
- The critical Rayleigh number $Ra^{\text{cr}} \approx 2250$
- The counter-wind flux $\Phi^c / \Phi_z = -(0.5 \div 0.67)$

Unforced Convection: A = 1

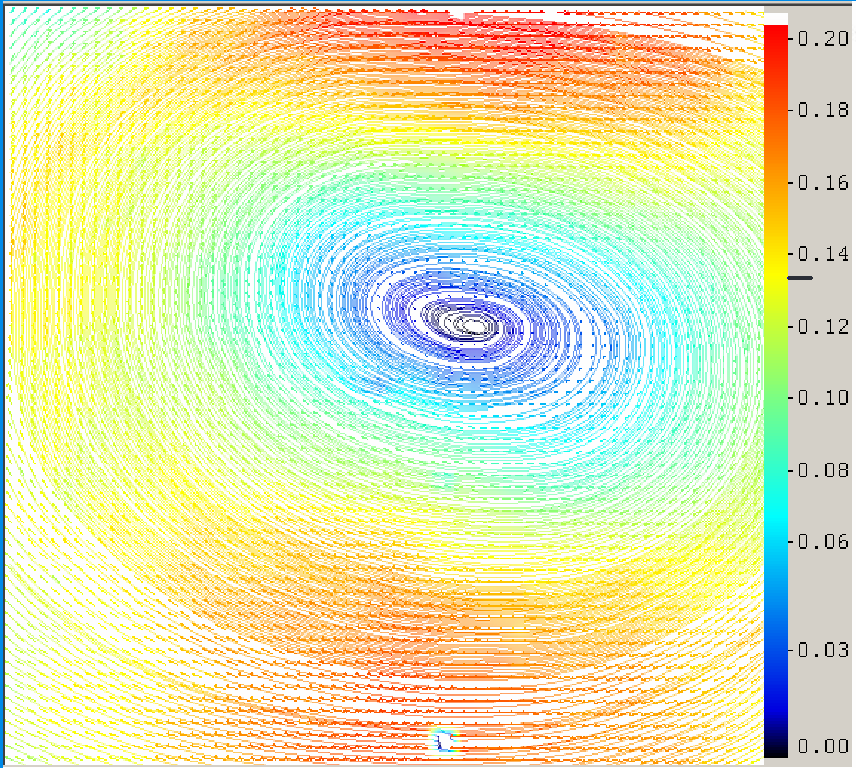

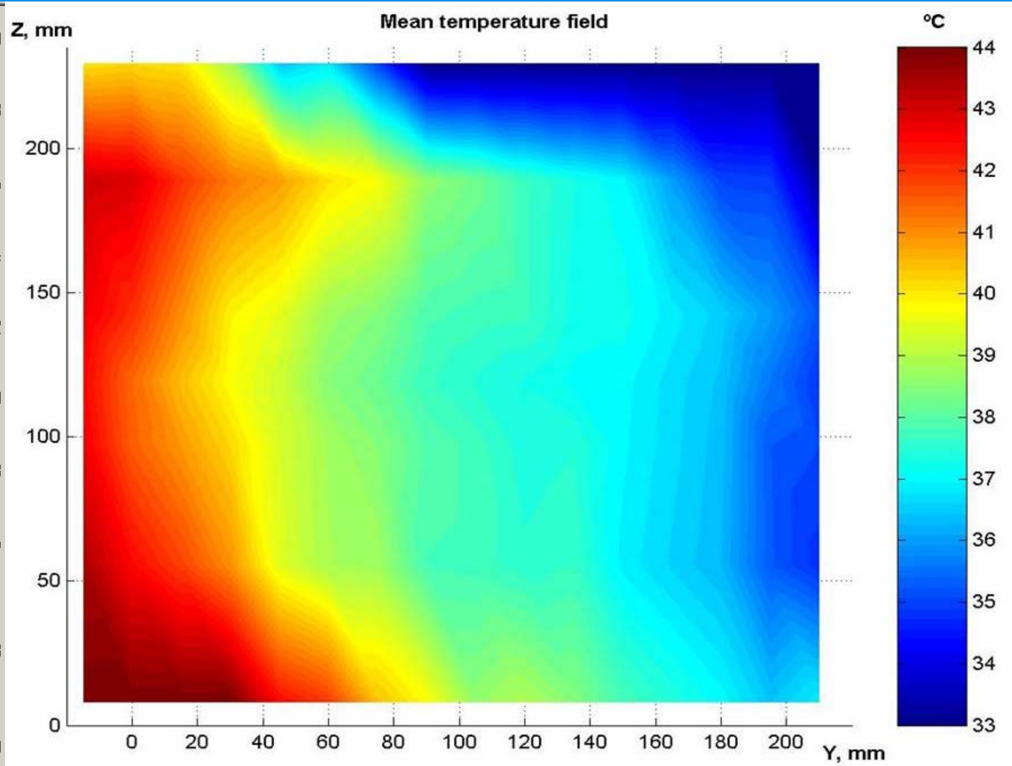

$\overline{U}(y,z)$ $\overline{T}(y,z)$

Experimental set–up for temperature measurements

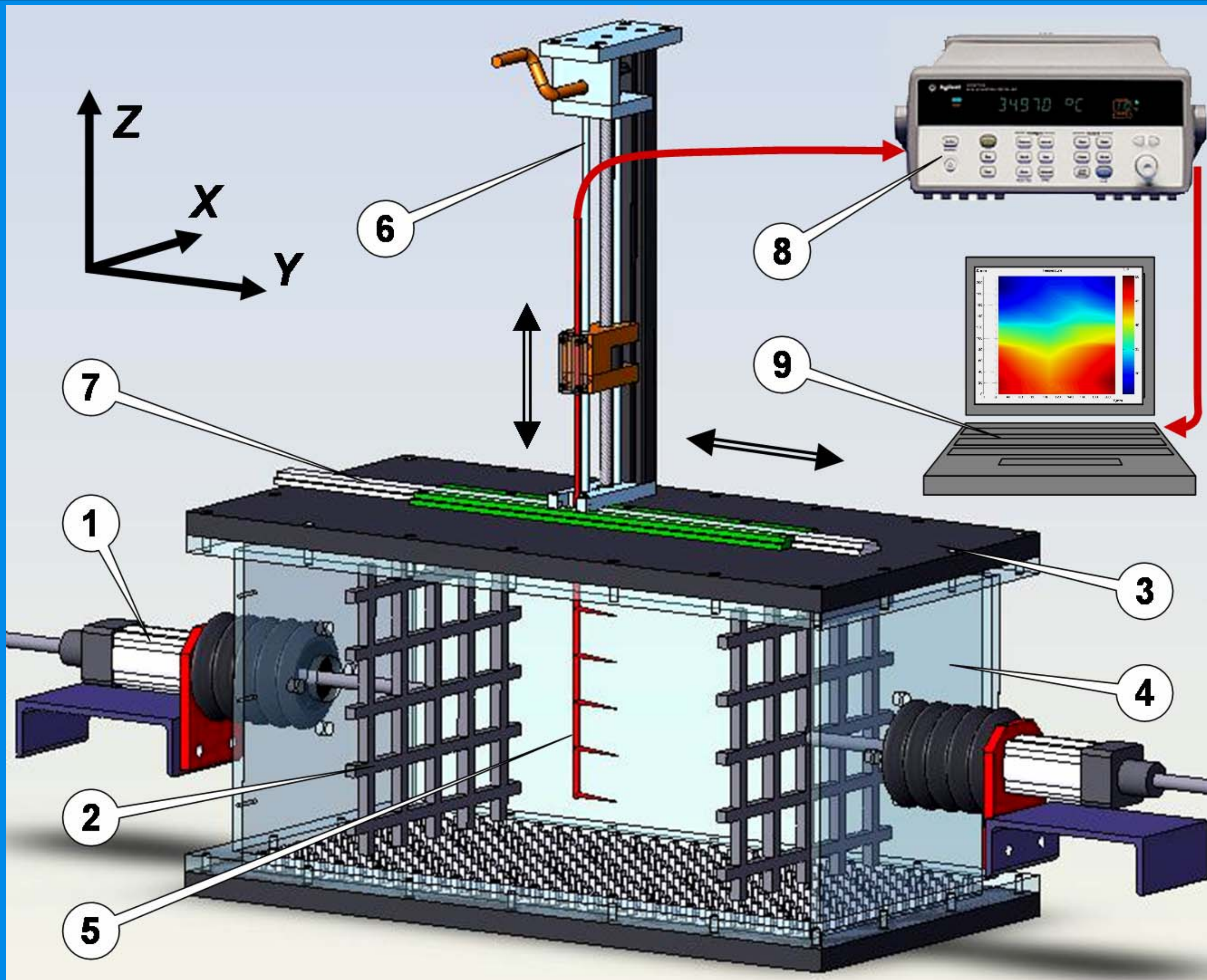

Temperature profiles

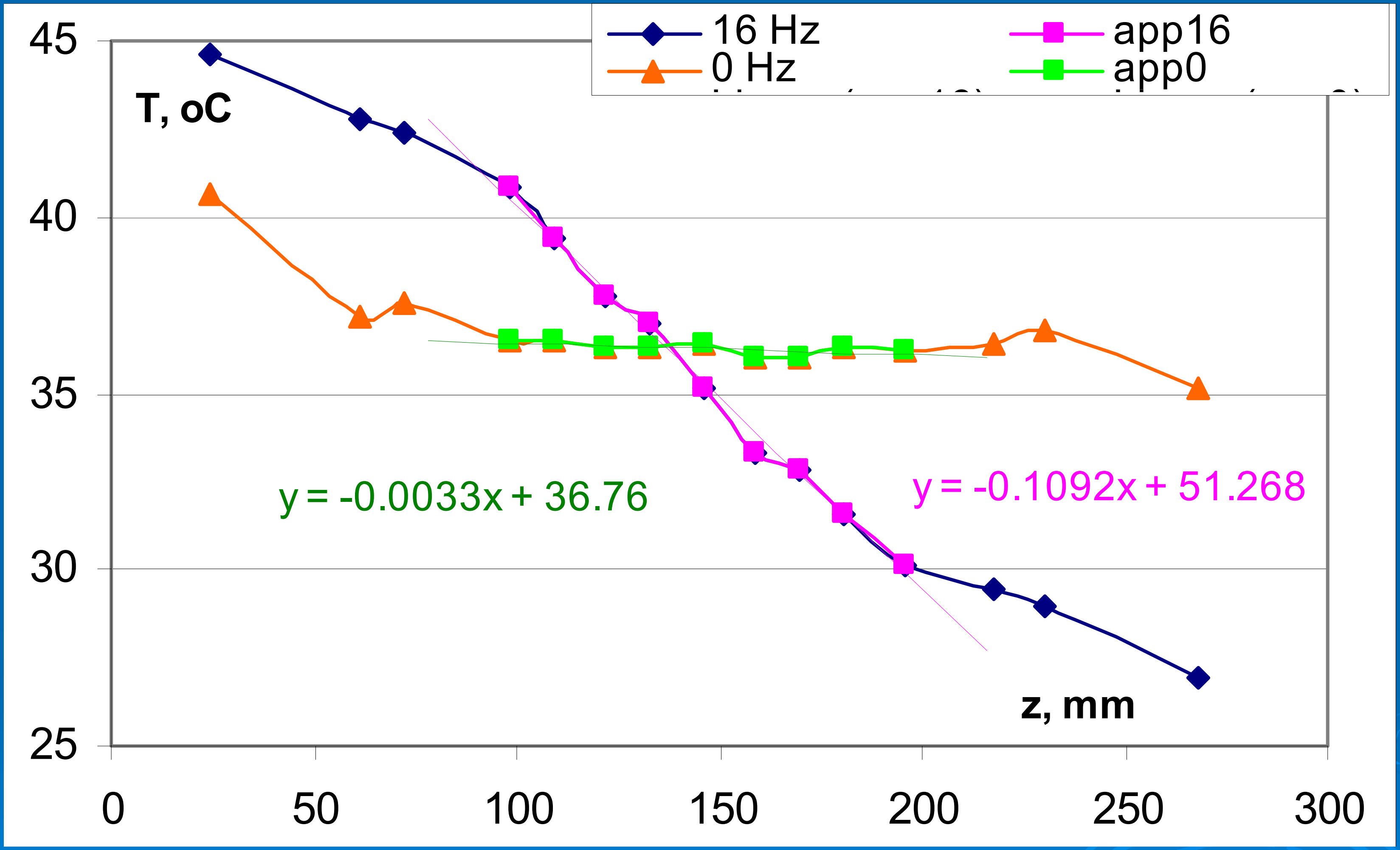

- ▲ **Pure convection**
- ◆ **Convection and oscillating grids forcing**

Unforced Convection: A=2

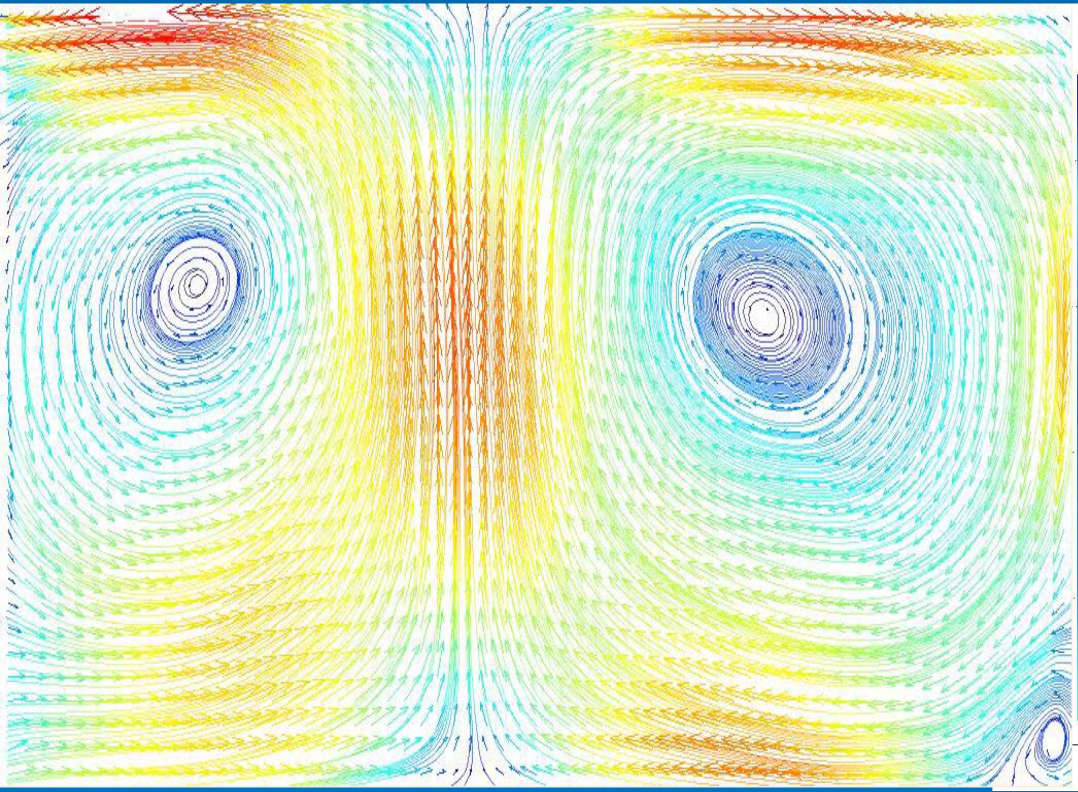

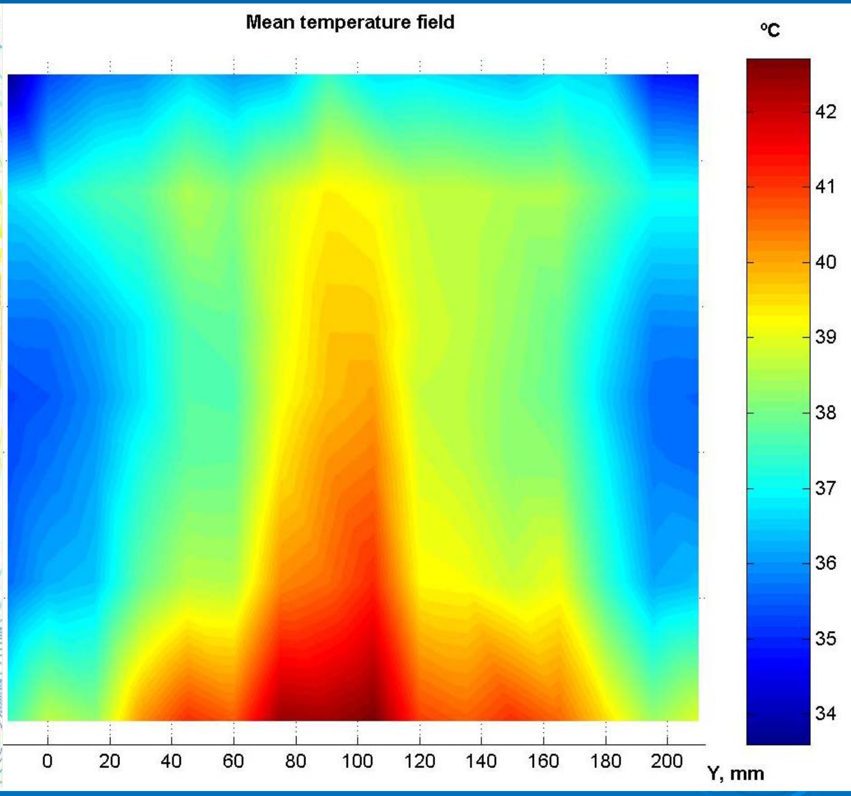

$\overline{U}(y,z)$

$\overline{T}(y,z)$

References

- **Elperin T**., **Kleeorin N**., **Rogachevskii I**., and **Zilitinkevich S**., Formation of large-scale semi-organized structures in turbulent convection, *Phys. Rev. E* **66**, 066305 (1—15), (2002).

- **Elperin T**., **Kleeorin N**., **Rogachevskii I**., and **Zilitinkevich S**., Tangling turbulence and semi-organized structures in convective boundary layers, *Boundary-Layer Meteorol*., **119,** 449-472 (2006).

- **Eidelman A**., **Elperin T**., **Kleeorin N**., **Markovich A**., and **Rogachevskii I**., Hysteresis phenomenon in turbulent convection, *Experiments in Fluids,* **40,** 723-732 (2006).

- **Elperin T**., **Golubev I**., **Kleeorin N**., and **Rogachevskii I**., Large-scale instabilities in turbulent convection, *Phys. Fluids,* ***18****, 126601 (1—11)*, (2006).

Conclusions

- A theory of formation of large-scale coherent structures in a turbulent convection is developed.

- In a shear-free turbulent convection this study predicts an instability which causes formation of large-scale coherent fluid motions in the form of cells (cloud cells).

- The theory predicts also the convective-shear instability in a sheared turbulent convection which results in appearance of large-scale coherent convective rolls (cloud "streets").
  - This instability can cause also a generation of convective-shear waves which have a nonzero hydrodynamic helicity.
  - The increase of shear promotes excitation of the convective-shear instability.

Conclusions

- It is demonstrated that the heat flux (which is modified by gradients of large-scale motions) plays a crucial role in these phenomena.

- Predictions of this theory are in a good agreement with the observed coherent structures.

- Experimental study of the large-scale circulations by Particles Image Velocimetry in a closed box with an imposed mean temperature gradient is performed.

- A hysteresis phenomenon in turbulent convection was found experimentally by changing of the temperature difference in the box. The developed theory explains the observed phenomenon.

THE END

Formation of a horizontal component of a mean heat flux

$$\mathbf{\Phi} \propto \tau_0 \left(\alpha + \frac{3}{2} \right) \left(\overline{\mathbf{W}} \times \mathbf{\Phi}_{\parallel}^{*} \right)$$

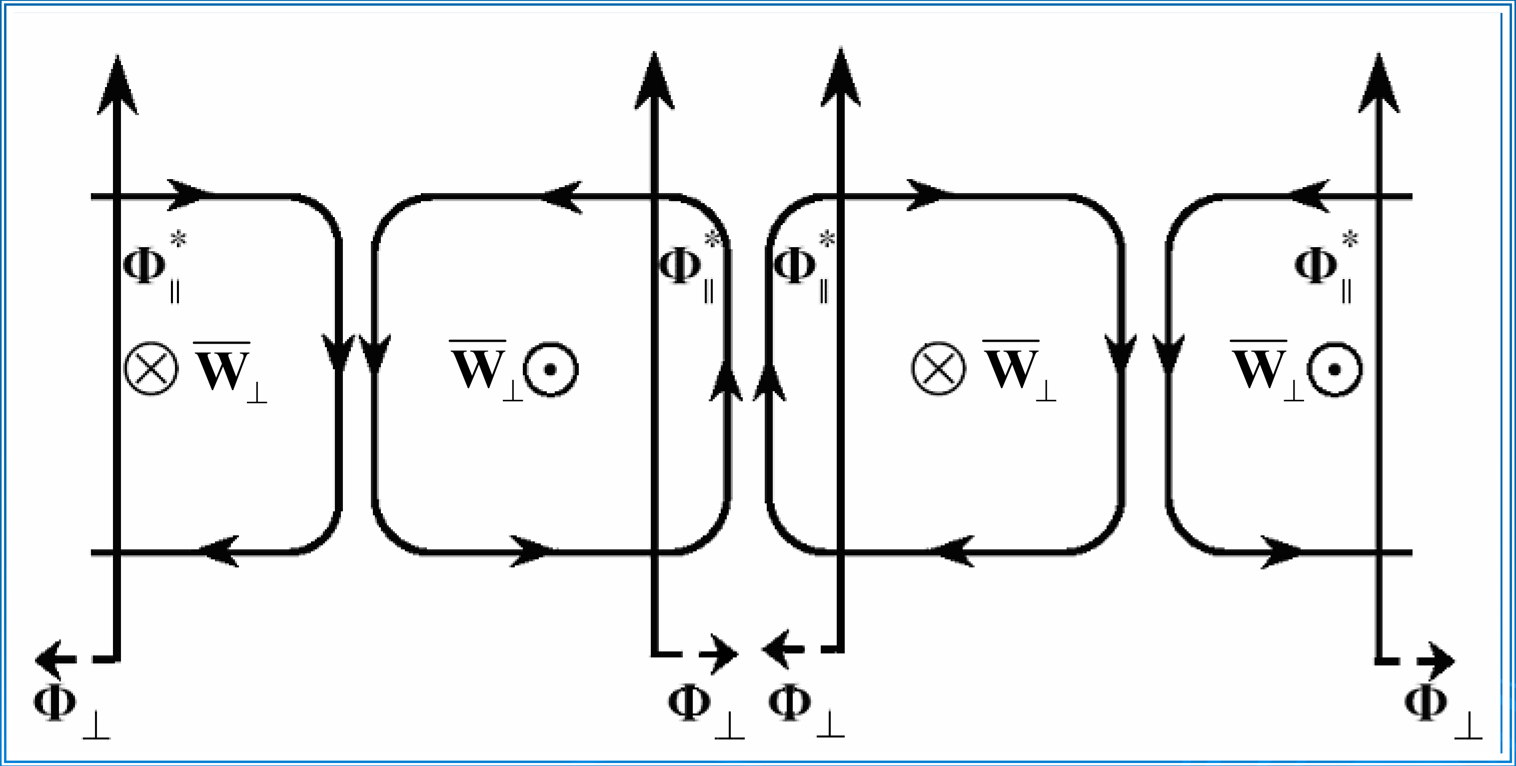

$\alpha < -\frac{3}{2}$ (column-like thermal structures)

Hysteresis in Turbulent Convection

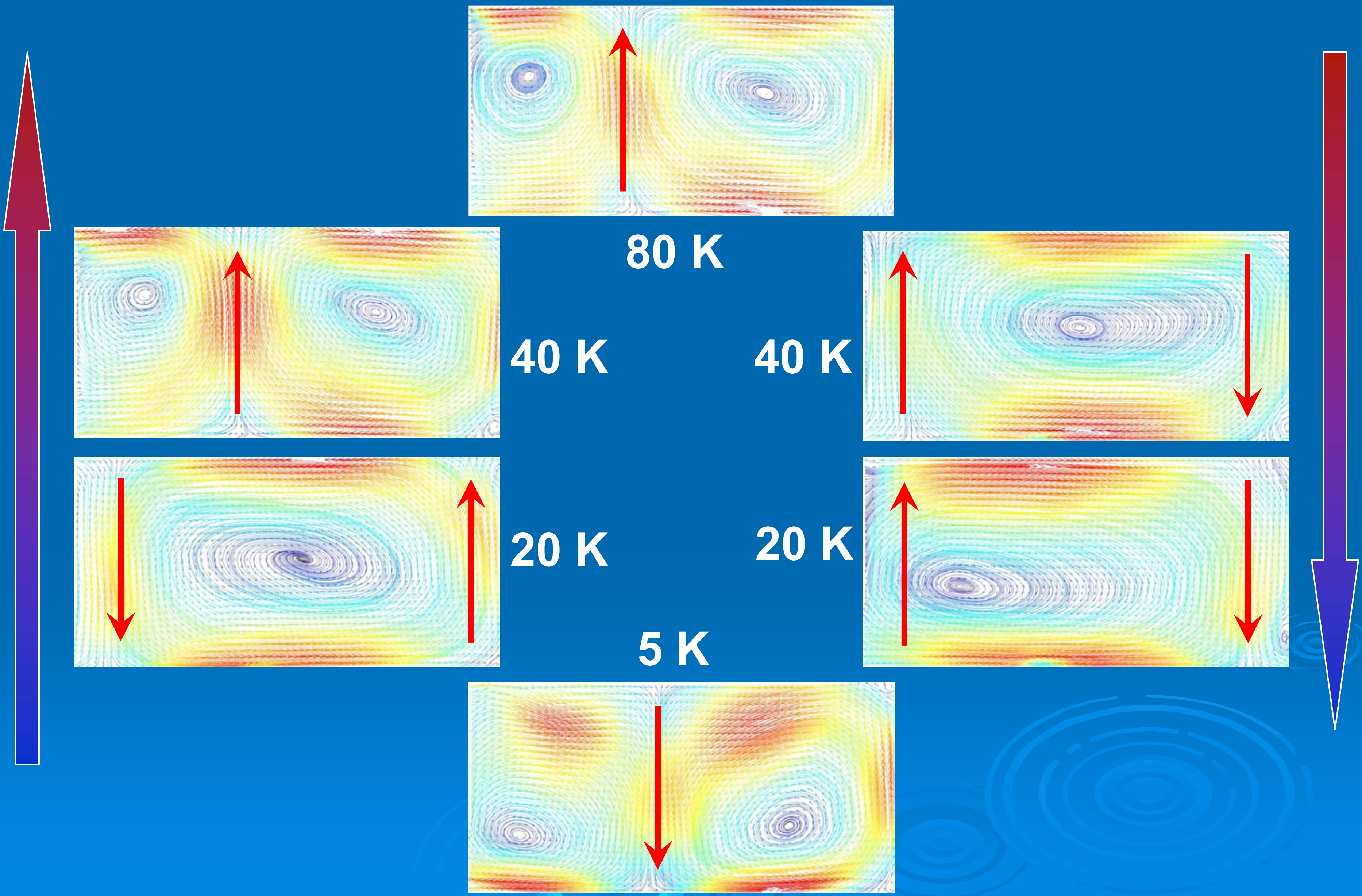

Hysteresis in Turbulent Convection

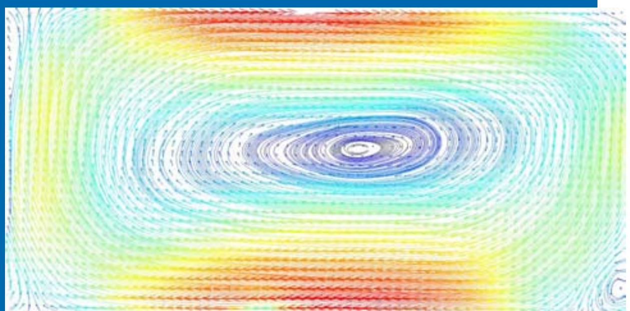

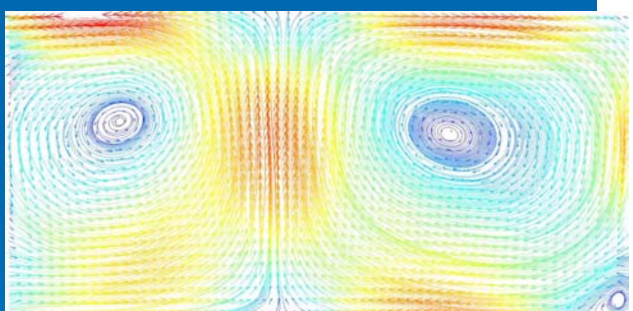

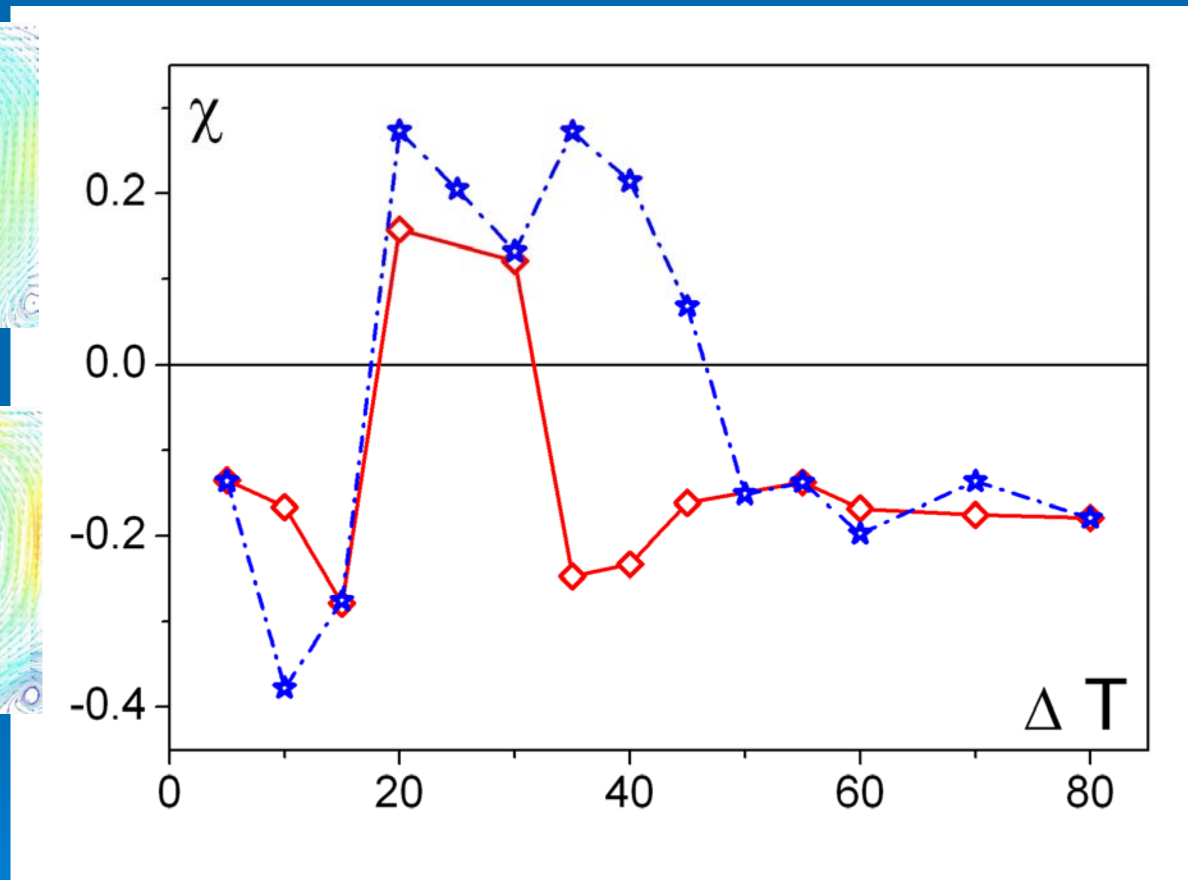

$$\chi = \frac{4}{3}\left(\frac{\langle u_y^2 \rangle}{\langle u_z^2 \rangle} - 1\right)$$

$\Delta T_{increase}$ (red)

$\Delta T_{decrease}$ $(blue)$

Growth rate of large-scale instability versus the degree of anisotropy for one-cell (red) and two-cell (blue) flow patterns

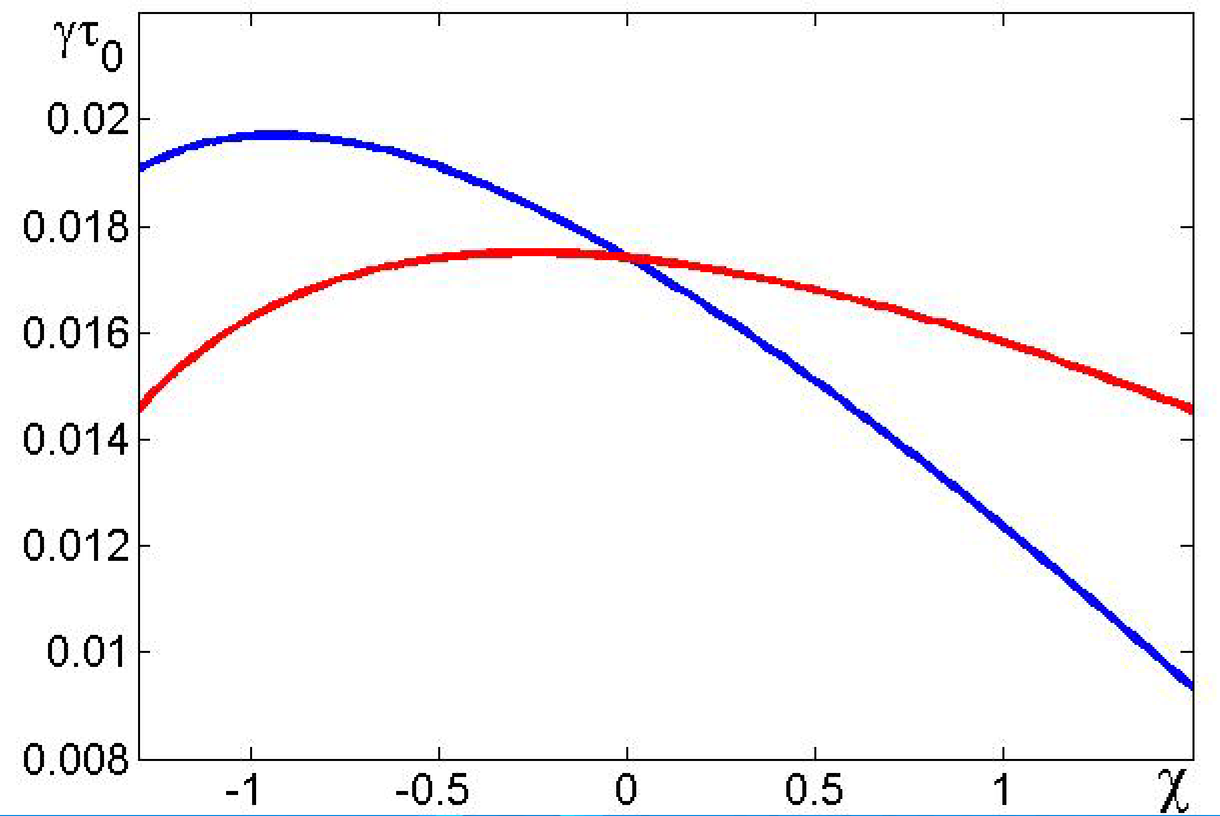

Mean field equations

$$\left(\frac{\partial}{\partial t}+\overline{\mathbf{U}}\cdot\vec{\nabla}\right)\overline{U}_i=-\nabla_i\left(\frac{\overline{P}}{\rho_0}\right)-\nabla_j\left\langle u_i u_j\right\rangle-g_i\overline{\Theta}+\nu\Delta\overline{\mathbf{U}},$$

$$\left(\frac{\partial}{\partial t}+\overline{\mathbf{U}}\cdot\vec{\nabla}\right)\overline{\Theta}=-\nabla_i\left\langle\theta\, u_i\right\rangle+\kappa\Delta\overline{\Theta}$$

$\mathbf{\Phi}\equiv\left\langle\theta\,\mathbf{u}\right\rangle$ is the heat flux

$\left\langle u_i u_j\right\rangle$ are the Reynolds stresses

Heat flux

Traditional parameterization

$$\left\langle \theta\, \mathbf{u} \right\rangle = -\kappa_T \vec{\nabla}\, \overline{\Theta}$$

Modification of the heat flux by tangling turbulence

$$\boxed{\left\langle \theta\, \mathbf{u} \right\rangle = \mathbf{\Phi}^* + \frac{\tau_0}{6}\left[-5\alpha\left(\vec{\nabla}\cdot\overline{\mathbf{U}}_\perp\right)\mathbf{\Phi}_\parallel^* + \left(\alpha + \frac{3}{2}\right)\left(\overline{\mathbf{W}}\times\mathbf{\Phi}_\parallel^*\right) + 3\left(\overline{\mathbf{W}}_\parallel\times\mathbf{\Phi}^*\right)\right]}$$

$$\mathbf{\Phi}^* = -\kappa_T \vec{\nabla}\,\overline{\Theta} - \tau_0\left(\Phi_\parallel^*\cdot\nabla\right)\overline{\mathbf{U}}^{(0)}(z)$$

$$\overline{\mathbf{W}} = \vec{\nabla}\times\overline{\mathbf{U}}$$

Problems

- The Rayleigh numbers based on the molecular transport coefficients are very large:

$$\boxed{Ra = \frac{g\,\beta\,\Delta T\,L^3}{\nu\;\;\kappa} \approx 10^{11} \div 10^{13}}$$

This corresponds to fully developed turbulent convection in atmospheric and laboratory flows.

- The effective Rayleigh numbers based on the turbulent transport coefficients (the turbulent viscosity and turbulent diffusivity) are not high.

$$\boxed{Ra^{eff} = \frac{g\,\beta\,\Delta T\,L^3}{\nu_T\;\;\kappa_T}}$$

They are less than the critical Rayleigh numbers required for the excitation of large-scale convection.

Hence the emergence of large-scale convective flows (which are observed in the atmospheric and laboratory flows) seems puzzling.

Anisotropy of velocity field

$$\boxed{\chi = \frac{2}{3}\left(\frac{\langle u_{\perp}^{2}\rangle}{\langle u_{z}^{2}\rangle} - 2\right)}$$

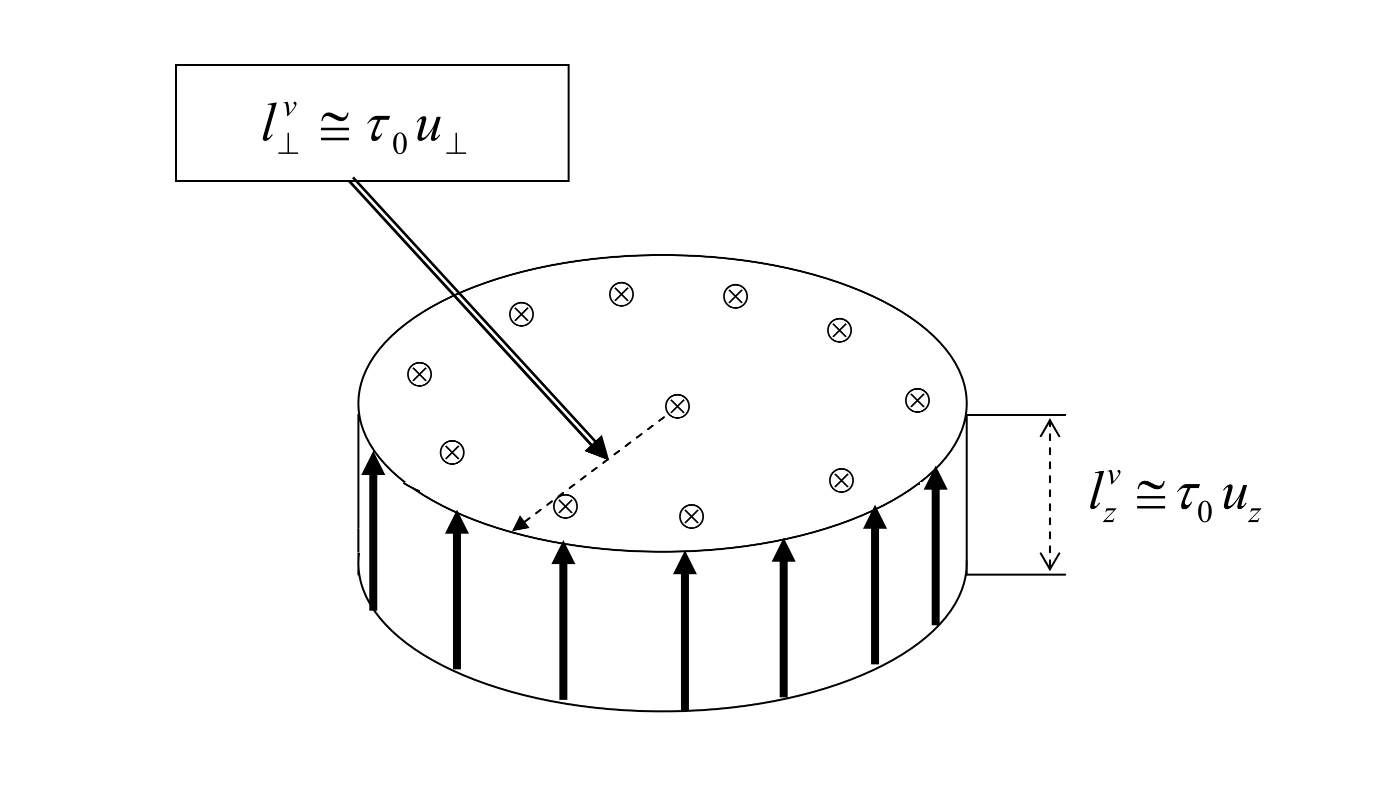

Thermal anisotropy

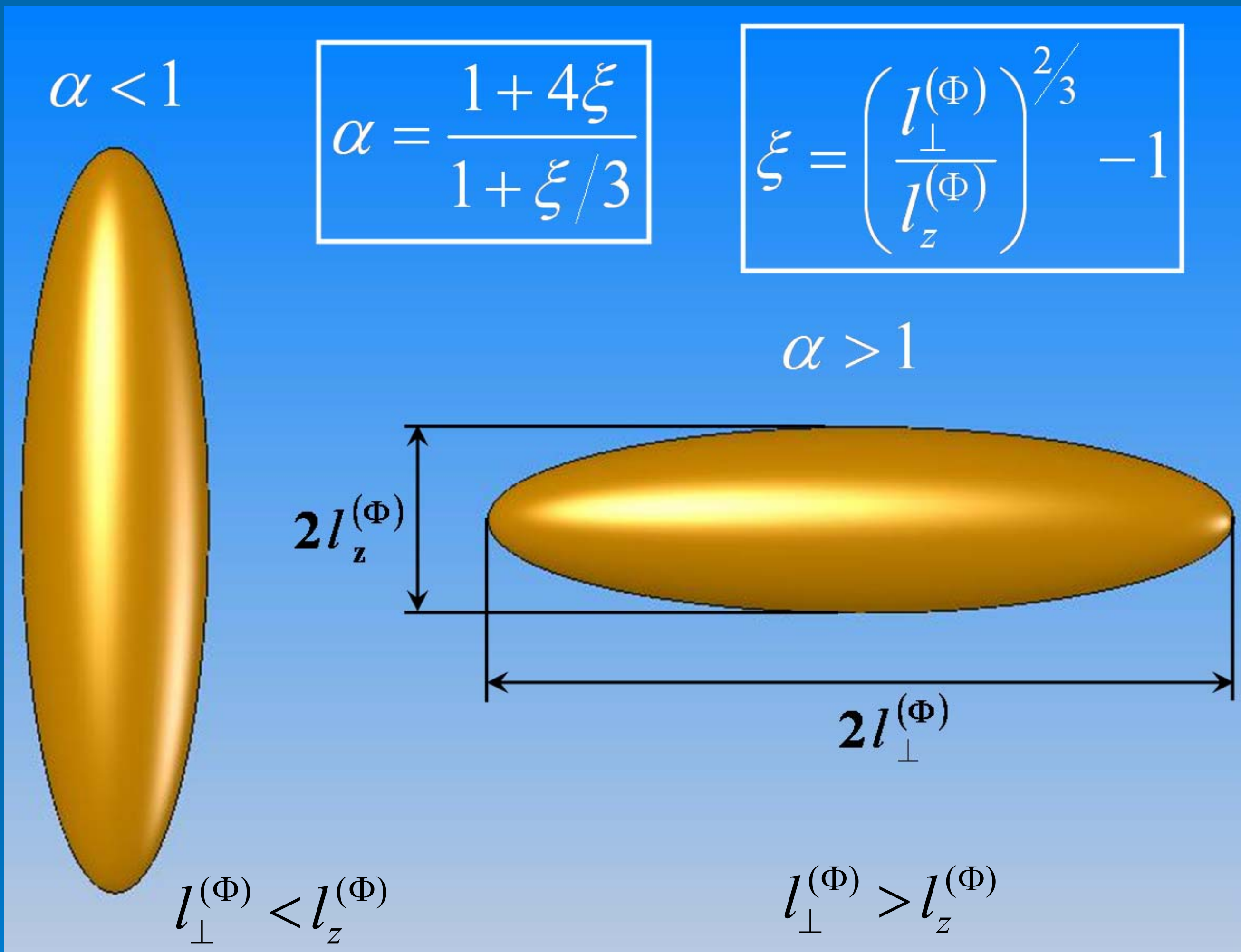

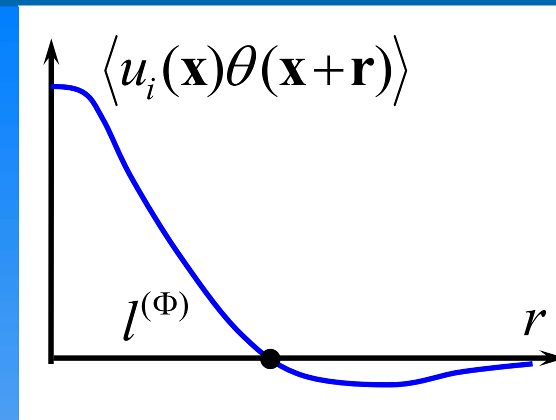

“Column”-like thermal structure

“Pancake”-like thermal structure

Laboratory Turbulent Convection

- R. Krishnamurti and L.N. Howard, *Proc. Natl.Acad. Sci. USA* **78,** 1981 (1981).
- M. Sano, X.Z. Wu and A. Libchaber, *Phys. Rev. A* **40**, 6421 (1989).
- S. Ciliberto, S. Cioni and C. Laroche, *Phys. Rev. E* **54**, R5901 (1996).
- S. Ashkenazi and V. Steinberg, *Phys. Rev. Lett.* **83**, 3641 (1999).
- J.J. Niemela, L. Skrbek, K.R. Sreenivasan and R.J. Donnelly, *J. Fluid Mech.* **449**, 169 (2001).

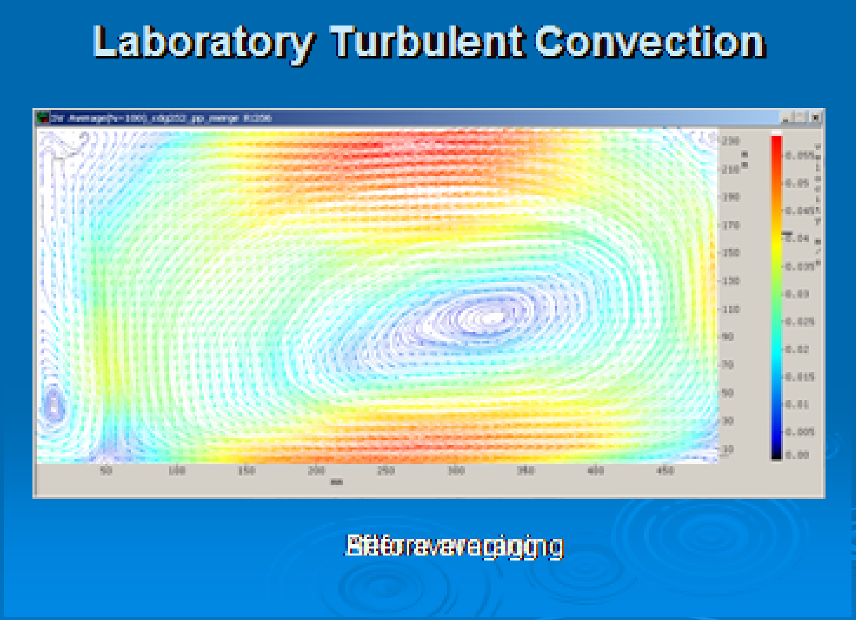

Critical Rayleigh Number

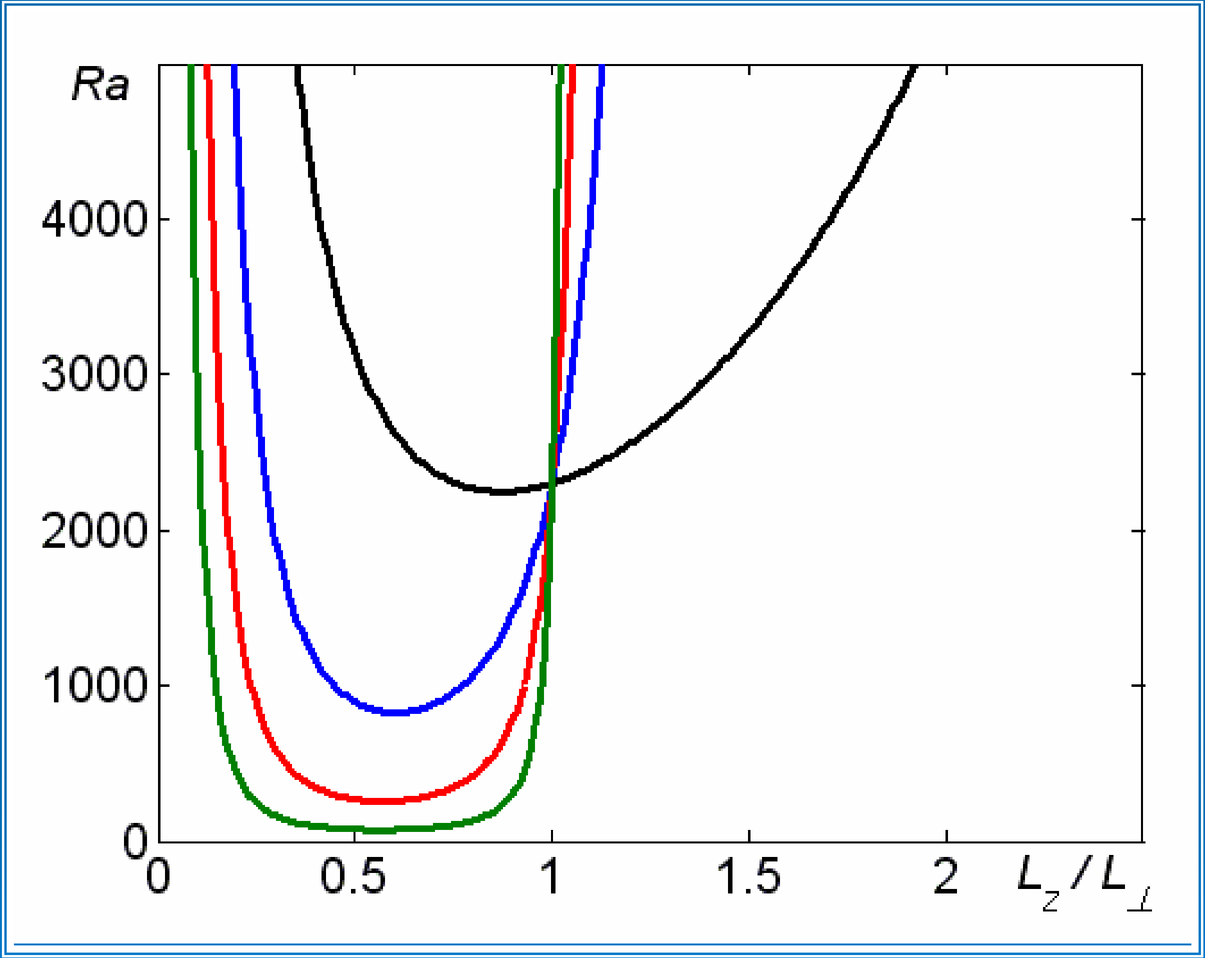

$Ra^{cr} = 2247$

$\mu = 0.7$ $Ra^{cr} = 826$

$\mu = 2$ $Ra^{cr} = 256$

$\mu = 5$ $Ra^{cr} = 72$

$$\mu = 0.15\left(\frac{T_0}{\Delta T}\frac{u}{g\tau}\right)^{2/3}$$

In laminar convection:

$Ra^{cr} = 657.5$

Laboratory Turbulent Convection

- In laboratory turbulent convection several organized features of motion, such as plumes, jets, and large-scale circulation patterns are observed.
- The large-scale circulation in a closed box with the heated bottom (in the Rayleigh-Benard apparatus) is often called the "mean wind".

There are several unsolved theoretical questions concerning these flows:

- How do they arise ?
- What are their characteristics and dynamics?

Hysteresis in Laminar Convection

- F. H. Busse, J. Fluid Mech. **30**, 625-649 (1967).
- F. H. Busse, Rep. Prog. Phys. **41**, 1929-1967 (1978).
- G. E. Willis, J. W. Deardorff, R. C. J. Somerville, J. Fluid Mech. **54**, 351-367 (1972).

The hysteresis phenomenon in laminar convection was found by Busse (1967) who defined it as follows: "The fact that the convection at a certain Rayleigh number depends on the way in which the Rayleigh number has been reached is called the hysteresis effect".

In the laminar convection the hexagon flow structures transform into roll structures by increasing the Rayleigh number. Decreasing the Rayleigh number causes the transition from the roll structure to the hexagons. Similar phenomena were observed in a number of numerical simulations and laboratory experiments.

The typical size of structures versus Ra

Experiments by Willis, Deardorff, Somerville (1972):

$$\mathrm{Ra} = (0.2 - 3) \times 10^4 \qquad A = 31.5$$

- In the experiments performed in air, water and a silicon oil, it was demonstrated that in convection the average dimensionless roll diameter, L, increases as Ra is increased.
- The hysteresis phenomenon was found in dependence of the roll diameter L versus Ra only for large Pr (for water and silicon oil).

DNS of convection by Hartlep, Tilgner, Busse (2003):

$$\mathrm{Ra} = 10^3 - 10^6 \qquad A = 10$$

The typical size of the large-scale structures broadly increases with increasing Ra, but the hysteresis phenomenon was not observed in DNS.

Experimental set–up

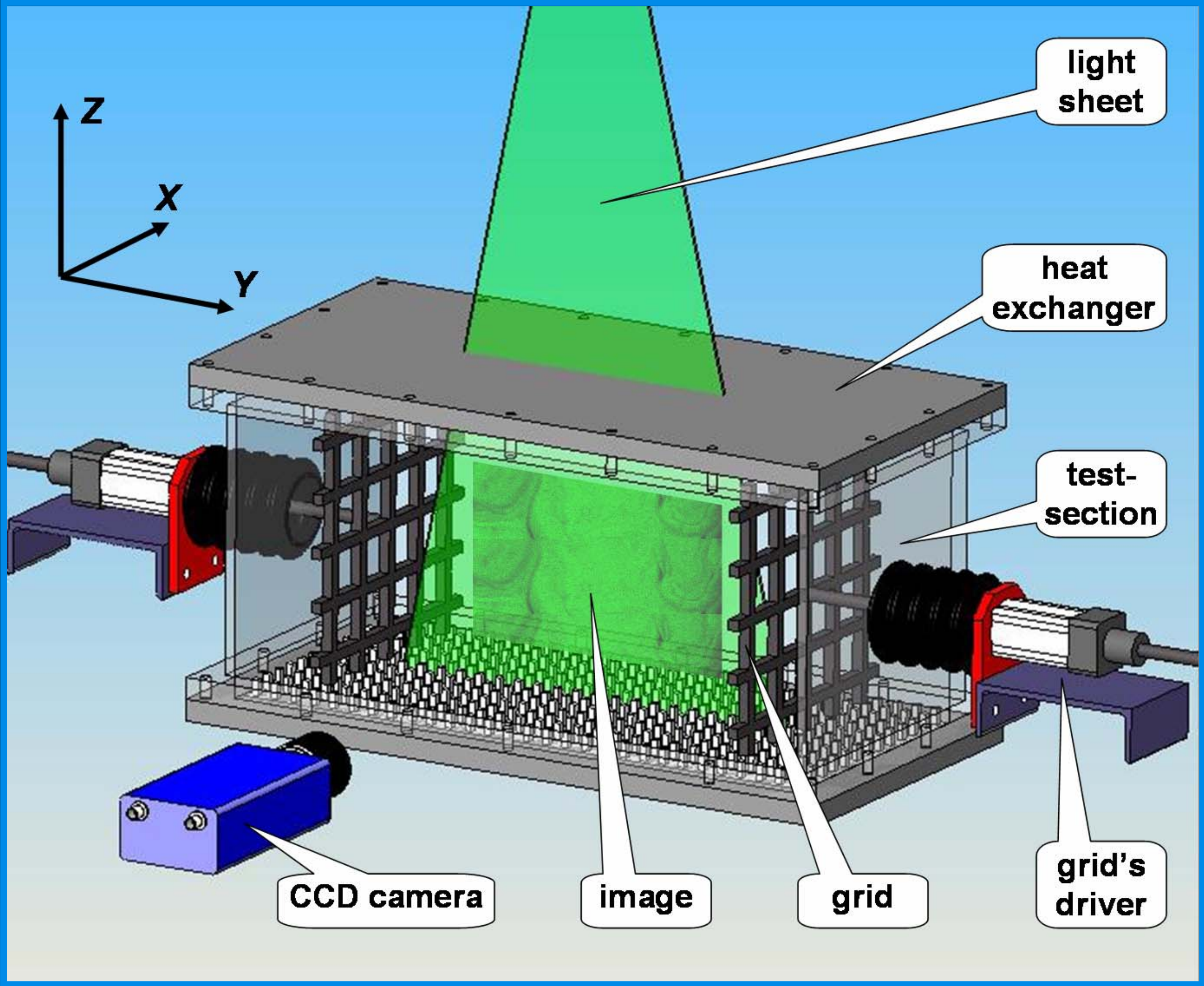

Particle Image Velocimetry System

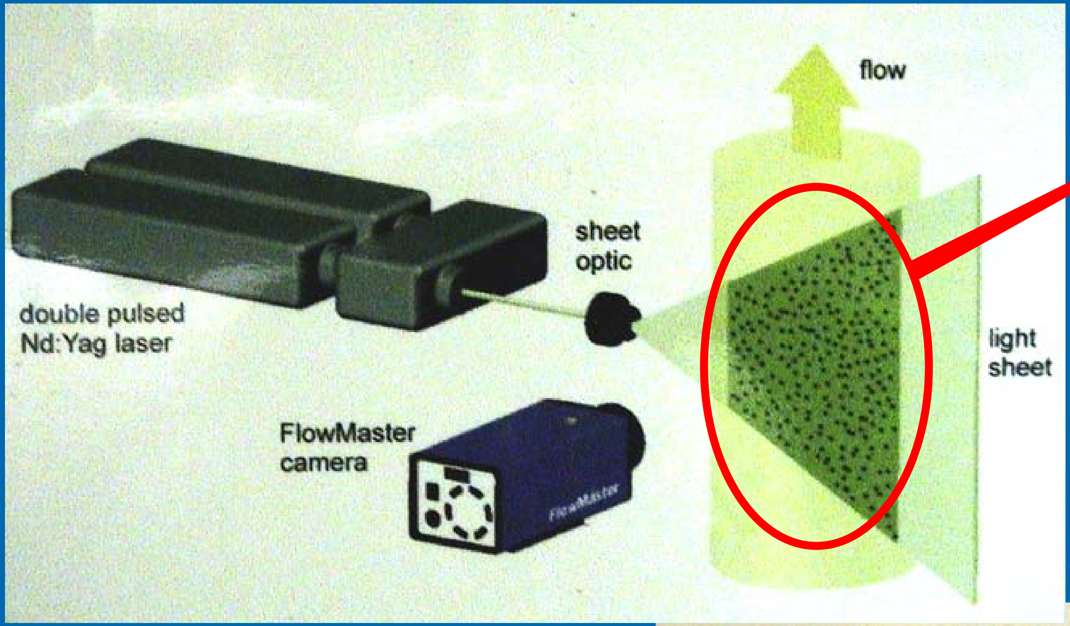

Raw image of the incense smoke tracer particles in oscillating grids turbulence

Particle Image

Velocimetry Data

Processing

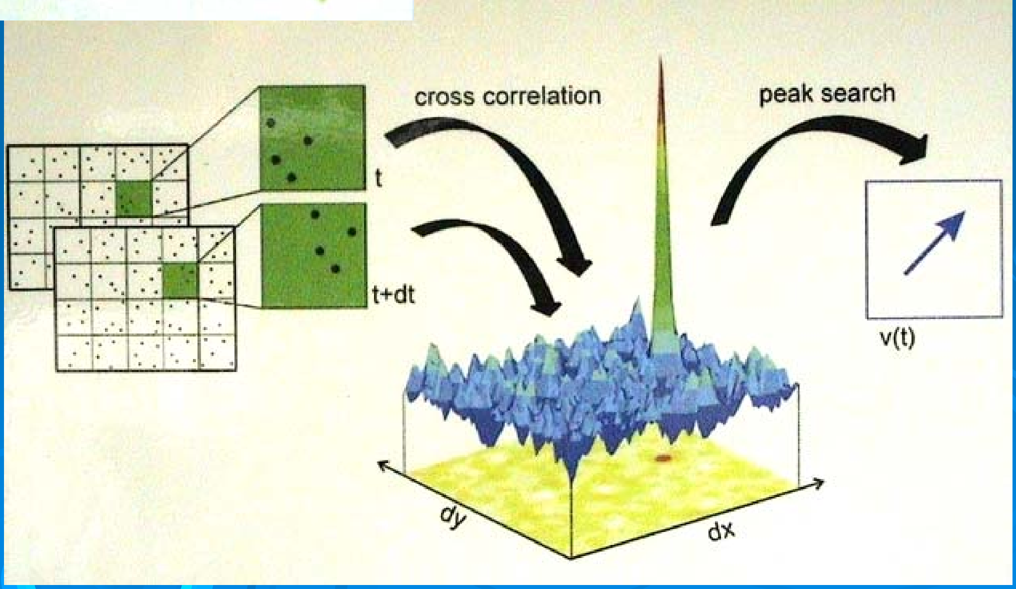

Velocity Fields

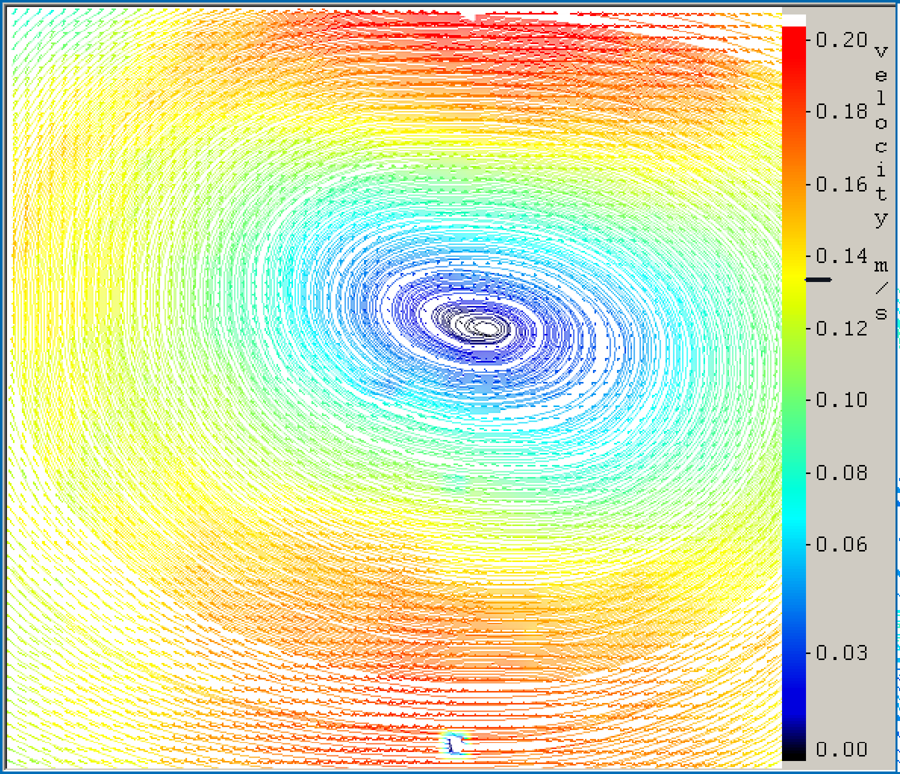

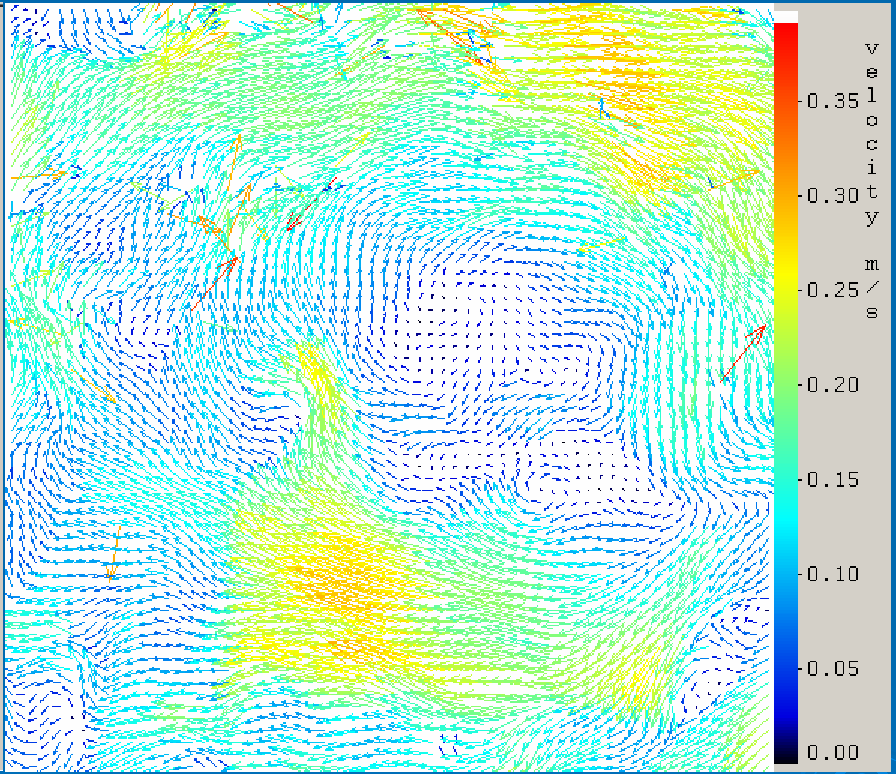

$$A = \frac{L_{\perp}^{B}}{L_{z}^{B}} = 1$$

Temperature Field in Forced and Unforced Turbulent Convection

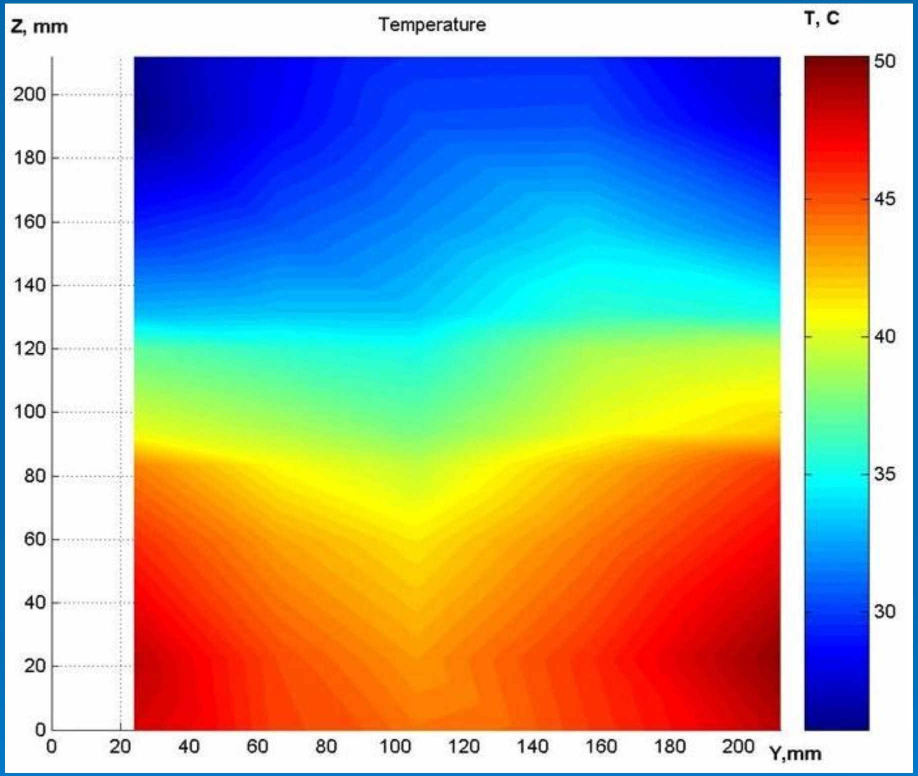

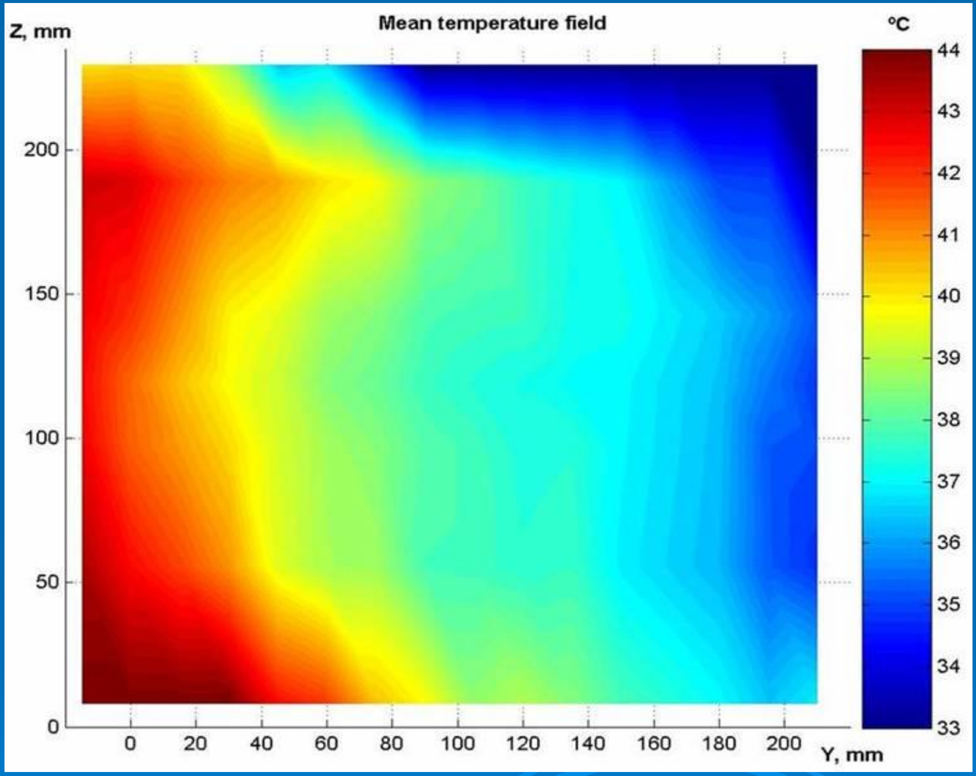

Forced turbulent convection
(two oscillating grids)

Unforced convection

Hysteresis in Turbulent Convection

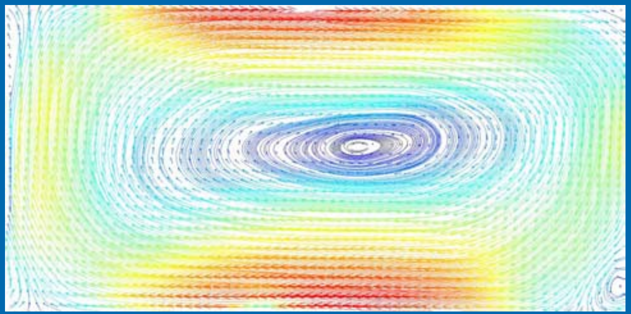

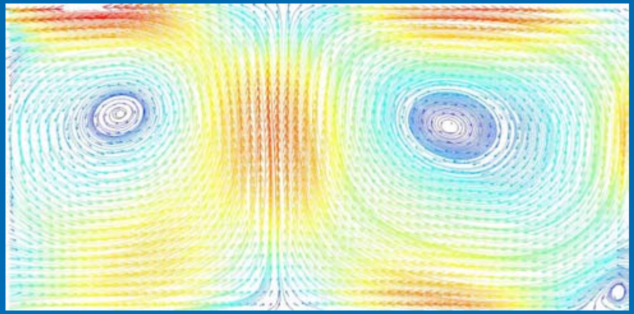

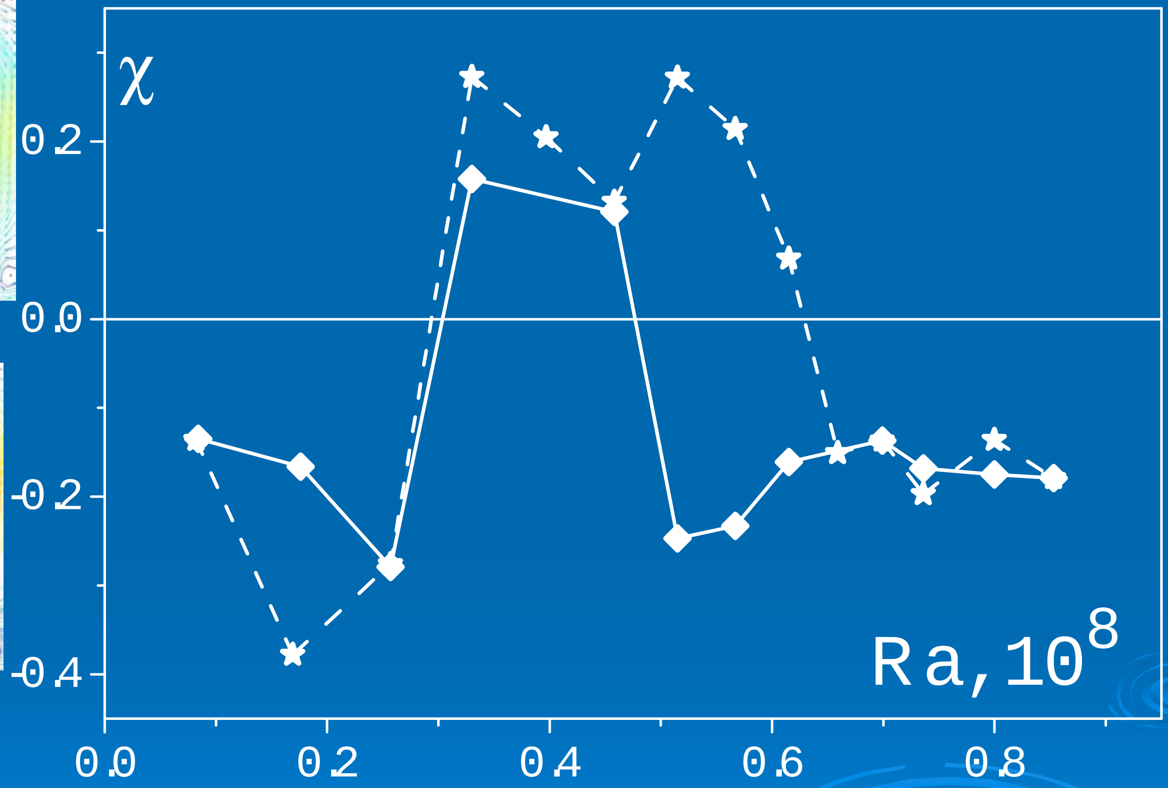

$$\chi = \frac{4}{3}\left(\frac{\langle u_y^2 \rangle}{\langle u_z^2 \rangle} - 1\right)$$

$\mathrm{Ra}_{\mathit{increase}}$ (*solid*)

$\mathrm{Ra}_{\mathit{decrease}}$ (*dashed*)

Method of Derivation

Equations for the correlation functions for:

- The velocity fluctuations $(M_{ij}^{(II)})_u \equiv \langle u_i u_j \rangle$
- The temperature fluctuations $M_\theta^{(II)} \equiv \langle \theta\, \theta \rangle$
- The heat flux $(M_i^{(II)})_\Phi \equiv \langle \theta\, u_i \rangle$

The spectral τ-approximation (the third-order closure procedure)

$$\hat{D}M^{(III)}(\mathbf{k}) - \hat{D}M_K^{(III)}(\mathbf{k}) = -\frac{M^{(II)}(\mathbf{k}) - M_K^{(II)}(\mathbf{k})}{\tau_c(\mathbf{k})}$$

$$\left(\hat{D}M_{ij}^{(III)}\right)_u = -\langle u_j(\mathbf{u}\cdot\nabla)u_i \rangle - \langle u_i(\mathbf{u}\cdot\nabla)u_j \rangle$$

$$\left(\hat{D}M_{ij}^{(III)}\right)_\theta = -2\langle \theta(\mathbf{u}\cdot\nabla)\theta \rangle$$

$$\left(\hat{D}M_i^{(III)}\right)_\Phi = -\langle u_i(\mathbf{u}\cdot\nabla)\theta \rangle - \langle \theta(\mathbf{u}\cdot\nabla)u_i \rangle$$

The difference in the growth rate for two-cell and one-cell flow patterns versus the degree of thermal anisotropy

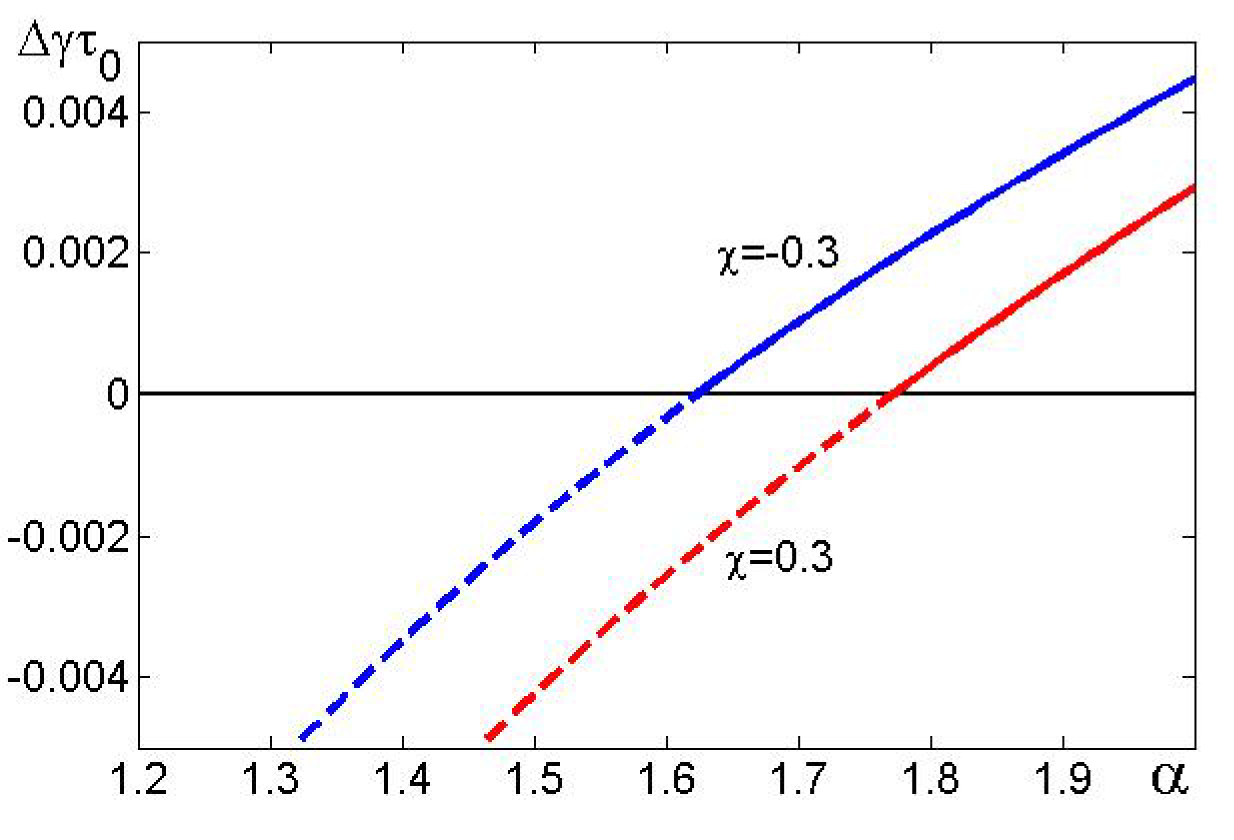

Bifurcation point versus the degree of thermal anisotropy

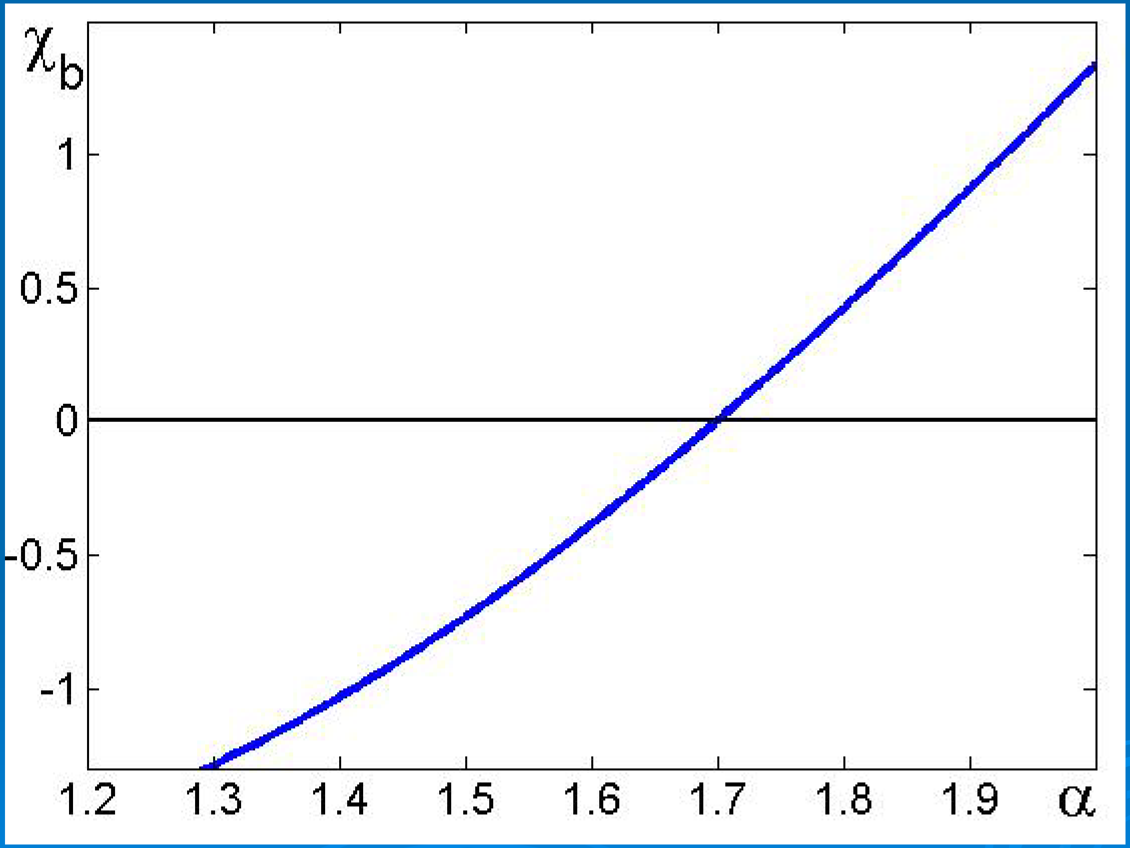

Turbulent Energy Flux

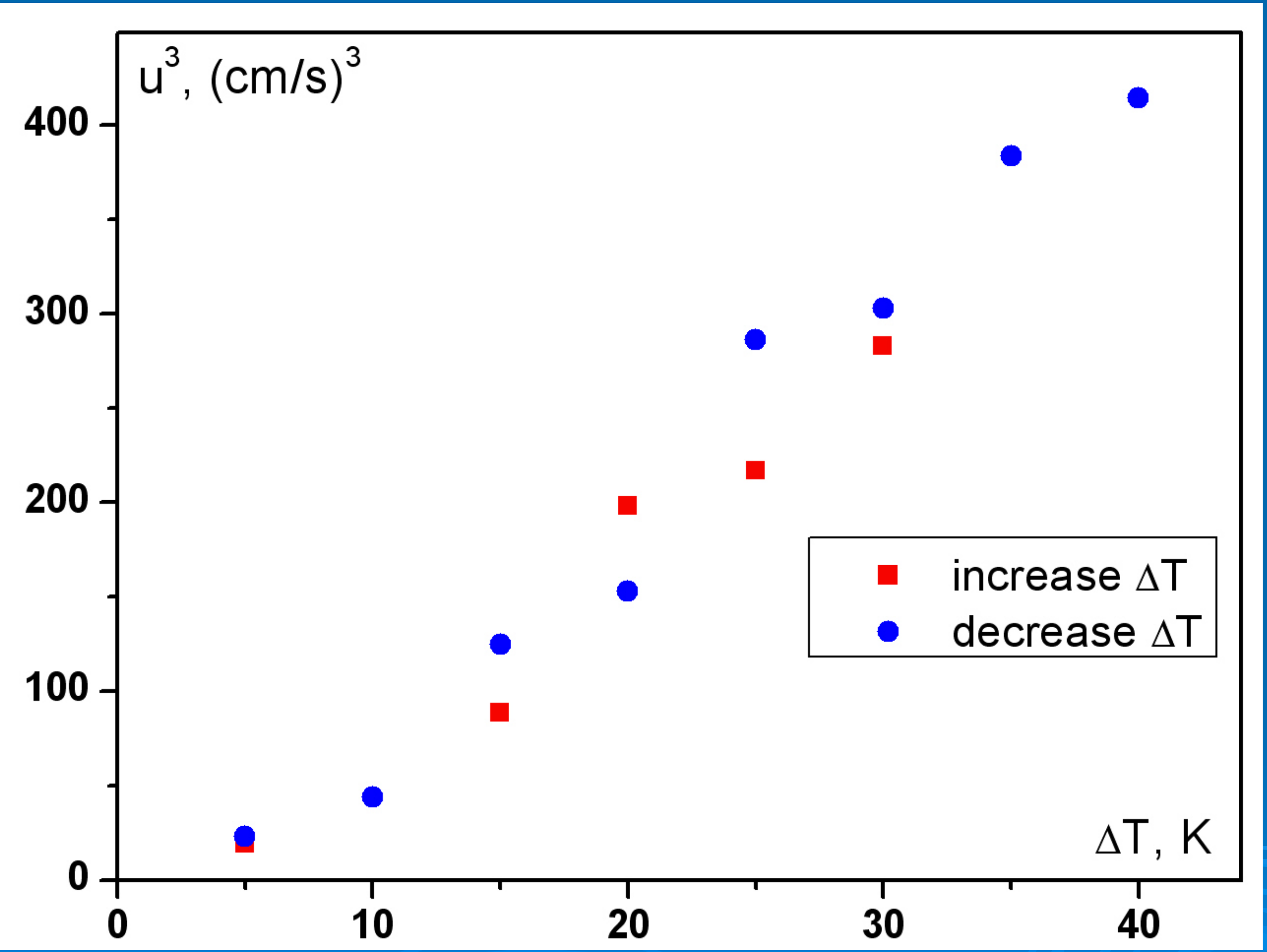

Linearized equations

Linearized equations for the small perturbations from the equilibrium

$$\tilde{U}_z = \overline{U}_z - \overline{U}_z^{(eq)}, \quad \tilde{W}_z = \overline{W}_z - \overline{W}_z^{(eq)}, \quad \tilde{\Theta} = \overline{\Theta} - \overline{\Theta}^{(eq)}$$

$$\left[\left(\frac{\partial}{\partial t} + \overline{U}_y^{(0)} \nabla_y - \nu_T \Delta\right)\Delta + \sigma \nabla_y \nabla_z\right]\tilde{U}_z = g \Delta_\perp \tilde{\Theta}$$

$$\left(\frac{\partial}{\partial t} + \overline{U}_y^{(0)} \nabla_y - \nu_T \Delta\right)\tilde{W}_z = -\sigma \nabla_x \tilde{U}_z$$

$$\left(\frac{\partial}{\partial t} + \overline{U}_y^{(0)} \nabla_y\right)\tilde{\Theta} = -\left(\vec{\nabla} \cdot \tilde{\mathbf{\Phi}}\right) - \left(\nabla_z \overline{\Theta}^{(0)}\right)\tilde{U}_z$$

where $\Delta_\perp = \Delta - \frac{\partial^2}{\partial z^2}$, $\quad \nu_T$ is the turbulent viscosity,

$$\boxed{\vec{\nabla} \cdot \tilde{\mathbf{\Phi}} = -\frac{4\tau_0}{45}\left[\left(\mathbf{\Phi}^* \cdot \mathbf{e}\right)\left[10\alpha \Delta_\perp - (8\alpha - 3)\Delta\right]\tilde{U}_z + 6\left((\mathbf{\Phi}^* \times \mathbf{e}) \cdot \vec{\nabla}\right)\tilde{W}_z\right] - \kappa_T \left[\Delta + \frac{3}{2}(4-\gamma)\frac{\partial^2}{\partial z^2}\right]\tilde{\Theta},}$$

κ_T is the turbulent heat conductivity and γ is the ratio of specific heats,

$$\overline{\mathbf{U}}^{(0)}(z) = \sigma z \mathbf{e}_y$$

Convective-shear instability

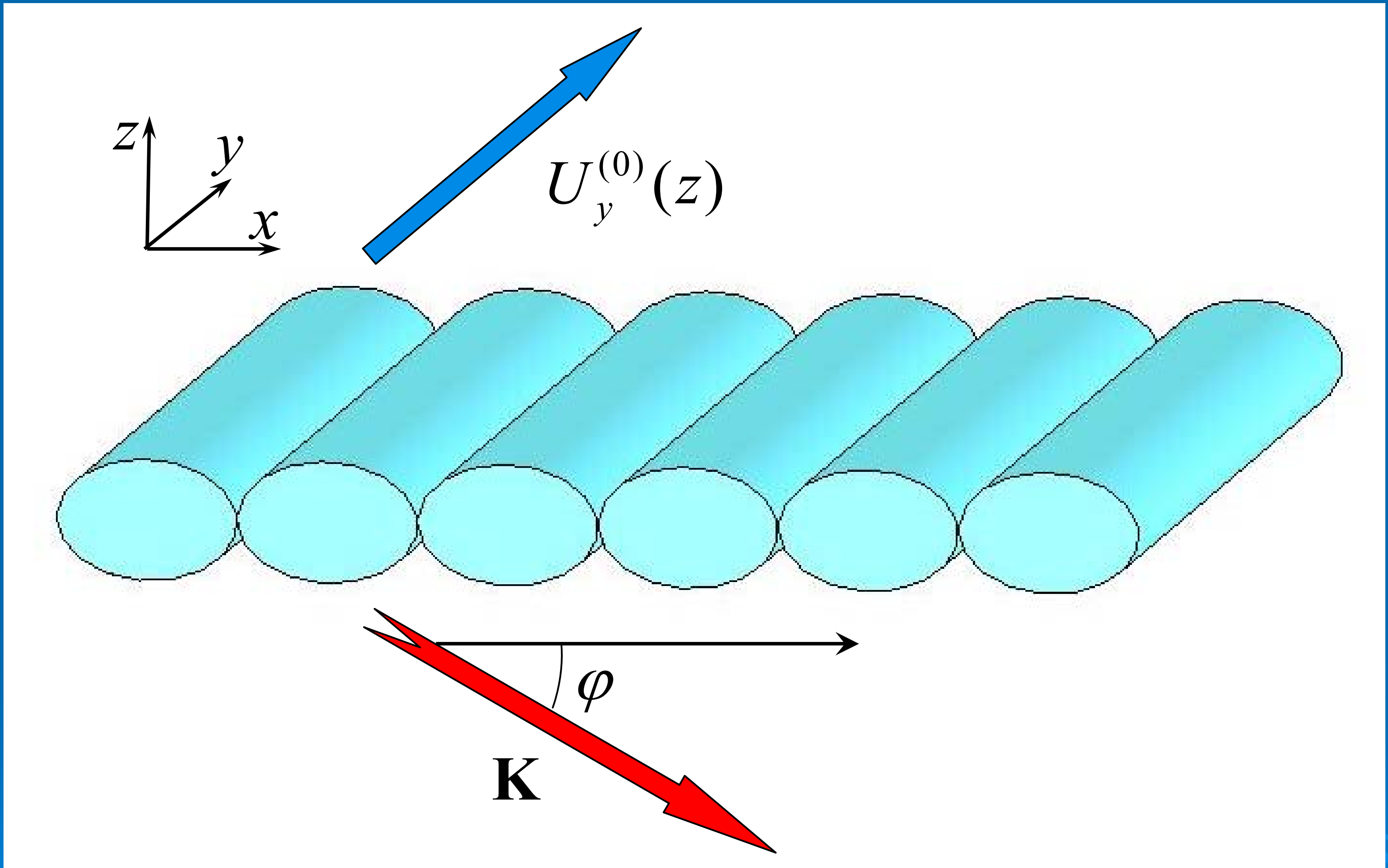

Conditions for the instability

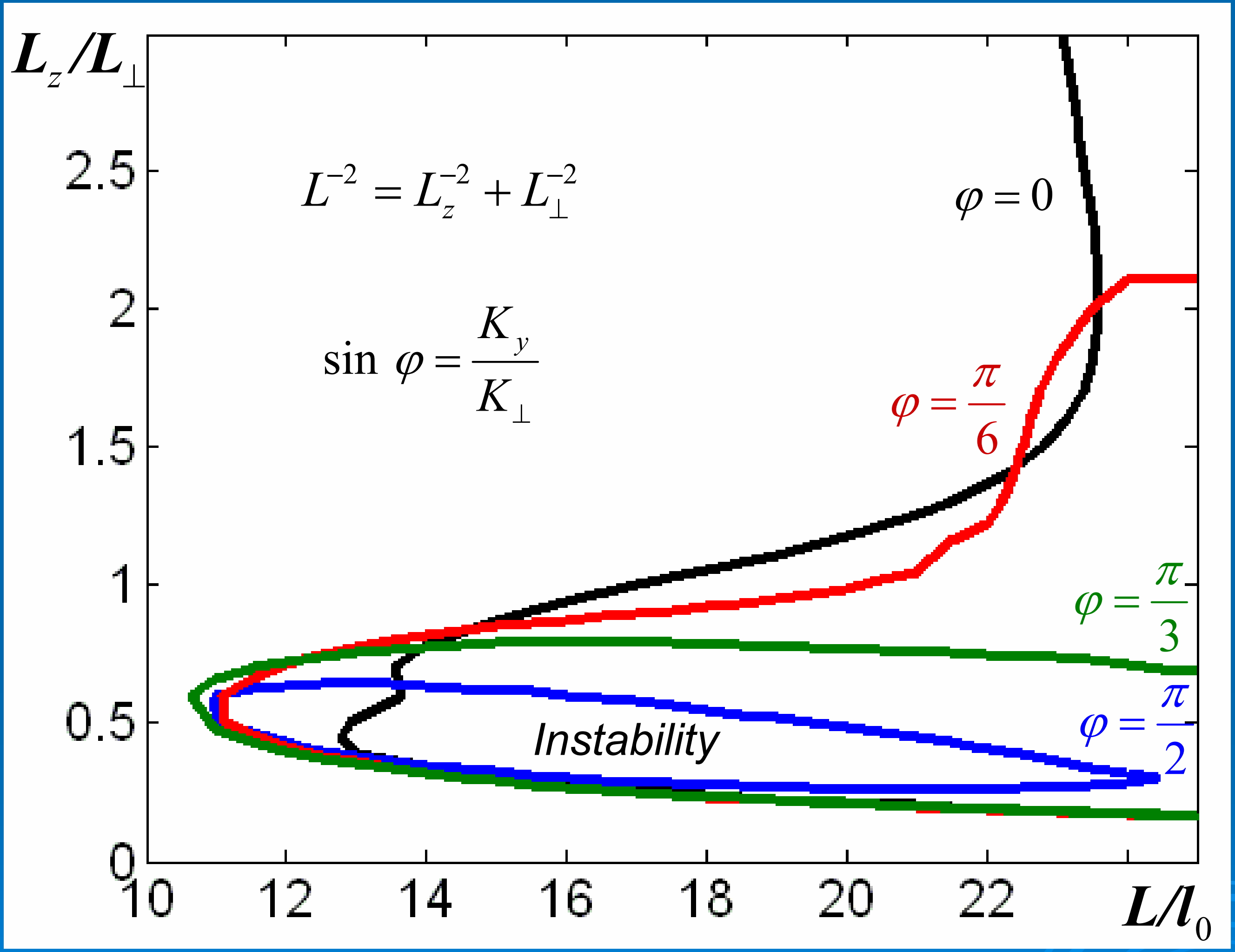

The range of parameters $L_z / L_\perp$ and L / l_0 for which the convective shear instability occurs

Maximum growth rate

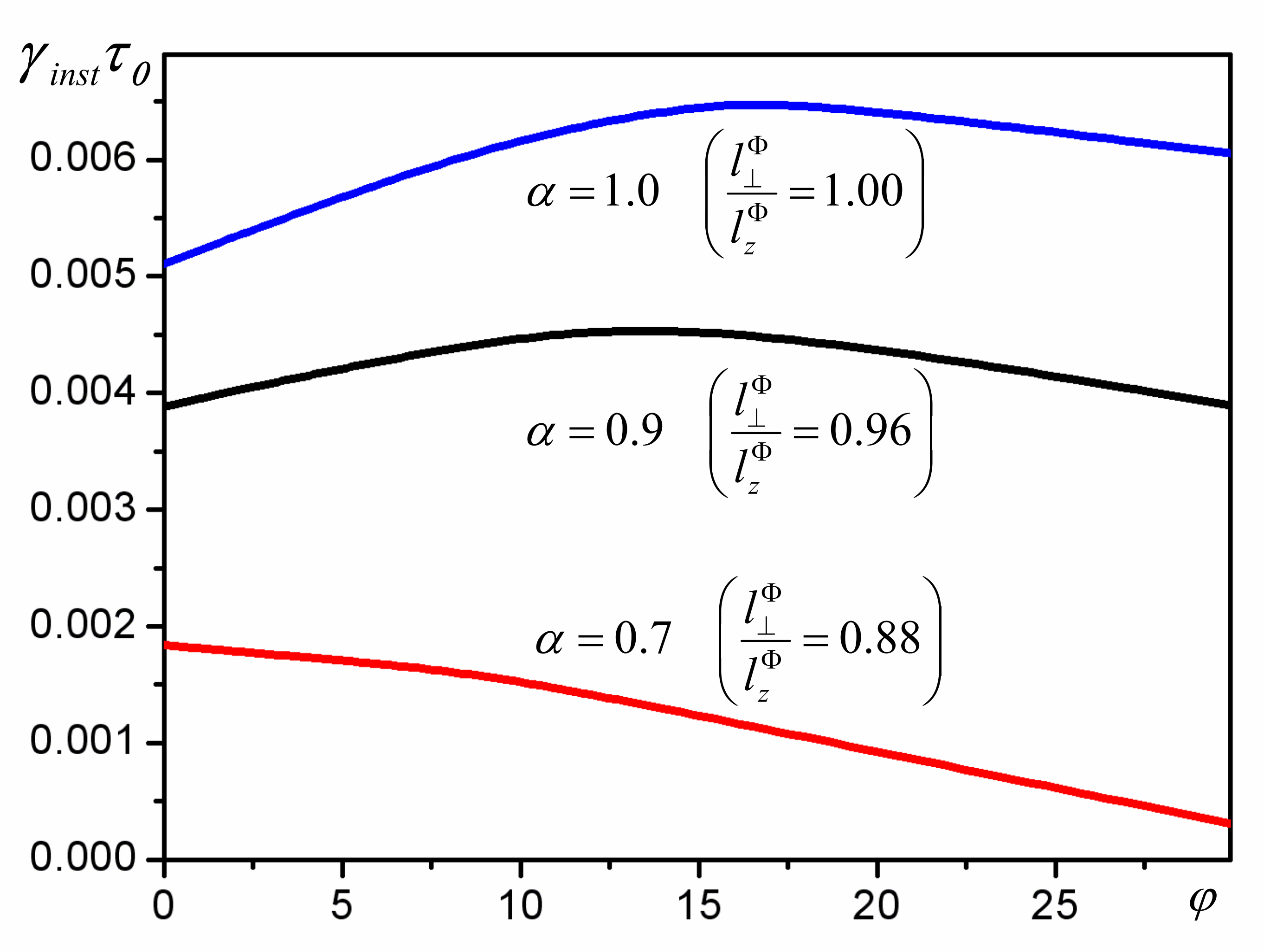

The growth rate of the convective shear instability
for different thermal anisotropy

Mean Velocity and Temperature Fields (One Grid Forcing)

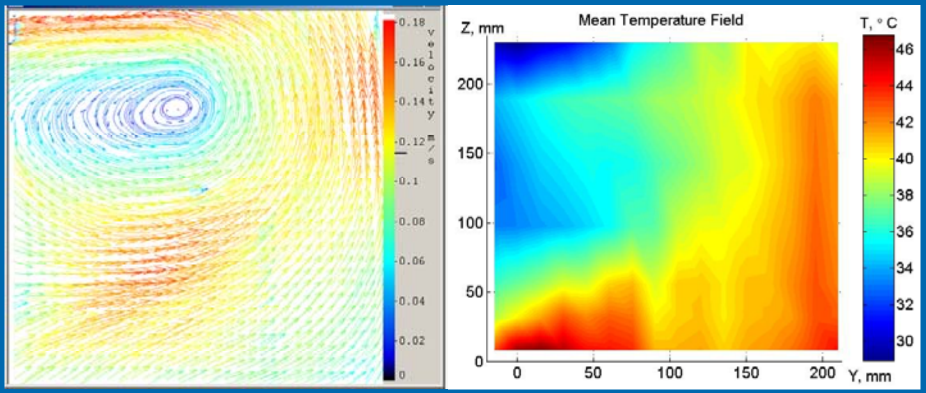

2.2 Hz

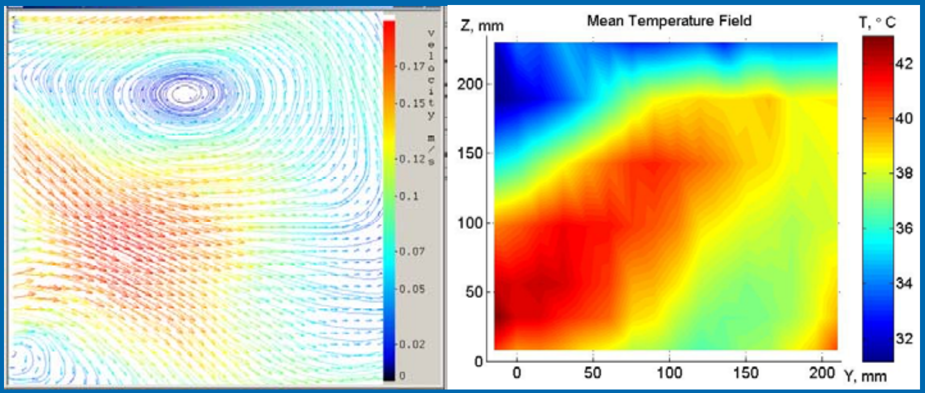

4.4 Hz

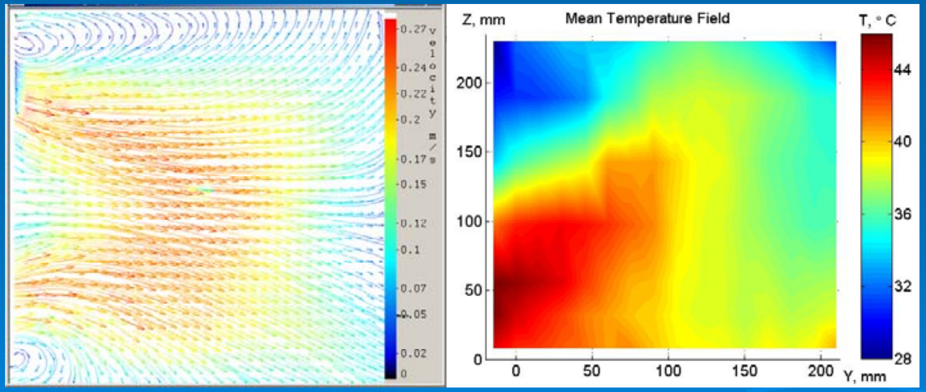

6.4 Hz

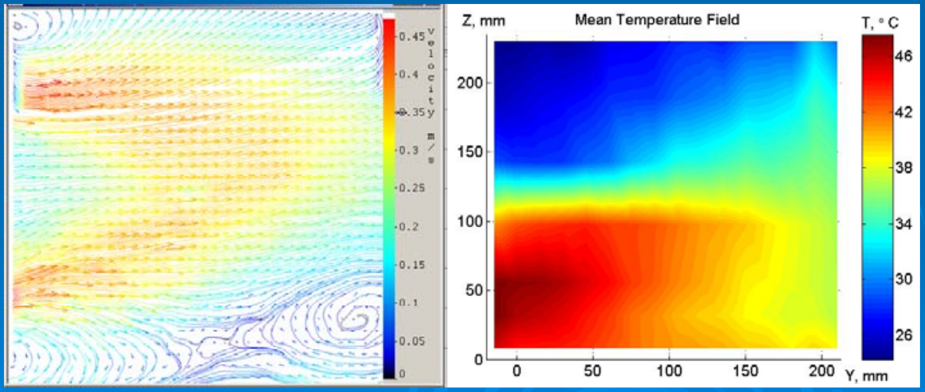

10.4 Hz